Master of Science Thesis

Comparison of classification systems to define Atmospheric Stability
and their impact on Wind Turbine Design

J.J.W. Hutschemaekers

September 8, 2014

Wind Energy Research Group, Faculty of Aerospace Engineering · Delft University of Technology

TU Delft Delft University of Technology

Challenge the future

RE Power 3.2M114 Prototype (Winter 2011)

Comparison of classification systems to define Atmospheric Stability

and their impact on Wind Turbine Design

MASTER OF SCIENCE THESIS

For obtaining the degree of Master of Science in Sustainable Energy Technology at Delft University of Technology

J.J.W. Hutschemaekers

September 8, 2014

Faculty of Aerospace Engineering & Applied Physics · Delft University of Technology

DELFT UNIVERSITY OF TECHNOLOGY
DEPARTMENT OF
WIND ENERGY

The undersigned hereby certify that they have read and recommend to the Faculty of Aerospace Engineering & Applied Physics for acceptance a thesis entitled **"Comparison of classification systems to define Atmospheric Stability"** by **J.J.W. Hutschemaekers** in partial fulfillment of the requirements for the degree of **Master of Science**.

Dated: September 8, 2014

Head of department: _____
Prof.dr. G.J.W. van Bussel

Supervisor: _____
Dr.ir. W.A.A.M. Bierbooms

Reader: _____
Dr. S.R. de Roode

Reader: _____
Ir. M.C. Holtslag

Summary

The world's energy consumption is rising, which will eventually result in the depletion of fossil fuels. A transition from fossil fuels to renewable energy sources as main energy supply has to be achieved to ensure the world's energy supply on the long term [9]. To ensure the world's energy supply, the European Commission adopted the climate and energy package with binding legislations, known as the 20-20-20 targets. To reach the targets set by the European Commission, renewable energy sources have to become less dependent on governmental subsidies and therefore the cost price of renewable energies has to be lowered.

For wind turbines, this results in an reduction of the Levelized Cost of Electricity (LCoE) by reducing the CAPEX (Capital Expenditures) and OPEX (Operational Expenditures). One way to do this is to take the Atmospheric Stability into account. More accurate load and power predictions can be executed, which could eventually lead in reduction of CAPEX and OPEX by increasing the accuracy of wind profiles and description of Turbulence Intensity.

- Load calculations: More accurate load calculations could result in cost reductions of production, material etc.
- Power calculations: More accurate power calculations could result in decrease of uncertainty of the power predictions leading to reduction of the OPEX through decrease of the interest rate.

For the estimation of the atmospheric stability multiple classifications systems and methodologies can be used. In this master thesis, the focus will be on the classification of the atmospheric stability with the Monin-Obukhov Similarity Theory (MOST) using multiple methodologies which are used in the industry and research. However, each methodology results to different values for the atmospheric stability. The goal of the project is to compare different methodologies, determine the best for each case and develop guidelines for atmospheric stability estimations.

To achieve the goal, a comparison of multiple methodologies is executed using measurement campaigns on multiple levels at three locations. In the research significant differences in distribution, friction velocity and heat flux could be observed as a result of using different multiple methodologies and measurement heights. This is even noticed for the reference methodology, the Eddy

Covariance Method, differences are found between different heights at the same site.
Analysis of the atmospheric stability distributions, slope and correlation of both the friction velocity and heat flux showed that the Profile Method 2 gives the best approximation of the atmospheric stability conditions, due to the found high correlation and consistency using various measurements heights.
The Profile Method 2 uses one wind speed measurement at the tower and two temperature measurements, at the surface and tower. A preference was found for tower measurements around a measurement height of 40-60 meters. At lower altitudes the sensory accuracy significantly influences the temperature difference and at higher altitudes it is often outside of the Surface Boundary Layer where MOST not any more is applicable.

The research also showed that the methodologies based on the Richardson Number are strongly influenced by measurements outside the Surface Boundary Layer. Using the approximation of the Surface Boundary Layer height and filtering the timesteps where the measurement height is outside of the Surface Boundary Layer, results in a large data reduction. The resulting distribution can deviate with the local conditions, while equivalent load calculations require typical conditions of the Surface Boundary Layer.

Translating various distributions found by different methodologies to the impact on the bending moment of the blade root of a wind turbine, by comparing the equivalent loads resulted in significant differences. The differences in equivalent load vary from 1-2% between the Eddy Covariance Methods at different heights up to around 15% for the Profile Method 1 and Gradient Richardson Number. Using the Profile Method 2, preferred methodology for onshore conditions, gave a difference of only 3% with the reference. Comparing this with the equivalent load found using the IEC guideline, where a 30% difference in equivalent load was found between the IEC guideline and the Eddy Covariance Method. This shows the impact and importance of the accurate determination of the atmospheric stability and possible reduction of LCoE which could be realized, by selecting the most suitable methodology.

Finally resulting in the development of an appropriate guideline for atmospheric stability estimation.

Acknowledgements

"I have made this longer than usual,
because I have not had time to make it shorter."
- Blaise Pascal

This master thesis concludes my career as a student at Delft University of Technology. I wish to thank the my supervisors prof.dr. G.J.W. van Bussel and dr.ir. W.A.A.M. Bierbooms for the valuable supervision and feedback and especially ir. M. Holtslag for the long discussions and brainstorm sessions. I also would like to thank dr. S.R. de Roode & ir. J. Schalkwijk for broadening my scope and providing the Large-Eddy Simulation results of Cabauw.

I would like to thank several institutes for their help by providing valuable data for my research. The Royal Dutch Meteorological Institute (KNMI) for providing the Cabauw data and especially P. Baas and F. Bosveld at the KNMI. The ICDC, CliSAP/KlimaCampus, University of Hamburg and F. Beyrich, W.K. Adam for the Lindenberg Boundary Layer Measurement Tower data [6] NoordzeeWind B.V. (NZWBV) and its contractors for providing the Offshore Windpark Egmond aan Zee (OWEZ) met mast data. The Federal Ministry for the Environment, Nature Conservation and Nuclear Safety (BMU), Projekttraeger Juelich, project executing organisation (PTJ) and DEWI GmbH (Deutsches Windenergie Institut) for the FINO1 data and help with the data analysis. The Danish Technical University for providing me with the data of the Danish wind turbine test site in Høvsøre.

Delft, The Netherlands
September 8, 2014

J.J.W. Hutschemaekers

Contents

List of Figures

List of Tables

Nomenclature

Latin symbols

A	Weibull scale parameter	m/s
c_i	Stability constant	
C_p	Specific heat capacity	J/K
d_i	Partial damage	
D_J	Julian day of the year	
D_L	Number of days skipped due to leap years	
f_c	Coriolis parameter	$1/s$
F_D	Fatigue strength	Nm
F_eq	Equivalent load	Nm
F_i	Actual fatigue load	Nm
g_M	Mean anomaly of the Sun	$^\circ$
H	Turbulent sensible heat flux	W/m^2
k	Weibull shape parameter	
L_M	Longitude of the Sun	$^\circ$
L	Monin-Obukhov length	m
N_{JD}	Number of days from start of the Julian year in 2000	
N_D	Fatigue limit (number of cycles)	
n_{eq}	Number of equivalent cycles	
n_i	Actual fatigue cycles	
u_*	Friction velocity	m/s
u	Horizontal wind velocity	m/s
v	Vertical wind velocity	m/s
w	Horizontal wind velocity perpendicular to u	m/s
z_i	Boundary Layer height	m
z_s	Surface Boundary Layer height	m
z	Height	m

Greek symbols

α_s	Solar elevation angle	$^\circ$
α	Hellman exponent	
δ	Solar declination angle	$^\circ$
$\frac{g}{\theta_v}$	Buoyancy parameter	m/s^2K
κ	Von Karman constant	
λ_{ec}	Ecliptic longitude of the Sun	$^\circ$
$\overline{w'\theta'_v}$	Heat flux	W/m^2
ϕ_m	Relationship between dimensionless momentum gradient and stability parameter $\frac{z}{L}$	
ϕ_h	Relationship between dimensionless heat gradient and stability parameter $\frac{z}{L}$	
ϕ_q	Relationship between dimensionless moisture gradient and stability parameter $\frac{z}{L}$	
ψ_M	Momentum function for wind profile	
ψ_H	Heat function for temperature profile	
ψ_Q	Moisture function for moisture profile	
ρ	Density	kg/m^3
σ_u	Standard deviation of wind speed	m/s
σ_ϕ	Standard deviation of wind direction angle ϕ	$^\circ$
σ_Ω	Standard deviation of the vertical wind speed	m/s
σ_Θ	Standard deviation of the horizontal wind speed	m/s
θ_*	Temperature scale	K
θ_s	Solar Zenith angle	$^\circ$
θ_v	Virtual potential temperature	K
θ	Potential temperature	K
$\zeta = \frac{z}{L}$	Stability parameter	

Abbreviations

AEP	Annual Energy Production
AMSL	Above Mean Sea Level
BMSL	Below Mean Sea Level
CAPEX	CAPital EXpenditures
DTU	Technical University of Denmark
EPC	Engineering Procurement Construction
IEC	International Electrotechnical Commission
TKE	Turbulent Kinetic Energy
KNMI	Royal Dutch Meteorological Institution
LCoE	Levelized Cost of Electricity
LES	Large-Eddy Simulation
MOST	Monin-Obukhov Similarity Theory
NN	Near Neutral
NREL	National Renewable Energy Laboratory
OPEX	OPerational EXpenditures
OWEZ	Offshore Windpark Egmond aan Zee
S	Stable
US	UnStable
VS	Very Stable
VUS	Very UnStable
WRF	Weather Research and Forecasting

Chapter 1

Introduction

1.1 Project background and motivation

The world's energy consumption is rising, which will eventually result in the depletion of fossil fuels. The largest part of the world's energy consumption is supplied by fossil fuels and only a small percentage is from renewable sources, demonstrating the world's dependency on fossil fuels (Figure 1.1).
A transition from fossil fuels to renewable energy sources as main energy supply has to be achieved to ensure the world's energy supply on the long term.

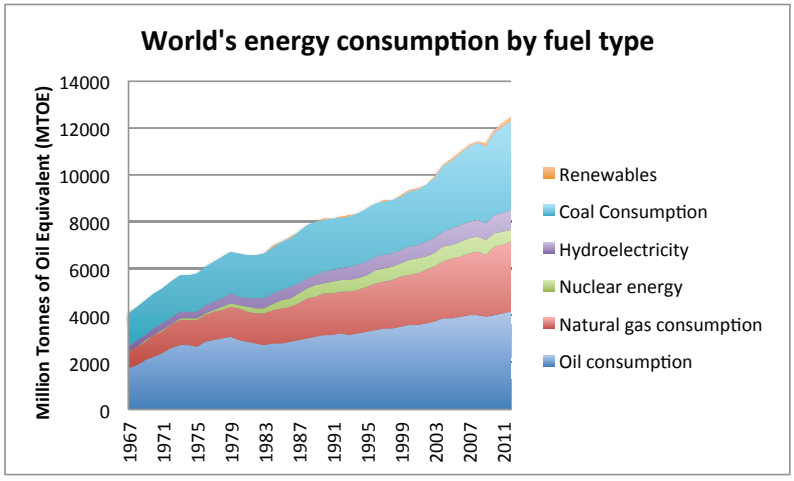

Figure 1.1: World's Energy Consumption by fuel type between 1967 to 2011 [9]

In 2009 the European Commission adopted the climate and energy package with binding legislations, known as the 20-20-20 targets. In specific, these targets are [16]:

- Reduction of EU greenhouse gas emissions of at least 20% below the 1990 levels.

- Increase to 20% of EU gross final energy consumption produced by renewable energy sources.
- Increase to 10% of transport final energy consumption produced by renewable energy sources.
- Reduction of primary energy use of 20% compared to projected levels.

In order to reach the climate and energy package, renewable energy sources have to become less dependent on governmental subsidies and therefore, the cost price of renewable energies has to be lowered. At the current market conditions, subsidies are necessary policies to increase the market share of renewable energy in the total power production arena. In order to be competitive with other energy sources, a decrease of the cost price will have to be realized to increase the renewable energy market share due to natural development of the market.

Wind energy is a big contributor to the total produced energy from renewable sources [12]. In order to reduce the cost price of the energy generated by wind turbines, we have to take a look at the Levelized Cost of Electricity (LCoE):

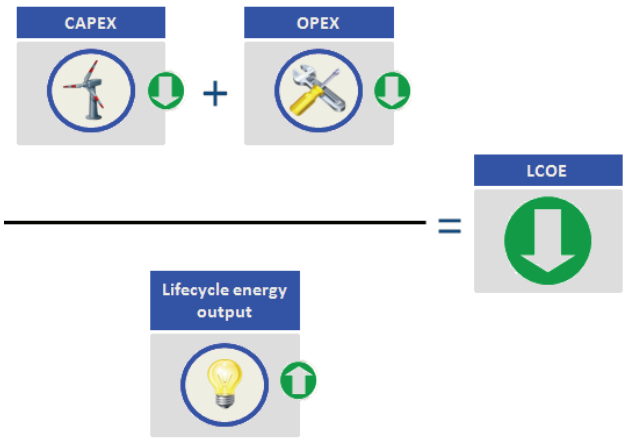

Figure 1.2: Levelized Cost of Electricity with CAPEX (Capital Expenditures or initial cost) and OPEX (Operational Expenditures or variable cost) in the numerator and the lifecycle energy output in the denominator, the total produced energy during the lifetime of the turbine.

Figure 1.2 shows that the required decrease of LCoE can be achieved by either decreasing the CAPEX and OPEX or increasing the lifecycle energy output. The CAPEX and OPEX together form the total lifecycle cost, where the CAPEX (Capital Expenditures) represents the cost of development, construction and installation of the wind turbine. This can also be described as the initial investment of the investor. The second part of the total life cycle cost is the OPEX (Operational Expenditures), which are the recurring costs, or variable cost. OPEX consists of operations and maintenance cost during the lifetime of the wind turbine. The recurring costs depend on the production of the turbine and therefore the AEP (Annual Energy Production).

1.1.1 CAPEX

The CAPEX or initial investment can be reduced by optimizing the turbine suitability for a particular site. The wind climate, extreme wind speed and turbulence intensity determines the critical design loads, which a turbine (of a specific IEC class) must withstand during its lifetime. IEC is the International Electrotechnical Commission which determines which turbine is suitable for the normal conditions of a particular site. As a result, the selection of a suitable wind turbine model for a project is often dependent on the extreme wind speed conditions at the specific site. An over-estimation of the wind climate, could result in a higher IEC classification and therefore increasing the critical design loads of the turbine and resulting in an overdimensionalized wind turbine. The wind turbine is not optimized for this particular site, introduces extra cost (CAPEX). With more insight into project-specific wind climate, firmer conclusions about the suitability of a specific turbine type will be possible, resulting in possible cost reductions and reducing the CAPEX of the turbine.

1.1.2 OPEX

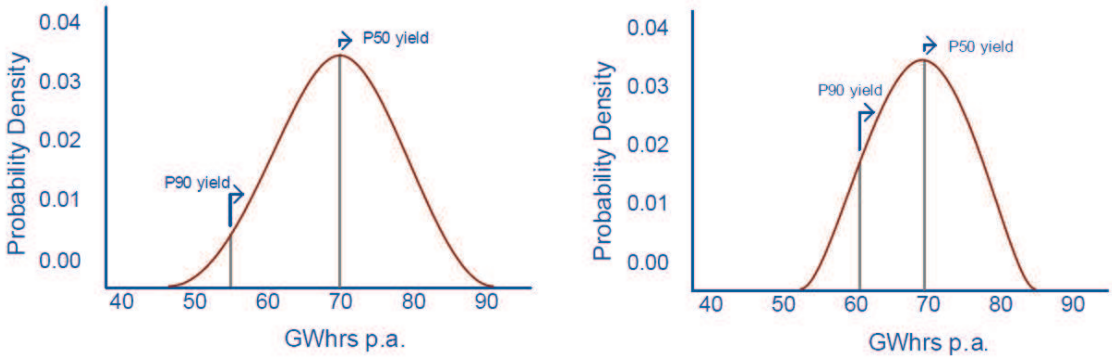

Figure 1.3: Scottish and Southern Energy P50-P90 AEP with increased certainty from left to right [52]

In figure 1.3 two normal distributed energy outputs of a wind turbine are shown. With P90 indicating the expected power output which is exceeded 90% of the time over a period of 10 years and P50 with the resulting 50% of the time. The operations and maintenance costs (OPEX) is paid per MWh, using the expected power output P90. More accurate power predictions result in a tighter normal distribution (right side of figure 1.3), which results in a close P90:P50 relationship indicating an increased certainty. An increase in certainty of the AEP prediction will result in higher P90 and eventually resulting in a lower fee per MWh thus lowering the OPEX.
A reduction of the CAPEX and OPEX due to more accurate load and power predictions would result in better conditions for finance and therefore increasing the share of renewable wind energy in the world.

1.2 Problem definition

In order to reduce the CAPEX and OPEX by more accurate load and power predictions, one can take a look at the turbine design. Both the power production and load predictions are significantly influenced by the assumed wind profile and turbulence intensity at the location of interest. Currently the wind profile is represented in the IEC design requirements by either a logarithmic profile without the diabatic correction or by an empirical power law with the power exponent depending on only the wind speed. Surface roughness and atmospheric stability are not taken into account in the current studies. Using atmospheric stability more accurate wind profiles and turbulence intensity predictions can be made using diabatic corrections for the wind profile. Previous studies from Sathe et al. [49] and Wharton et al. [58] showed the impact and importance of atmospheric stability estimations for accurate power production calculations and load calculations.

Atmospheric stability estimations can be done on the basis of Monin-Obukhov Similarity Theory (MOST). Currently there are multiple methodologies that are used in the industry and research to estimate the atmospheric stability, using the Monin-Obukhov length (L). However each methodology results to different values for the atmospheric stability and therefore the goal of this master thesis project is:

- To compare different methodologies estimating the atmospheric stability and determine which is the best for each case.
- To determine the impact of different methods on the atmospheric stability distribution and on the wind turbine design.
- To create guideline for atmospheric stability estimations.

1.3 Content

This report will take you through the following:

- In chapter 2 an introduction in atmospheric stability is given. The important theory for the understanding, execution and impact of the estimation of the atmospheric stability will be discussed. Subsequently multiple methodologies for the estimation of atmospheric stability will be explained.
- In chapter 3, multiple papers are discussed comparing different methods to estimate the atmospheric stability. The research is executed using measurement data from four locations. The study starts with the paper using measurement data of Rødsand, followed by papers using Horns Rev, OWEZ and FINO1.
- Chapter 4 focuses on the comparison of five methods to estimate the atmospheric stability at the met mast of the Royal Dutch Meteorological Institute (KNMI) in Cabauw. The comparison will focus on the differences of the atmospheric stability based on yearly, seasonal, hourly and wind speed distributions. After which a direct comparison of the momentum and heat fluxes will be executed. The chapter concludes with a short summary based on the Cabauw data.

- The next chapter is similar to the previous chapter, but focuses on the met mast in Lindenberg.
- As described in chapter 1 (the project background, motivation and problem definition), the goal of this thesis is to reduce the LCOE though better wind profile and load calculations using atmospheric stability corrections. In chapter 6, the equivalent load for a wind turbine blade root using different stability distributions found in chapter 4 and 5 is calculated, showing the impact on the design of the wind turbine of the different methodologies estimating the atmospheric stability.
- In chapter 7, the conclusions, recommendations and a guideline to gain the best atmospheric stability estimations is presented.

Chapter 2

Theoretical concepts

In this chapter the basics of the atmospheric stability will be discussed, starting with an introduction to numerous classifications systems to define atmospheric stability developed over the years. The second part of chapter two includes the explanation of main parameters for a better understanding of the phenomenon stability concluding with the explanation of five methodologies to determine the atmospheric stability.

2.1 Introduction in atmospheric stability

Atmospheric stability is a condition describing the state of the earth's atmosphere. The atmospheric stability indicates the variation of different properties in the vertical direction and therefore the existence of different horizontal layers and the mixing of these layers.

During the years, numerous classification systems have been developed to define the atmospheric stability. A small selection of relevant classification systems can be found below:

- Pasquill-Gifford (P-G) Method [35]
  Pasquill-Gifford is one of the oldest classification system used. This classification system uses the following parameters for the determination of the atmospheric stability: horizontal wind speed, cloud cover, ceiling height of clouds and the time of observation.
- STability ARray (STAR) Method [35]
  The computational method does not require special instruments. It relies on the weather observations made by meteorologists at National Weather Service stations.
- Brookhaven National Laboratory (BNL) Scheme [35]
  The BNL scheme uses only the horizontal wind direction fluctuations to estimate the atmospheric stability.
- σ_ϕ Method [35]
  The standard deviation of the wind direction angle ϕ (in the vertical direction) is used to

estimate the atmospheric stability. σ_ϕ gives an indication of the order of magnitude and intensity of the vertical motions in the atmosphere.

- σ_Ω Method [35]
  In this method, σ_ϕ is indirectly calculated using the standard deviation of the vertical wind speed , σ_Ω and the average horizontal wind speed.

- σ_Θ Method [35]
  The σ_Θ method, uses the standard deviation of horizontal wind direction, σ_Θ to estimate the atmospheric stability.

For this research, the primary focus will be on the following classification system:

- Monin-Obukhov Similarity Theory (MOST)

The Monin-Obukhov Similarity Theory is developed by Monin and Obukhov in the 1950's. The Monin-Obukhov length (L) plays a vital role in this theory [40]. There is a number of methodologies to determine the Monin-Obukhov length from measurements, which will be analysed in this research.

First, the basic theory will be explained, followed by the atmospheric stability and the different methodologies used to determine it.

2.1.1 Virtual and Potential Temperature

In order to understand the atmospheric stability completely, the difference between absolute temperature, potential temperature and virtual temperature will be explained.

Potential temperature

The potential temperature of an air particle at pressure P is the temperature that the particle would acquire if adiabatically (no heat exchanged with the surroundings) brought to a standard reference pressure P_0, usually $1 \cdot 10^5$ Pa. The potential temperature is described in equation 2.1

$$\theta = T \left(\frac{P_0}{P} \right)^{R/C_P} \tag{2.1}$$

where T is the temperature of the air particle in K, R is the gas constant of air, and C_P is the specific heat capacity at a constant pressure P.

In figure 2.1 the temperature, $T(z)$ and the potential temperature $\theta(z)$ of an air particle is visualised during movement from height z_1 to height z_2. Darker shades in the center sketch represent warmer temperatures, indicating an decrease in temperature during the movement due to the decrease of pressure and no exchange of heat with the surrounding. The decrease in temperature with height is visible on the left side of the figure. The right side of the figure shows the potential temperature, which is constant.

The decrease in temperature with increased height, is shown in figure 2.1 on the left. This is called the lapse rate. The lapse rate of dry (adiabatic) air is 9.8 $\frac{K}{km}$, denoting that for every kilometer of altitude gained, the temperature will be decreased by 9.8 K [53].

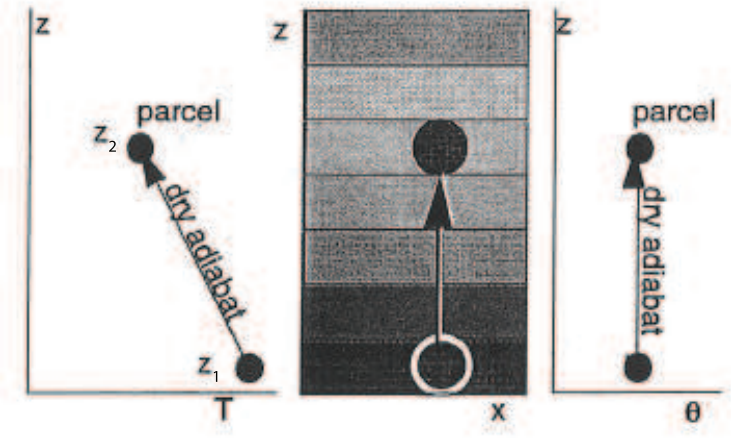

Figure 2.1: Comparison of temperature T(z) and potential temperature $\theta(z)$ methods of representing parcel movement through the environment. Darker shades in the center sketch represent warmer temperatures T. [53]

Virtual temperature

So far, we have only discussed dry air, however in reality, air also contains moisture. In order to take this into account, the virtual temperature is employed. The virtual temperature (T_v) is the temperature of dry air with the same density as the moist air at constant pressure. The virtual temperature of unsaturated moist air is always higher than that of actual air. For the virtual temperature the following equation applies:

$$T_v = T\frac{1+\frac{r_v}{\varepsilon}}{1+r_v} \tag{2.2}$$

where T is the temperature in K, r_v is the mixing ratio between moist and dry air and ε the ratio between the molecule masses of water vapour and dry air.

2.1.2 Stability conditions

Three main stability conditions in the atmospheric boundary layer can be observed: neutral, stable and unstable conditions. These stability conditions can be explained by an example of a moving air particle.

Neutral, stable and unstable conditions

Due to the movement of air in the atmosphere, the lapse rate is different at each moment in time and space. If it is assumed that at a certain moment in time the atmospheric lapse rate is equal to the standard lapse rate, then when a air particle is moved up, without heat exchange with the surroundings. The air particle has the same potential temperature as the surroundings, but the actual temperature is higher. Due to the lower pressure, the particle will expand and the temperature will drop. Because the environment and particle are cooled down with the standard

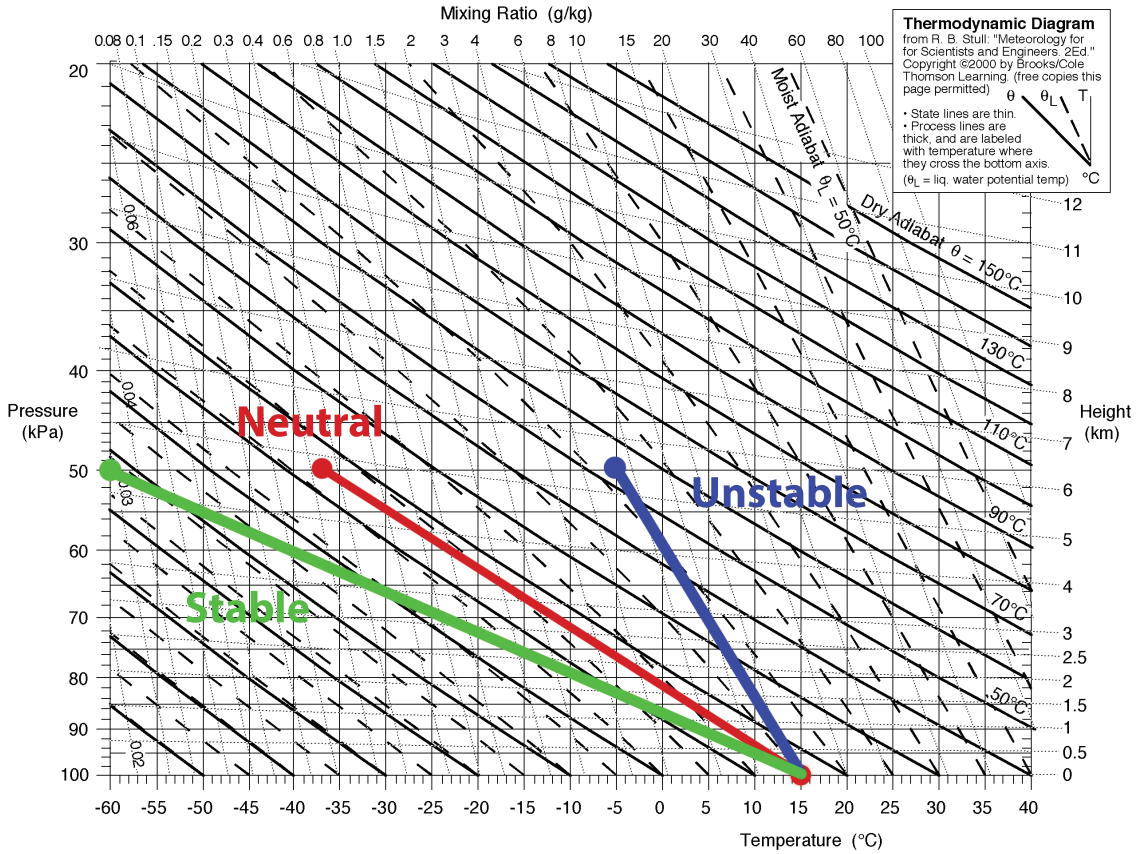

Figure 2.2: Thermodynamic diagram with temperature against pressure with three stability conditions. [53]

lapse rate, this means that there will be no difference in temperature between the surroundings and the air particle and the particle therefore will stay at the new acquired height. The atmospheric stability is at this moment neutral. In figure 2.2, the red line indicates the neutral conditions parallel to the potential temperature θ.

Now assume that at a certain moment in time the atmospheric lapse rate is higher than the standard lapse rate (green line in figure 2.2). When an air particle is moved up, the potential temperature stays the same, but it is higher in comparison to the surroundings because the environment is cooled below the standard lapse rate. The particle will have a lower temperature than the surroundings and will therefore move downwards until its initial position. The atmospheric stability at this moment is stable. In figure 2.2 the green line indicates the stable conditions.

Finally assuming that at a certain moment in time the atmospheric lapse rate is lower than the standard lapse rate (blue line in figure 2.2). Then the particle will have a higher temperature than the surroundings and will as a result move upwards. The atmospheric stability at this moment is unstable. In figure 2.2, the blue line indicates the unstable conditions.

Influence of stability conditions on wind profile and turbulence intensity

As explained before, the atmospheric stability indicates the variation of temperature and wind speed in the vertical direction. Based on the explanation of the three main conditions, the impact on the wind profile and turbulence intensity can be explained in the following paragraph.

Under stable conditions, the air particle will return to its initial position. The mixing of different layers therefore will be low, resulting in a low turbulence intensity compared to neutral conditions. Due to the fact that the mixing of air of different layers is lower, the wind shear will decrease with height. This results in a small increase of mean wind speed due to the stable conditions, which can be seen in figure 2.3.

For unstable conditions on the other hand, the air particle will not return to its initial position but continue to move. The mixing of different layers in the surface boundary layer therefore will be high. Due to strong mixing, the turbulence intensity will therefore be higher compared to the neutral conditions. The wind profile will also be more uniform because layers at low altitudes with low wind speeds will be mixed with layers at higher altitudes resulting in a lower mean wind speed which can be seen in figure 2.3.

An introduction of the atmospheric stability is provided. The following sections will now explain the Monin-Obukhov Similarity Theory (MOST) in more detail.

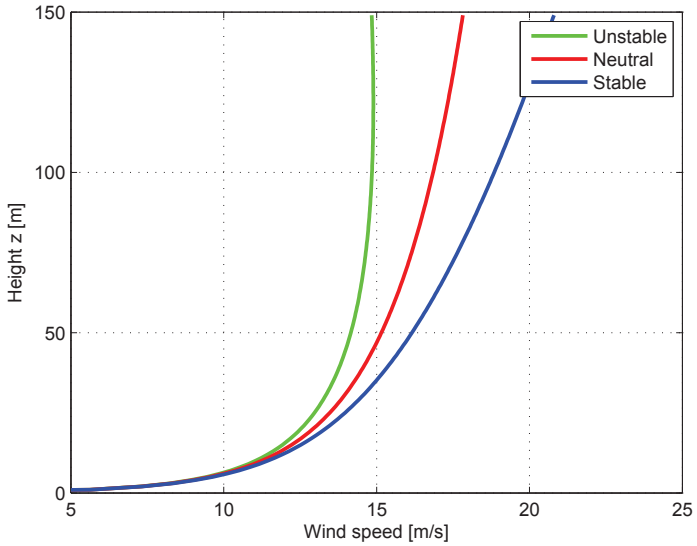

Figure 2.3: Typical wind speed profiles in the surface boundary layer for stable, neutral and unstable conditions

2.2 Monin-Obukhov Similarity Theory

The Monin-Obukhov Similarity Theory is a similarity theory describing the mean wind profile in the atmospheric surface layer as a function of dimensionless numbers. It is derived from the Turbulent Kinetic Energy equation, introduced below:

$$\overbrace{\frac{\partial \overline{q}}{\partial t} + \overline{U_j}\frac{\partial \overline{q}}{\partial x_j}}^{1} = \overbrace{-\overline{u_i' u_j'}\frac{\overline{U_i}}{\partial x_j}}^{2} + \overbrace{\frac{g}{\overline{\theta}}\overline{u_i'\theta'}\delta_{i3}}^{3} - \overbrace{\frac{\partial}{\partial x_j}\left(\frac{1}{2}\overline{u_i' u_i' u_j'} + \frac{1}{\overline{\rho}}\overline{P' u_j'} - \overline{\nu u_i'\frac{\partial u_i'}{\partial x_j}}\right)}^{4} - \overbrace{\nu\left(\frac{\partial u_i'}{\partial x_j}\right)^2}^{5} \tag{2.3}$$

where $\overline{q}$ is the Turbulent Kinetic Energy (TKE), ρ is the density, g is the acceleration of gravity, δ_{i3} is the Kronecker delta function, P is the pressure, ν the dynamic viscosity and the subscripts $i, j = 1,2,3$ denote the x, y, z directions.

The equation is divided into five terms. The first term represents the change in turbulent kinetic energy, the second is the mechanical production, the third is the buoyant production, the fourth the turbulent transport and finally the fifth one refers to the dissipation energy.

Equation 2.3 is derived from the Navier Stokes equation. Using a Boussinesq approximation, the Reynolds averaged Navier Stokes equation can be derived from which the Turbulent Kinetic Energy equation can be derived. This derivation is explained in [45].

The Turbulent Kinetic Energy equation cannot be solved easily. In the Monin-Obukhov Similarity Theory it was suggested that the average surface layer wind and temperature fields only depend on four parameters, the sensible heat flux (H), the height from the ground (z), the buoyancy parameter ($\frac{g}{\theta_v}$) and the surface shear stress (τ_0). Together these parameters can be used to define the length (z) and L (from equation 2.4), velocity (u_*) and temperature (T_*) scales. Where L is the Monin-Obukhov length, which gives a physical representation of the MoninâĂŞObukhov Similarity Theory. For unstable conditions, -L represents the height at which the buoyant production of turbulent kinetic energy is equal to the shear production. The Buckinham-π theorem/ dimensional analysis, comes in handy to describe the fluxes and gradients in a dimensionless form as a function $\frac{z}{L}$.

$$L = -\frac{u_*^3}{\kappa \frac{g}{\theta_v}\overline{w'\theta_v'}} \tag{2.4}$$

In equation 2.4 u_* is the friction velocity, κ is the Von Karman constant, g is gravity, θ_v is the virtual potential temperature ($\frac{g}{\theta_v}$ the buoyancy parameter), $\overline{w}$ is the mean wind velocity, w' is fluctuating term of the wind velocity, $\overline{\theta_v}$ is the mean virtual potential temperature and $\theta_v{}'$ the fluctuating term of the virtual potential temperature together with the $\overline{w'\theta_v'}$ is the covariance wind velocity and virtual potential temperature. The steps from the ambient air temperature to the virtual potential temperature are explained in section 2.1.1.

The covariance of the virtual potential temperature and the wind velocity are related to the sensible heat (H), as shown in equation 2.30.

$$H = \rho C_P \overline{w'\theta_v'} \tag{2.5}$$

where ρ is the air density and C_P is the specific heat of air at constant pressure P.

However, there are three assumptions which restrict the similarity analysis. The occurrence of the following assumptions is rare, but it is important to be taken into account. These assumptions are:

- Steady state: Mean values of parameters do not change in time.
- Homogeneity (horizontal direction): There is no variation in the horizontal direction.
- Homogeneity of the momentum and heat fluxes (vertical direction): There is no variation of the momentum and heat fluxes in the vertical direction.
  Therefore the theory is only generally applicable to the Surface Boundary Layer.

Based on the assumptions of MOST, the non-dimensional wind velocity gradient can be written as:

$$\frac{\kappa z}{u_*}\left(\frac{\partial U}{\partial z}\right) = \phi_m\left(\frac{z}{L}\right) \tag{2.6}$$

where ϕ_m is the relationship between the dimensionless gradient and stability parameter $\frac{z}{L}$ and U is the mean wind speed at height z. Similar equations can be derived for the non-dimensional temperature and moisture gradients (equation 2.7).

$$\frac{\kappa z}{\theta_*}\left(\frac{\partial \theta_v}{\partial z}\right) = \phi_h\left(\frac{z}{L}\right), \qquad \frac{\kappa z}{q_*}\left(\frac{\partial q}{\partial z}\right) = \phi_e\left(\frac{z}{L}\right) \tag{2.7}$$

where θ_v is the virtual potential temperature, q_* the moisture scale. The following relationships between the dimensionless gradients and stability parameter $\zeta = \frac{z}{L}$ can be described by the Bussinger-Dyer flux relationships [10]. The Bussinger-Dyer functions are derived from the Kansas experiment where few very stable and very unstable data was available. This resulted in a reasonable approximation of neutral stabilities, which can be found in table 2.1. For very stable and very unstable conditions, an updated version can be found in literature [5].

Table 2.1: Relationships between the dimensionless gradients and stability parameter $\frac{z}{L}$ for unstable and stable conditions

Unstable	$(\frac{z}{L} < 0)$	Momentum (ϕ_m)	$\phi_m = (1 - 16\frac{z}{L})^{1/4}$	(2.8)
		Heat (ϕ_h)	$\phi_h = (1 - 16\frac{z}{L})^{1/2}$	(2.9)
		Moisture (ϕ_e)	$\phi_e = (1 - 16\frac{z}{L})^{1/2}$	(2.10)
Stable	$(\frac{z}{L} > 0)$	Momentum (ϕ_m)	$\phi_m = (1 - 5\frac{z}{L})$	(2.11)
		Heat (ϕ_h)	$\phi_h = (1 - 5\frac{z}{L})$	(2.12)
		Moisture (ϕ_e)	$\phi_e = (1 - 5\frac{z}{L})$	(2.13)

2.3 Description of wind, temperature and moisture profiles

As stated in the problem description of this project, in the IEC classification the wind, temperature and moisture profiles are described without taking the atmospheric stability into account. The description of the wind profile without taking atmospheric stability into account is called the logarithmic law (equation 2.14).

$$U = \frac{u_*}{k} ln(\frac{z}{z_0}) \tag{2.14}$$

The temperature and moisture profiles can also defined.

$$\theta_{2v} = \theta_{1v} + \frac{\theta_{*v}}{k} ln(\frac{z}{z_t}), \qquad q_2 = q_1 + \frac{q_*}{k} ln(\frac{z}{z_q}) \tag{2.15}$$

where the subscripts $1,2$ denote different locations on the profile for respectively θ_v the virtual potential temperature and q the moisture. As described in literature [47], the effect of atmospheric stability on the three profiles is important and is described in the following equations:

$$U = \frac{u_*}{\kappa} [ln(\frac{z}{z_0}) - \psi_M(\frac{z}{L})] \tag{2.16}$$

$$\theta_{2v} = \theta_{1v} + \frac{\theta_{*v}}{\kappa} [ln(\frac{z}{z_t}) - \psi_H(\frac{z}{L})] \tag{2.17}$$

$$q_2 = q_1 + \frac{q_*}{\kappa} [ln(\frac{z}{z_q}) - \psi_Q(\frac{z}{L})] \tag{2.18}$$

where ψ_M, ψ_H and ψ_Q are the functions for respectively momentum, heat and moisture. The ψ_M and ψ_H functions are derived from equation 2.8-2.13 via integration.

Table 2.2: ψ functions for unstable and stable conditions

ψ_M	Unstable ($\frac{z}{L} < 0$)	$\psi_M = 2ln(\frac{1+x}{2}) + ln(\frac{1+x^2}{2}) - 2tan^{-1}(x) + \frac{\pi}{2}$	(2.19),
		where $x = \frac{1}{\phi_m}$	
	Stable ($0 < \frac{z}{L} < 0.5$)	$\psi_M = -\alpha(\frac{z}{L}$	(2.20), where $\alpha = 5$
	Stable ($\frac{z}{L} > 0.5$)	$\psi_M = -a(\frac{z}{L}) + b(\frac{z}{L} - \frac{c}{d})e^{(-d\frac{z}{L})} + \frac{bc}{d}$	(2.21),
		where $a = 1$, $b = 0.667$, $c = 5$ and $d = 0.35$	
ψ_H	Unstable ($\frac{z}{L} < 0$)	$\psi_H = 2ln(\frac{1+y}{2})$	(2.22), where $y = \frac{1}{\phi_h}$
3	Stable ($\frac{z}{L} > 0$)	$\psi_H = \psi_M$	(2.23)

2.4 Derivation of the Monin-Obukhov length

In this section, the derivation of the Monin-Obukhov length (L) will be explained using five different methodologies. Starting in paragraph 2.4.1 with the Eddy Covariance Method, which will be used as a reference. After which the Profile Method and Richardson Number methodologies with each two variants will be explained in respectively paragraphs 2.4.2 and 2.4.3.

2.4.1 Eddy Covariance Method

Airflow can be seen as horizontal flow of multiple eddies. At the level of single air particle, one eddy moves an air particle up-/ downwards with speed w, with a certain gas concentration c, temperature and humidity. A schematic overview of the Eddy Flux can be seen in figure 2.4.

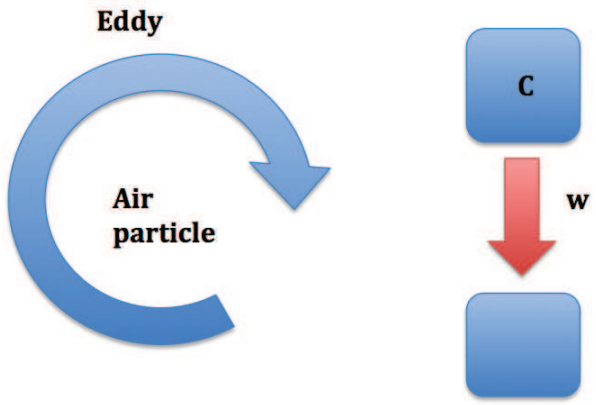

Figure 2.4: Schematic overview of Eddy Flux

The momentum, temperature and moisture flux can be determined by measuring the movement of particles and their characteristics. From these measured characteristics, the change of the temperature and moisture can be determined. Together with the movement of the particles, the netto flux can be determined as the sum of upward and downward stream of particles.

Scientifically flux can be explained by how many particles move through a unit area per unit time. Therefore the flux depends on three parameters:

- Number of particles crossing the area with their characteristics (gas concentration, speed, temperature and humidity)
- Size of the area (boundary conditions)
- The time that particles crossed the area

The general principle is explained and can be used for the Eddy Covariance Method to calculate the Monin-Obukhov length by measuring the parameters according to table 2.3.

Table 2.3: Required parameters for the Eddy Covariance Method

Parameter	**Measurement frequency**
u horizontal wind speed [m/s] v horizontal wind speed perpendicular to u [m/s] w vertical wind speed [m/s] T absolute temperature [$^{\circ}C$]	High frequent $(10-20Hz)$
RH relative humidity [%] P pressure [Pa]	Low frequent ($\frac{1}{600}Hz$)

Momentum and temperature flux is calculated as a covariance of fluctuations of vertical wind speed and fluctuations in the other measured characteristics.

Measurements of the wind speed in different directions and temperature are used in the Eddy Covariance Method to finally derive the Monin-Obukhov length (L). The wind speed and temperature are measured using a high frequency sonic anemometer. The high frequentcy measurements are used to determine the fluctuations in time of the temperature and wind speed in the vertical and the horizontal direction by coupling the fluctuations of the temperature and the horizontal wind speed with the vertical wind speed measurements. The turbulent fluxes of momentum ($w'u'$ and $w'v'$) and heat flux ($w'\theta'_v$) are therefore determined. Using the covariance of the fluctuations of the horizontal wind speed with respect to the vertical wind speed the friction velocity is computed, following [45]:

$$u_* = \sqrt[4]{\overline{w'u'}^2 + \overline{w'v'}^2} \tag{2.24}$$

By rotating the coordinate system in the direction of the surface stress ($w'v' = 0$), a simpler versionof equation 2.24 can be derived for u_*.

$$u_* = \sqrt{-\overline{w'u'}} \tag{2.25}$$

From the determined friction velocity (u_*) and heat flux $w'\theta'_v$ the Monin-Obukhov length can be determined using equation 2.4.

It has to be taken into account that the measurement frequency determines the perceptibility of turbulent flux carrying eddies [42][38]. The smallest eddies are determined with the highest frequency and largest eddies with the lowest measurement frequency. The measurement response time and separation distances between the sonic anemometers limit perceptibility of the turbulent flux carrying eddies. In order to determine the fluxes, an averaging period is selected (between 10 and 60 minutes). The length of the averaging period is a compromise between perception of the eddies with the highest contribution of momentum, heat flux and the requirement of stationary conditions.

2.4.2 Profile Method

The profile method is one of the methodologies to determine the parameter L, by determining the heat and momentum surface fluxes. Two variations of the profile method will be used in this research, with each slightly varying the input parameters. Depending on what data is available, one of these variations can be used [24][41][45] The profile method assumes a logarithmic wind profile with an adiabatic correction and iteratively estimates the fluxes to determine the atmospheric stability.

- Variant 1 - Two wind speeds and air temperatures are available at heights z_1, z_2.
- Variant 2 - A single wind speed at height z, air temperature at height z, surface temperature and surface roughness length z_o are available.

Variant 1 - Profile method difference in wind speed and temperature

For the Profile Method, two parameters have to be approximated: the friction velocity u_* and the temperature scale θ_*. The friction velocity u_* is given by:

$$u_* = \frac{k(U_2 - U_1)}{ln(\frac{z2}{z_1}) - \psi_M(\frac{z_2}{L}) + \psi_M(\frac{z_1}{L})} \tag{2.26}$$

where ψ_M is the momentum function, calculated using table 2.2.

The temperature scale θ_* can be approximated as followed:

$$\theta_* = \frac{k\delta\theta_v}{ln(\frac{z_2}{z_1}) - \psi_H(\frac{z_2}{L}) + \psi_H(\frac{z_1}{L}))} \tag{2.27}$$

where the ψ_H is the heat function, computed using table 2.2.

Using both equations, a first estimation of the friction velocity u_* and temperature flux θ_* can be calculated, with $L = \infty$ resulting to $\psi_H = \psi_M = 0$. Using this together with equation for the sensible heat flux equation 2.28, equation 2.30 and equation 2.4 the Monin-Obukhov length can be calculated.

$$H = -\rho C_p u_* \theta_* \tag{2.28}$$

$$-\overline{w'\theta'_v} = u_*\theta_* \tag{2.29}$$

$$\overline{w'\theta'_v} = \frac{H}{\rho C_p} \tag{2.30}$$

The first estimation of the Monin-Obukhov length can be used to get improved estimates of the u_* and θ_*. Therefore it can be used to recalculate the Monin-Obukhov length. This iterative process has to be repeated until the Monin-Obukhov length converges to a value assuming 5% the convergence tolerance.

Variant 2 - Profile method surface temperature

The second variant of the Profile Method is very similar to the first one. The second variant only uses one air temperature measurement. The other temperature measurement is the surface temperature. The following equations can be used to determine the friction velocity (equation 2.31) and temperature scale (equation 2.32).

$$u_* = \frac{k(U_z)}{ln(\frac{z}{z_0}) - \psi_M(\frac{z}{L})} \tag{2.31}$$

$$\theta_* = \frac{k\delta\theta}{ln(\frac{z}{z_0}) - \psi_H(\frac{z}{L}))} \tag{2.32}$$

In the same manner as the first variant of the Profile Method the Monin-Obukhov length can be determined iteratively.

For this methodology it has to be taken into account that the surface temperature is not always available. Due to height differences of the water level, measuring the surface water temperature is difficult for offshore locations, therefore usually the water temperature is measured at a depth of around 2 meter or deeper. Due to the cool skin effect the measured temperature is on average slightly higher than the surface water temperature [17]. Leading to a small over-prediction of the temperature difference $\overline{\Delta\theta_v}$ and the measured air temperature, which consequently leads to over-prediction of the stability parameter $\frac{z}{L} = \zeta$. This results in an under-prediction of the Monin-Obukhov length (L) for stable and over-prediction for unstable conditions.

Both variations of the Profile Method are now explained. The next section will focus on the Richardson Number.

2.4.3 Richardson Number

The Richardson Number (Ri) is named after Lewis Richardson (1881 - 1953). It is a dimensionless number that expresses the ratio of potential to kinetic energy.

$$Ri = \frac{potential \quad energy}{kinetic \quad energy} = \frac{gh}{u^2}$$

where g is the acceleration of gravity, h is the representative vertical length scale and u is velocity scale. However, in the wind energy, the flux Richardson number is used, which represents the ratio of buoyant production of turbulence over the shear term in the TKE equation.

Variant 1 - Gradient Richardson Number

The Gradient Richardson Number (Ri_g) method can be used to determine the Monin-Obukhov length (L) from the measurements of wind speed in horizontal direction and temperature at two heights. By using the buoyant production and shear term of the TKE equation (2.33) , assuming horizontal homogeneity results in the follow equation of the flux Richardson Number (derived from [53]).

$$Ri_f = \frac{\frac{g}{\overline{\theta_v}}\overline{w'\theta'}}{\overline{w'u'}\frac{\delta U}{\delta z}} \tag{2.33}$$

Assuming that the correlation is proportional to their vertical gradients, results to the following relation for the Gradient Richardson number. More detailed information of the derivation can be found in appendix F.1 and [36][45][39].

$$Ri_g = \frac{g\overline{\Delta\theta_v}\Delta z}{\overline{\theta_v}(\Delta\overline{U})^2} \tag{2.34}$$

where Ri_g can be used to derive the Monin-Obukhov length (L) using:

$$\zeta = Ri_{g|Ri_g<0} \quad with \quad \zeta = \frac{z}{L} \tag{2.35}$$

$$\zeta = \left(\frac{Ri_g}{1-5Ri_g}\right)_{|0<Ri_g<0.2} \tag{2.36}$$

Variant 2 - Bulk Richardson Number

The second variant of the Richardson Number is the Bulk Richardson Number (Ri_b), which is similar to the Gradient Richardson Number. Both use two temperature measurements at different heights, however for the Bulk Richardson Number one of these measurement is the surface temperature in contrast with the gradient method where two air temperature measurements are used. This results in the following equation for the Ri_b.

$$Ri_b = \frac{g\overline{\Delta\theta_v}z}{\overline{\theta_v}(\Delta\overline{U})^2} \tag{2.37}$$

Resulting in the following stability parameter ζ.

$$\zeta = 10Ri_{b|Ri_b<0} \tag{2.38}$$

$$\zeta = (\frac{10Ri_b}{1-5Ri_b})_{|0<Ri_b<0.2} \tag{2.39}$$

2.4.4 Summary Methods based on MOST

Section 2.4 can be summarized into the following figure. The required parameters for each method are indicated in figure 2.5 with the corresponding height.

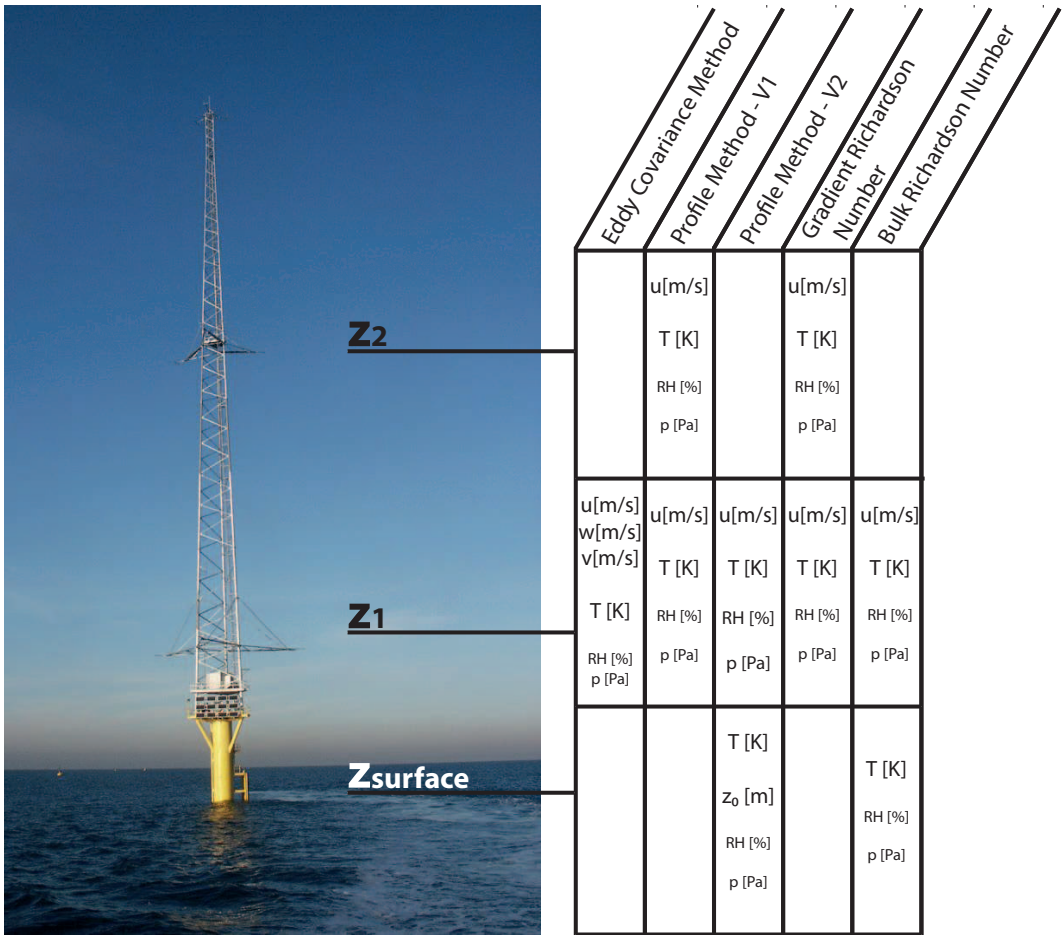

Figure 2.5: Graphical representation of required measured variables for the determination of the Monin-Obukhov length using different methodologies, with the photograph of the OWEZ met mast [34].

2.5 Additional classification systems

This report will mainly focus on the atmospheric stability estimation methodologies using the Monin-Obukhov Similarity Theory. These methodologies use meteorological data from met masts. However, it is important to note that this data is not always available. In order to estimate the atmospheric stability, multiple other methodologies can be used. In this section two methodologies will be explained, using various inputs to estimate the atmospheric stability:

- Pasquill-Gifford Method
- Eddy Covariance Method using data obtained from a Large-Eddy Simulation model.

More detailed information is given in the following paragraphs.

2.5.1 Pasquill-Gifford Method

The Pasquill-Gifford Method uses basics meteorological data. Unlike MOST, the Pasquill-Gifford Method does not use the Monin-Ubukhov length but instead uses seven categories for the atmospheric stability. These categories can be found in table 2.4. For the classification of the atmospheric stability using the Pasquill-Gifford Method the following parameters are required.

- Horizontal wind speed at a height of 10 meters [m/s]
- Cloud coverage
- Ceiling heights of clouds
- Time of the observation, daytime and nighttime

These parameters can be used to classify the atmospheric conditions according to table 2.4. As can be seen in the table, the daytime insolation is divided into four categories. The distribution in those categories takes place using the daytime insolation, which will be explained in more detail in next paragraph.

Daytime insolation

During the day, the temperature of the earth surface greatly influences the stability. The surface temperature depends on the solar radiation and cloud coverage. An estimation of the solar radiation can be given in two ways. First by measuring the solar radiation directly or secondly by calculating the solar elevation angle. In this sub-paragraph the estimation of the solar radiation will be explained using the solar elevation angle, more detailed information can be found in [29]. The solar elevation angle is the angle between the horizon and the centre of the Sun. This angle fluctuates during the day between different seasons and locations. In figure 2.6, the variations of the solar elevation angle and therefore the declination angle are indicated due to the seasonal and location variations. The solar elevation angle $(\alpha_s) = 90^\circ -$ solar zenith angle (θ_s) as shown in figure 2.6.

	Daytime insolation				Night-time conditions**	
Surface wind speed (m/s)	Strong	Moderate	Slight	Overcast	Thin overcast or > 4/8 low cloud	<= 4/8 cloudiness
< 2	A	A - B	B	C	E	F or G*
2 - 3	A - B	B	C	C	E	F
2 - 5	B	B - C	C	C	D	E
5 - 6	C	C - D	D	D	D	D
> 6	C	D	D	D	D	D

Table 2.4: Atmospheric stability defined by Pasquill-Gifford stability classes with A - Extremely unstable, B - Moderately unstable, C - Slightly unstable, D - Neutral, E - Slightly stable, F - Moderately stable and G - Extremely stable.
* Modification of the Pasquill-Gifford method, during nighttime the atmosphere could be categorised with G, with wind speeds below 0.5 m/s
** Night is the period from 1 hour before sunset to 1 hour after sunrise.[35]

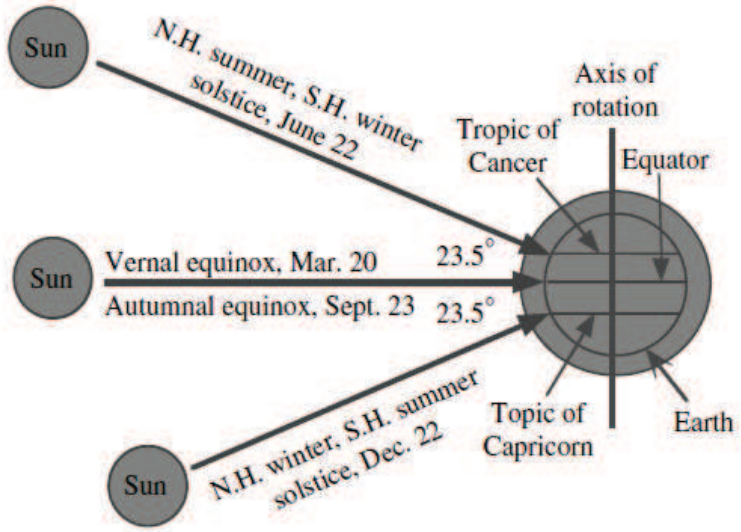

Figure 2.6: Seasonal variations of the solar zenith angle. Solstice is when the Sun reaches the highest or lowest excursion relative to the equator. Equinox is when the equators plane passes the centre of the Sun.[29].

In this paragraph, a short description of the calculation of the solar elevation angle will be provided. This will be used to determine atmospheric stability with the Pasquill-Gifford method according to the solar insolation. In table 2.5 a summary of the descriptions of the relevant angles in the solar system is presented.

As explained on the previous page, the solar elevation angle can be used to categorize the atmospheric stability according to the Pasquill-Gifford Method. First, the calculation of the solar elevation angle will be explained, after which the various parameters required for the calculation are discussed. The solar elevation angle can be calculated using equation 2.41 [29].

$$sin\alpha_s = sin\phi sin\delta + cos\phi cos\delta cosH_a \tag{2.40}$$

where α_s is the solar elevation angle, ϕ is the latitude, δ is the solar declination angle and H_a the

Angle		Description
Solar elevation angle	α_s	The angle between the horizon and the centre of the Sun.
Solar declination angle	δ	The angle between the Equator and the north or south latitude of the subsolar point, which is the point at which the Sun is directly overhead.
Solar Zenith angle	(θ_s)	The angle measured from directly overhead to the geometric centre of the sun's disc.
Local hour angle	H_a	The angle, between the longitude of the point at which the sun is directly overhead and the longitude of the research location.
Obliquity of the ecliptic	ε_{ob}	The angle between objects rotational axis and its orbital axis.

Table 2.5: Summary of angles in solar system

local hour angle of the sun. These can be found in figure 2.7.

The solar elevation angle can be divided into three insolation categories using table 2.6.

Sky Cover	Solar elevation angle		
	$\alpha_s > 60°$	$35 < \alpha_s < 60°$	$15 < \alpha_s < 35°$
Sky cover $\leq 4/8$ or High Thin Clouds *	Strong	Moderate	Slight
$4/8 <$ Sky cover $< 7/8$ or Middle High Clouds **	Moderate	Slight	Slight
$5/8 <$ Sky cover $< 7/8$ or Low Clouds ***	Slight	Slight	Slight

Table 2.6: Insolation as a function of solar elevation [1]
* High Thin Clouds > 4800 meters
** Middle High Clouds $2000 - 4800$ meters
*** Low Clouds < 2000 meters

Prior to the determination of the insolation, the solar declination angle and local hour angle have to be calculated.

The solar declination angle is:

$$\delta = sin^{-1}(sin\varepsilon_{ob} sin\lambda_{ec}) \quad [29] \tag{2.41}$$

where ε_{ob} is the obliquity of the ecliptic, which is the angle between the rotational axis of a object and its orbital axis also called axial tilt, and λ_{ec} is the ecliptic longitude of the sun.

The axial tilt or obliquity of the ecliptic can be approximated with the following equation:

$$\varepsilon_{ob} = 23.439 - 0.0000004 * N_{JD} \quad [29] \tag{2.42}$$

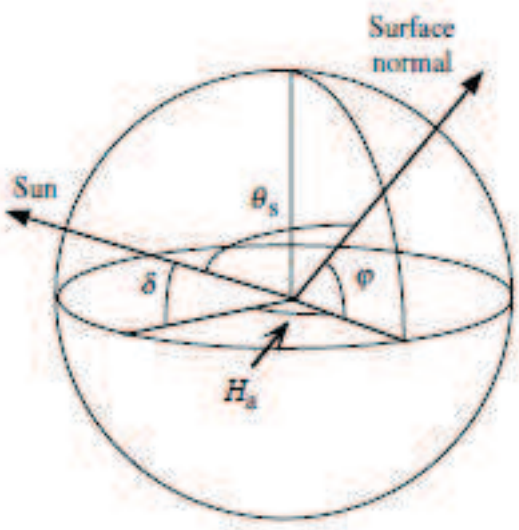

Figure 2.7: Geometry for a different solar zenith angle, with solar zenith angle (θ_s), solar declination angle (δ),solar azimuth angle (ϕ) and hour angles (H_a).[29]

where N_{JD} is the number of days from the start of the Julian year in 2000.

$$N_{JD} = 364.5 + (Y - 2001) * 365 + D_L + D_J \quad [29] \tag{2.43}$$

Y>2000	$D_L = (Y - 2001)/4$
Y<2001	$D_L = (Y - 2001)/4 - 1$

Table 2.7: Julian day of the year [29]

where Y= the current year, D_L is the number of days skipped because of the leap years since or before 2000 and D_J is he Julian day of the year.

The ecliptic longitude of the Sun can also be approximated, with the following equation:

$$\lambda_{ec} = L_M + 1.915 sing_M + 0.020 sin2g_M \quad [29] \tag{2.44}$$

where mean longitude of the Sun $L_M = 280.460 + 0.9856474 N_{JD}$ and the mean anomaly of the Sun $g_M = 357.528 + 0.9856003 N_{JD}$. The mean anomaly is the angular distance, from the point in the Earth's orbit where the Earth is closest to te Sun.

Lastly the local hour angle has to be approximated for the elevation height of the Sun. The highest point of the Sun during the day is already determined on variation of the location and season. The daily variation of the elevation angle has to be taken into account from sunrise to sunset, which can be done with the local hour angle (H_a) in degrees, as defined below:

$$H_a = \frac{360 t_s}{86400} \quad [29] \tag{2.45}$$

where t_s is the number of seconds past noon.

Using the following equations 2.41, 2.42, 2.43, 2.44 and 2.45, together with equation 2.40 the solar elevation angle can be calculated.

From the solar elevation angle and table 2.6, the solar insolation can be divided into four categories. Weak, slight, moderate and strong which together with the time of the day, cloud coverage and ceiling height can be used to give an estimation of the atmospheric stability according to table 2.4.

2.5.2 Large-Eddy Simulation

In the 1960's the modelling of the atmospheric boundary layer with a Large-Eddy Simulations (LES) started by Lilly in 1967 and was continued by Deardorff in 1972. After 1986, comparison studies of the LES model with observation data were conducted.

The Dutch Atmospheric Large-Eddy Simulation is a simulation method designed to study the physics of the atmospheric boundary layer. In combination with meteorological observations, LES can be used to parametrize boundary layer models, by resolving the turbulent scales with a size larger than a certain width and parametrize the smaller scales which contain less energy. The size or width of the scales corresponds to the grid size of the model, varying from 1 meter to 50 meters. A width of around 1 meter represents stable layers and 50 meters cloud-topped atmospheric boundary layer.

The LES model describes the atmospheric boundary layer using the conservation equations of momentum, heat and moisture. In order to determine the atmospheric stability, the description of the atmospheric boundary layer together with equation 2.4 can be used. Later, in this thesis a comparison between the atmospheric stability determined with the LES model and sonic measurements will be executed (section 4.7.2). The measurement data of Cabauw from January 1 to December 31, 2012 will be compared to the LES model using the weather model of the Royal Dutch Meteorological Institute (KNMI) with the pressure gradient, initial conditions and lateral forcing as input.

Using weather models as input for the LES model, the atmospheric stability can be determined using a LES model without on site measurement campaigns. However, it has to be taken into account that the LES model is very computational expensive. The simulation was executed on a single GPU of the Curie supercomputer, owned by GENCI.

In this chapter only a brief overview of the LES model is shown, more can be found in [22][30].

Chapter 3

Atmospheric stability analysis - Literature

In this chapter, multiple studies from literature are discussed focusing on the different methodologies to estimate the atmospheric stability. The comparison of atmospheric stability methodologies is divided into four sections. Each section corresponds to different geographic locations presented in the following four papers.

- Rødsand [36]
- Horns Rev [43]
- OWEZ [45]
- FINO1 [11]

3.1 Atmospheric stability corrections at Rødsand

At Rødsand in the Danish Baltic Sea, south of the island Lolland in Denmark, an offshore met mast is located with a height of 50 meters. It has been established in 1996 as part of a Danish study to determine the wind climate for proposed offshore wind farms.

The research of [36] can be divided into two main parts. The first part consists of a comparison of predicted and measured wind speed and power production using atmospheric stability corrections from different methods. The second part investigates different roughness models for offshore conditions.

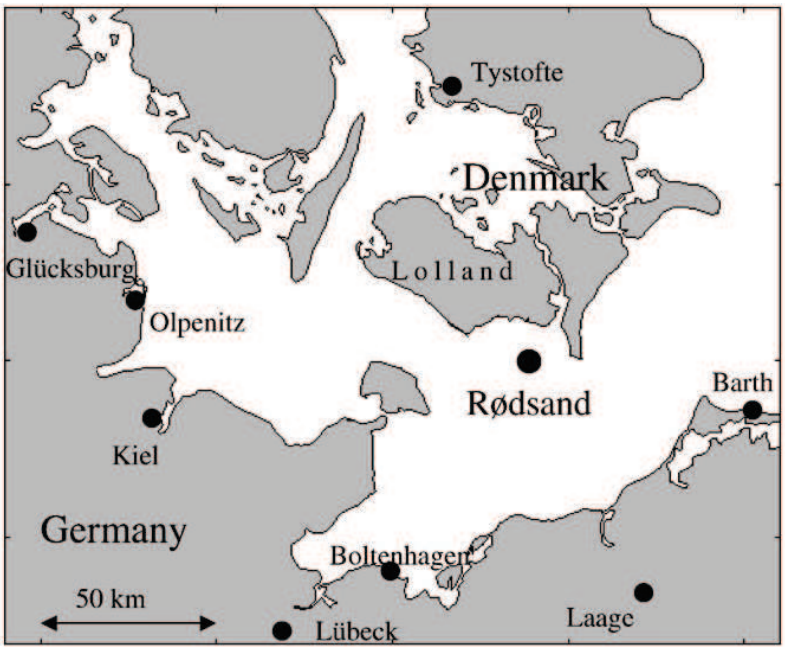

Figure 3.1: Map of Danish Baltic Sea with the location of the offshore met mast Rødsand [36]

3.1.1 Wind speed and power predictions based on the atmospheric stability corrections

In this study, [36] the impact of three methods was investigated in order to estimate the atmospheric stability to extrapolate the wind speed measurements on the predicted power production of the wind turbine. The wind speed measurements at a height of 10 meters are extrapolated using the logarithmic profile with stability corrections to estimate the wind speed at 50 meters. The wind profile with atmospheric stability corrections is described in section 2.3. The predicted wind speed is compared to the measured wind speed. The predicted power output uses computation the predicted wind speed with the P-V curve.

The following methods to estimate the atmospheric stability are investigated by Lange et al.

- Eddy Covariance Method based on high frequent sonic measurements
- Gradient Richardson Number
- Bulk Richardson Number

A direct comparison of the Bulk and Gradient Richardson Methods with the Eddy Covariance Method is executed using high frequency sonic measurements. In figure 3.2, it can be observed that the Bulk Richardson Number and the sonic measurements give very similar results in terms of the predicted wind profile. The predicted wind speed is within 5% of the measured wind speed. The error of the predicted power output varies between 4-6% for both the sonic and Bulk Richardson Number. The deviations in predicted power output between these two methods is only 1% as shown in figure 3.3.
Lange et al. also observed that often the bulk water temperature is used instead of the sea surface

temperature, because the last mentioned temperature is often not available. This will result into a small of overprediction of the stability parameter (z/L) on the stable side. This corresponds to the expectations in section 2.4.
From figure 3.2, a large underprediction of the wind speed can be observed for the Gradient Richardson Number. Especially for stable conditions, the error increases up to 20%. For stable conditions the Gradient Richardson Number, results in an underprediction of the power output with an error of around 8%.

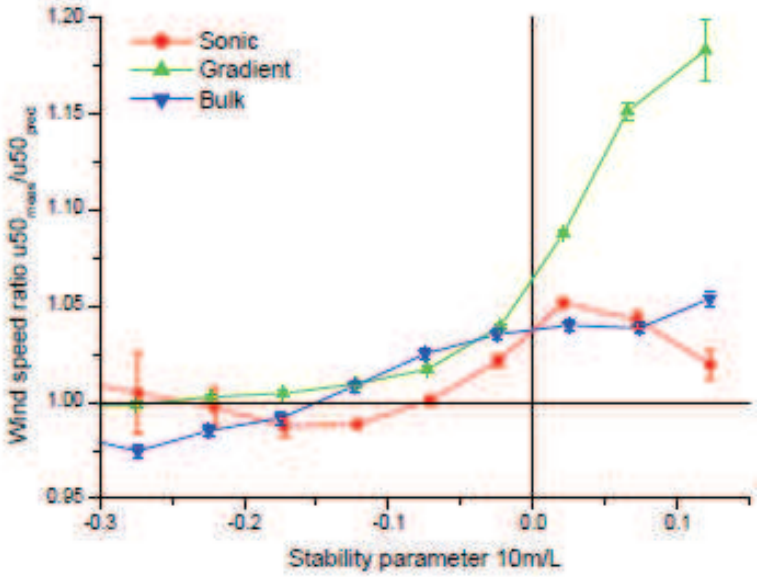

Figure 3.2: Comparison of Atmospheric Stability methods at Rødsand with on the y-axis the ratio measured/predicted wind speed and the stability parameter (z/L) on the x-axis [36].

3.1.2 Roughness modelling for offshore conditions

The main focus of this thesis is on the atmospheric stability, therefore the roughness modelling discussed in the paper of Lange et al. will not be discussed in details. Nonetheless, in this section the results will be discussed briefly.

MOST has been found to be generally applicable over the open sea, as explained in [15]. However, in coastal areas, wind blowing from land to sea is strongly influenced by roughness and heat transfer changes. This will result in strong inhomogeneity of the flow for distances up to 100-200 kilometers from the coast [18][32].

In addition to employing multiple methods to estimate the atmospheric stability, the impact of different roughness estimations is also investigated. The sea roughness depends on the wind speed, fetch and wave age. The following methods to model roughness are compared: constant roughness, Charnock relation, wave age and finally a fetch depended model. In figure 3.3 it can be observed that the Charnock relation, assuming that roughness only depends on wind speed, shows the smallest deviation compared to the real wind profile. The error of wind profile using the Monin-Obukhov length, caused by the change from land to open sea, can be decreased by a simple correction model of the inversion layer height.

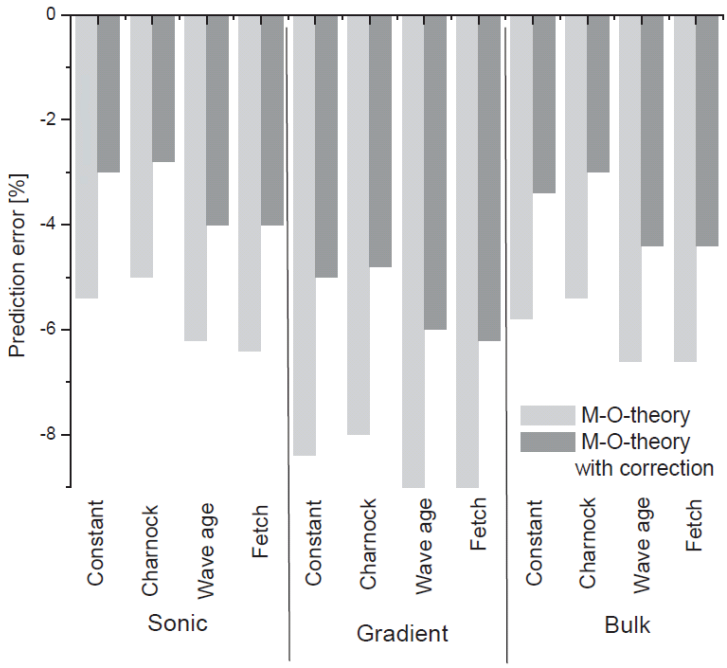

Figure 3.3: Error in power output prediction ($P_{measured} - P_{predicted}/P_{measured}$) of an example turbine for the data set; different methods to extrapolate the wind speed measurement at 10 meters height to 50 meters are used [36].

3.2 Atmospheric stability and turbulence fluxes at Horns Rev

A comparison of sonic, Bulk Richardson Number and Weather Research and Forecasting (WRF) model is conducted to estimate the atmospheric stability at Horns Rev by Peña and Hahmann[43] The Horns Rev met mast M2 was located in the North Sea near the Danish West Coast. The met mast was installed to investigate the wind climate for the Horns Rev offshore wind farm and was finally removed in 2007.

The met mast M2 contained the following measurement instruments:

- Two anemometers at 15 meters above mean sea level (AMSL)
- Sonic anemometer at 50 meters AMSL
- Wind vane at 28 meters AMSL
- Two temperature sensors at 4 meters below mean sea level (BMSL) and at 13 meters AMSL

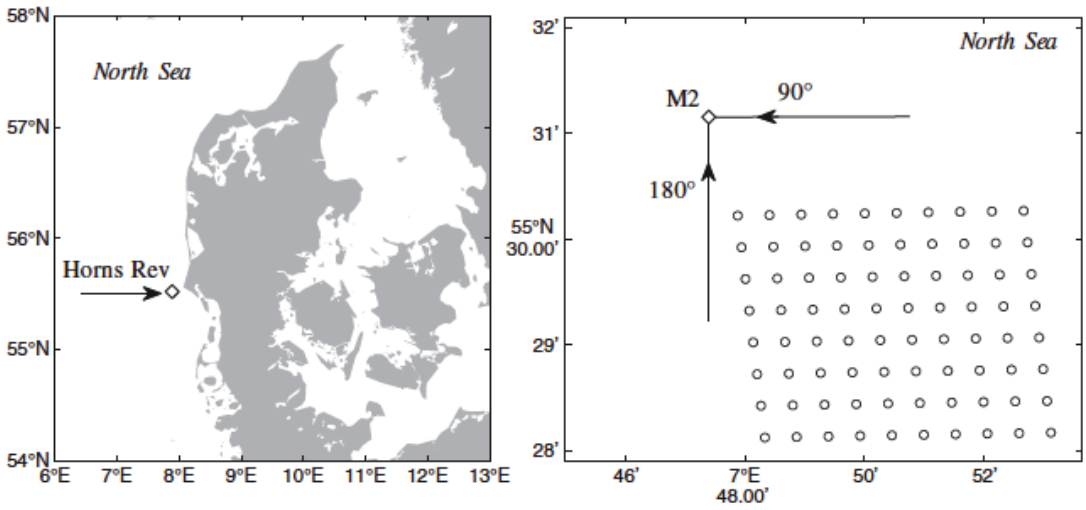

Figure 3.4: On the left the location of the Horns Rev met mast and wind farm in the Danish North Sea and on the right the layout of the wind farm [43]

Comparing the temperature at 4 meters BMSL to a satellite SST product showed that the surface temperature at Horns Rev can be assumed to be equal to the temperature measurement BMSL. The momentum and heat flux are determined from sonic measurements with a frequency of 12Hz and an averaging period of 10 minutes.

The above mentioned measurements are used to determined the atmospheric stability with three methods:

- Eddy Covariance Method based on high frequent sonic measurements
- Bulk Richardson Method
- Weather Research and Forecasting (WRF) model: Meso-scale numerical weather prediction system for both atmospheric research and operational forecasting needs.

3.2.1 Comparison of Sonic and Bulk estimations

From the direct comparison of the sonic measurements with the bulk estimation, Peña and Hahmann made a couple of observations summarized below.

The biggest uncertainty in the atmospheric stability estimation is assumed to be due to the temperature difference of measurements. This translates into an uncertainty of the heat flux estimation. The same was found by Sathe [48], where the uncertainty contribution of the temperature measurements for the Bulk Richardson Method was four orders of magnitude larger than that of the wind speed measurements for near-neutral conditions.

They also found that the error of the Monin-Obukhov length from the bulk estimation was smaller for unstable conditions than for stable conditions. This might be due the fact that measurements used in the bulk estimations are within the Surface Boundary Layer, compared to the sonic measurements, with a height of 50 meter, which could exceed the Surface Boundary Layer under stable conditions. It is worth to revisit the fact that MOST is only applicable within the Surface Boundary Layer, which could possible explain the differences.

The Bulk Richardson Number and the sonic measurements presented a high correlation of $R = 0.80$ for $1/L$, in the limited range of $-0.02m^{-1} \leq 1/L \leq 0.02m^{-1}$, excluding the very stable and very unstable conditions. The validity of this limited range is questionable, in multiple papers described above the biggest error occurred under extreme conditions, which lies outside of this limited range. Thus excluding of the extreme conditions results, in a correlation of $R = 0.80$ that does not represent whole dataset. Overall the Bulk Richardson Method estimates $\frac{1}{L_b}$ to be generally lower than the sonic estimate $\frac{1}{L_s}$. This can be explained by equation 2.4, where the u_* near the surface is nearly the same as the u_* at 50 meter height. The gradient of $\overline{w'\theta'_v}$ is larger, due to the decrease of heat flux with height [21]. This results in a small increase of L with height in the Surface Boundary Layer, thus decreasing $\frac{1}{L}$.

3.2.2 Comparison of Sonic and Weather Research and Forecasting estimations

The comparison of the sonic and WRF model showed similar results for the heat flux estimation. However, large scatter was found for the stable and unstable conditions, resulting in an correlation of only R=0.70 and slope of 1.12 for $1/L$. This can be explained by the large uncertainty of the output of the WRF model.
The heat flux estimation of the WRF model is also higher than the heat flux determined with the sonic measurements. This is expected because the heat flux decreases with height in the Surface Boundary Layer [21].

3.2.3 Conclusions based on the research of Peña and Hahmann at Horns Rev

The sonic fluxes estimated at 50 meter are not always representative of the Surface Boundary Layer, based on the analysis of Peña and Hahmann at the Horns Rev met mast M2. For higher wind speeds, the sonic friction velocity, u_{*s}, tends to be higher than u_{*b} and the WRF output u_{*WRF}. Due to the height of the measurements of the sonic and bulk measurements, a slight increase of u_* with height was found in the Surface Boundary Layer at Horns Rev.

The thickness of the Surface Boundary Layer under neutral conditions can be estimated to be 10% of height of the boundary layer (z_i) where $z_i = c_i * \frac{u_*}{f_c}$. Using this as a filter to determine when the thickness of the Surface Boundary Layer is below the height of the sonic measurements and exclude these measurements from the data, results in a reduction of 80% of the stable data. This however results in only a small difference in the results. Most of the stable data is during low wind speed conditions and because the sonic and bulk estimations of the friction velocity are better under low wind speed conditions the effect is insignificant.

A trend can be observed regarding the friction velocity determined by different methods:

$$u_{*s} \geq u_{*b} \geq u_{*WRF}$$

This could have multiple reasons, such as inaccuracy of the roughness (z_0) estimation. Therefore the results also match the trend found at Høvsøre [21]. There the u_* increased with height up to 60 meter and then decreased following the profile shape of Zilitinkevich and Esua [60].

3.3 Atmospheric stability estimation at OWEZ

In 2006 a joint venture, called NoordZeeWind (NZW) of Shell Wind Energy and Nuon Sustainable Energy entered a Engineering Procurement Construction (EPC) contract to install a wind farm off the Dutch coast near Egmond aan Zee, with the name Offshore Windpark Egmond aan Zee (OWEZ). Approximately 18 kilometres from the coast, at a water depth of 20 meters and near the site of the OWEZ wind farm, a met mast was installed in 2003, as can been seen in figure 3.5 at the red dot, in order to determine the weather and wave conditions of the North Sea[34].

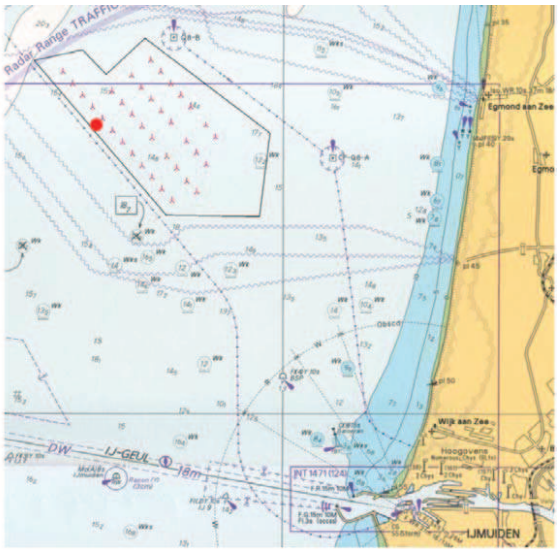

Figure 3.5: Map of the met mast and wind farm Egmond aan Zee with the met mast at the red dot[34]

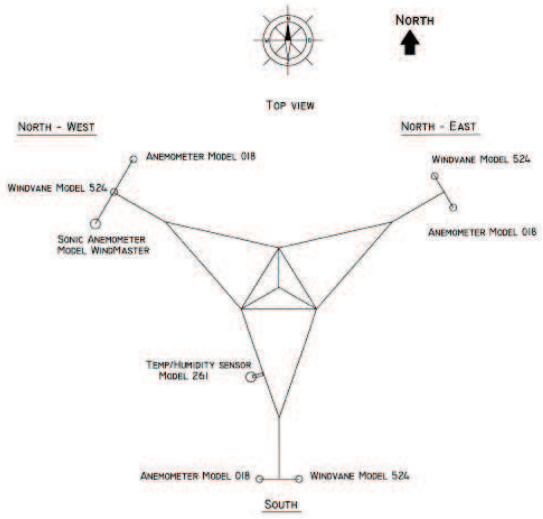

Figure 3.6: OWEZ met mast Layout [34]

In this research of Sathe et al. [45], an extensive comparison to estimate the atmospheric stability using OWEZ data is conducted. Four methodologies based on MOST are used namely: the Profile methods, Bulk and Gradient Richardson Number respectively. Unfortunately high frequent temperature measurements are not recorded at OWEZ and thus a direct comparison with the Eddy Covariance Method is not possible. Sathe et al. [45] used the data between July 2005 and April 2009 to conduct a comparison in four ways:

- The ratio between the measured and predicted wind speed against the stability parameter $\frac{z}{L}$.
- A comparison of different wind profiles: measured profile, log-law, power-law and wind profile based on MOST.
- Probability density function of L.
- Distribution of L per wind speed 4-25 m/s.

The above mentioned four ways of comparison will be used to conduct the comparison of the four methodologies. The results of Sathe et al. will be discussed separately in the next paragraphs.

3.3.1 Profile Method 1

The ratio between the measured and predicted wind speed corrected with the stability estimated with the Profile Method 1 shows huge scatter. For almost all values of the stability parameter $\frac{z}{L}$ the mean error is more than 10%. This results in an overall underprediction of the wind profile using the Profile Method 1.

3.3.2 Profile Method 2

For the Profile Method 2, the mean error of the ratio between the measured and predicted wind profile lies within 3% for unstable and very unstable conditions. However, the error increases significantly for near-neutral and stable conditions. This results in an underprediction of the wind profile for the near neutral and the stable conditions and a small overprediction for the unstable conditions.

3.3.3 Gradient Richardson Number

The ratio between the measured and predicted wind speed corrected with the stability estimated using the Gradient Richardson Number also shows huge scatter and with a large varying mean error for all conditions. For almost all values of the stability parameter zL^{-1} the mean error is more than 10%. This results in an overall underprediction of the wind profile using the Gradient Richardson Number.

3.3.4 Bulk Richardson Number

For the wind profile corrections using the Bulk Richardson Number the mean error of the ratio between the measured and predicted wind profile lies within 3% for unstable and very unstable conditions. For the near-neutral, stable and very stable conditions the mean error increases to 5%. Resulting in an underprediction of the wind profile for almost all values of the stability parameter.

3.3.5 Conclusions based on the research of Sathe at OWEZ

The research of Sathe showed, that each method gave significantly varying results. The results from the Profile Method 2 are in good agreement with that of the Bulk Richardson Number. The results of Profile Method 1 and the Gradient Richardson Number also match quite well. It is assumed that the Bulk Richardson Number is the most accurate method the wind profile, because the error of the wind speed ratio stays within 3% with the smallest scatter. For the prediction of the wind profile, two filters for the measured data are used which are of utmost importance of MOST, the stationary conditions and the estimated Surface Boundary Layer (SBL) height $z_s >$ measurement height. These filters, especially the SBL height, result in a large data reduction with an availability of only 6%. Without the SBL height filter the accuracy of predicted wind profile decreases significantly. However, that poses a question on validity. It seems that the Bulk Richardson Number performs the best but further investigation is required with extended wind profiles and direct comparison with sonic measurements to generalize the results and reach a final solid conclusion.

3.4 Atmospheric stability and fluxes estimation at the offshore mast FINO1

In 2003, FINO1, the first German offshore research platform was installed. It is part of the FINO programme, a research platform in the Baltic and North Sea with an extensive meteorological and biological measuring program. The FINO1 was installed in the North Sea, approximately 45 kilometers off the island of Borkum.

Deutsches Windenergie Institut (DEWI) is in charge of the technical measurements of the FINO1 platform and investigates the meteorological conditions in the Surface Boundary Layer. The measurements are obtained using multiple sensors, at different heights and facing different directions. At the South-East side of the platform, eight different levels ranging from 33.5 meters to 101.5 meters cup anemometers have been installed. At the North-West side of the platform, the wind vanes measure the wind direction at four levels (33.5, 50, 70 and 90 meters from sea level). In addition to the before mentioned measurements, high resolution ultra sonic anemometers are installed at three levels (40, 60 and 80 meters from sea level). More detailed information can be found in [14].

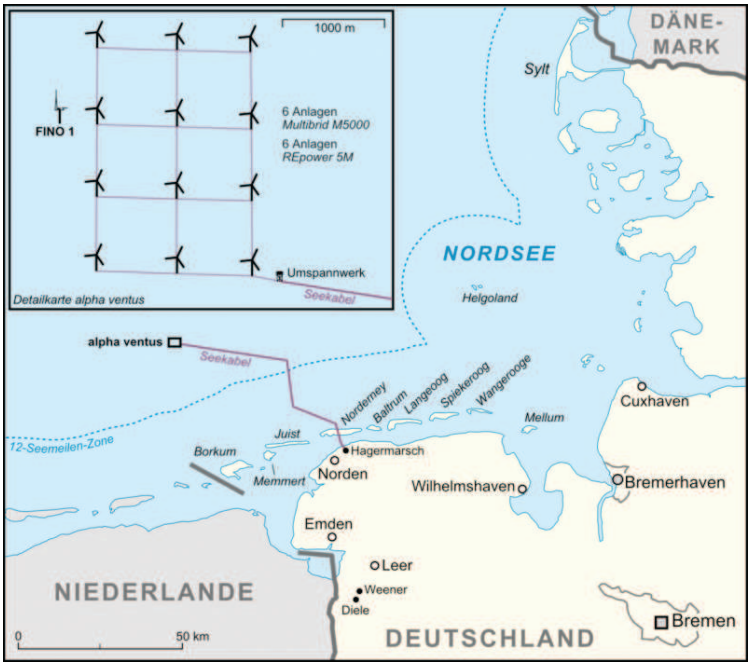

Figure 3.7: Map of with the FINO1 offshore research platform [14]

Figure 3.8: FINO1 - Offshore research platform [14]

In the research of Cañadillas et al.[11], the Eddy Covariance method is used to estimate the momentum and heat fluxes at the offshore met mast FINO1 for one year period (January 2010 - December 2010). In order to determine the fluxes, an averaging period is required, by minimizing the error distribution of the Ogive function. A averaging period of 30 minutes is selected, based on the Ogive function.

It has to be taken into account, that there were no high frequency humidity sensors at FINO1. Sonic anemometers measure the speed of sound, which depends on the air temperature and the humidity. Therefore a bulk formulation was used to correct the measurements [51].

$$\overline{w'\theta'}_{sonic} = \overline{w'\theta'} + 0.51\bar{\theta} + \overline{w'q'} \tag{3.1}$$

where $\overline{w'\theta'}$ is the heat flux, $\bar{\theta}$ is the mean potential temperature and $\overline{w'q'}$ is the humidity or moisture flux. Cañadillas et al.[11] compared the Monin-Obukhov length of the sonic measurements to the atmospheric stability estimation of the Bulk Richardson Number. A relative large scatter could be observed between the stability parameter determined with the Eddy Covariance method and the Bulk Richardson Number. The complex interplay of different parameters and different uncertainties of the different methods and sensors could explain the large scatter.

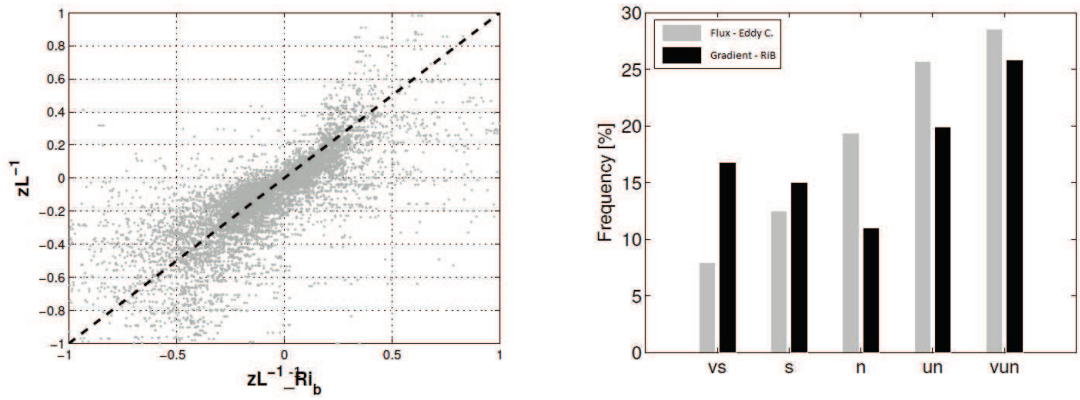

Figure 3.9: On the left a scatter plot of sonic (zL^{-1}) versus Bulk Richardson number (zL^{-1}_{RiB}) stability parameter at 41.5 meters. On the right side a histogram divided into five stability classes (according to table 3.1) [11]

Stability class	$\frac{z}{L}$
Very stable (VS)	$\frac{z}{L} > 0.2$
Stable (S)	$0.04 < \frac{z}{L} < 0.2$
Near Neutral (NN)	$-0.04 < \frac{z}{L} < 0.04$
Unstable (U)	$-0.2 > \frac{z}{L} > -0.04$
Very unstable (VU)	$\frac{z}{L} < -0.2$

Table 3.1: FINO1 -Stability classification according $\frac{z}{L}$ [11]

Based on right side of figure 3.9, the Bulk Richardson number tends to indicate more stable conditions than the Eddy Covariance Method, which could be caused due to the temperature difference between air and sea. Due to the fact that the sea temperature fluctuations more gradually, using sonic temperatures results in more extreme conditions, very unstable and stable. More can be found in the paper of Motta et al. [41]

The wind shear depended on the stability parameter zL^{-1} was compared with previous studies, and a good agreement was found for unstable and neutral conditions. For stable conditions, higher wind shear was found [23].

In the end the overall agreement between the datasets, stability distribution and wind shear, is found acceptable for Cañadillas et al..

Chapter 4

Atmospheric stability analysis - KNMI Met Mast Cabauw

4.1 Introduction

The Royal Dutch Meteorological Institute (KNMI), has a met mast of a height of 213 meter at Cabauw. The mast is used for meteorological measurements in the lower two hundred meters of the atmosphere, called the boundary layer. It was installed in 1972 and was one of the first meteorological stations whose data is collected automatically. At different heights of the mast, instruments were installed to take measurements of temperature, wind, humidity and radiation. [8]

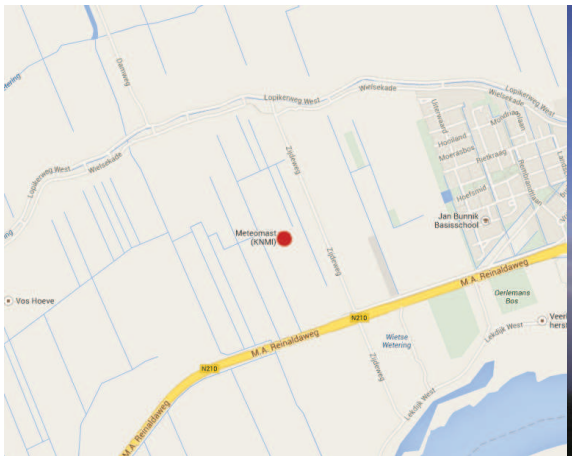

Figure 4.1: Area map around Cabauw with the met mast at the red dot [19]

Figure 4.2: Picture of the Cabauw met mast with low clouds [8]

The roughness length is equivalent to the height, measured from the surface, at which the wind speed theoretically transitions from zero to non-zero values. Describing the roughness of the

surroundings with the roughness length results in an approximation of the average roughness for a certain direction. The KNMI measurement mast is surrounded by various obstructions, mostly shelter belts (sequence of very high roughness and low roughness) influencing the flow and making it difficult to give a good approximation of the roughness length. In literature multiple papers discuss the modelling of the surroundings of Cabauw from which the roughness length per sector is derived [3][56] . More can be found in appendix B.2.

4.2 Measurement campaign

The KNMI Cabauw met mast data of the year 2010 is used in this research with measurements executed on eight heights: 0, 10, 20, 40, 80, 140, 200 meters and with high frequent sonic measurements at a height of 5 meters. At these levels various parameters are measured: temperature, wind speed,wind direction, pressure and relative humidity. The measurements of the wind speed and wind direction are executed at three and two brackets respectively. This is to avoid having a large influenced wind speed and direction measurements by tower shading. The 10 and 20 meter measurements are executed on a separate mast nearby the main tower.

The storage can be divided into two parts, high frequent sonic measurements and 10 minute average data.

4.2.1 High frequent sonic measurements

The data set obtained from the KNMI, contains 10 minute average measurements derived from high frequent sonic anemometer and temperature measurements together with low frequent cup and temperature sensors. The KNMI used the high frequent sonic anemometer and temperature measurements to directly determine the atmospheric stability from the heat and momentum flux measurements. From these high frequency measurements (frequency of 10 Hz) at a height of 5 meter the friction velocity (u_*) and turbulent sensible heat flux (H) are calculated using the Eddy Covariance Method, as explained in section 2.4.1. More information about the met mast in Cabauw can be found in [8].

4.2.2 Data averaging

The low frequency measurements of the wind speed, wind direction, air pressure and relative humidity are converted to 10 minute averages. In figure 4.3 the Weibull distribution of 6 levels is visible, from measurements at a height of 10 meters up to 200 meters. Showing the most occurrences of wind speeds around 4 m/s at a height of 10 meter and the same with a wind speed around 12 m/s at a height of 200 meter.

The average absolute temperature is stored every 10 minutes for 8 heights, including the surface temperature at a height of 10 centimeters. It is assumed that the temperature measurement at this height corresponds to the surface temperature. In appendix E.2, an sensitivity analysis is executed showing that small variations in temperature have no significant effect on the stability analysis.
In figure 4.4, the monthly average temperatures are shown. What can be observed is the strong seasonality of the average temperature, with high temperatures occurring during the summer months. It therefore can be expected, that in the summer months more unstable conditions occur.

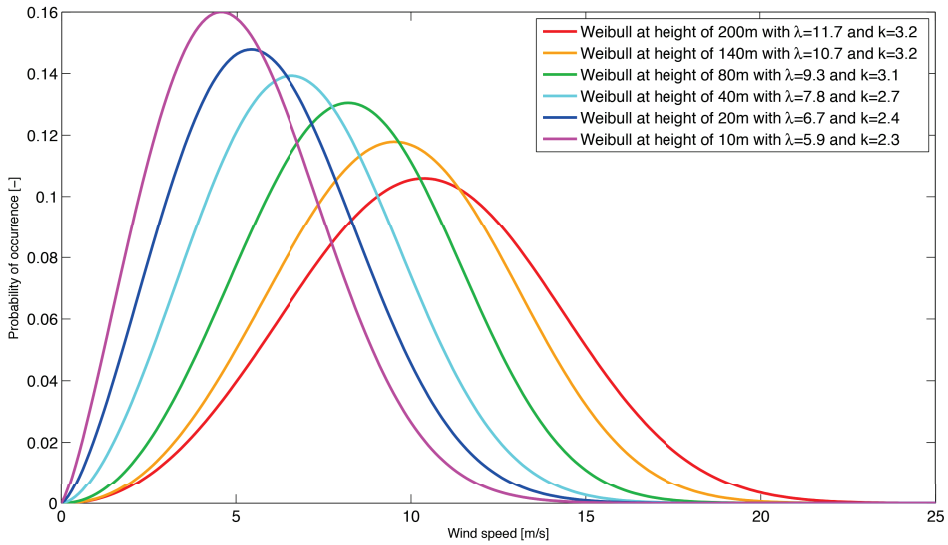

Figure 4.3: Cabauw - Weibull for different heights

In October, the average absolute temperature at 200 meter is the highest with respect to all other measurements, however this does not meet the expectations. Due to adiabatic expansion of air with increasing height the temperature at 200 meter is expected to be the lowest.
The selection of the measurement height will be discussed later in this report in section 4.3.3.

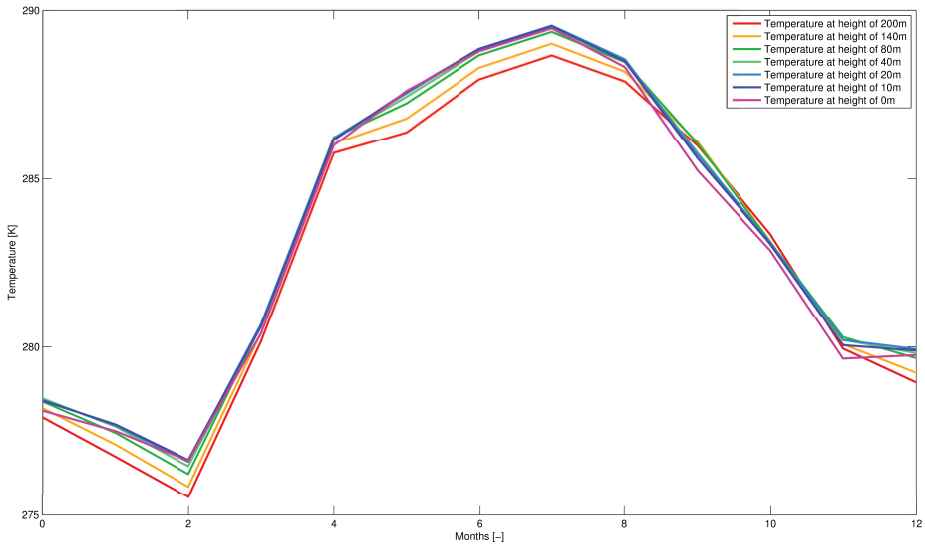

Figure 4.4: Cabauw - Monthly average absolute temperature for different heights

The air temperature, humidity and air pressure are used to determine the virtual potential temperature, explained in section 2.1.1, which is used for the estimation of the atmospheric stability.

It is important to note, that the wind speed and wind direction are measured respectively on two or three brackets, as stated before. The used dataset however contained only one wind speed at each measurement height. The sensor selection of the wind direction and wind speed, is already executed by the KNMI and therefore it is assumed that the effect of tower shading are not affecting the obtained data.

4.3 Data processing

Before the atmospheric stability can be determined from the given dataset, a couple of factors have to be taken into account, namely:

- Data filtering
- Tower shading
- Selection of measurement height

4.3.1 Data filtering

Data filtering is of utmost importance for the validity of the data and research. In this section two filters will be explained:

- Operational conditions & sensor errors
- Steady state conditions

Operational conditions & sensor errors

Use of measurement equipment can result in deviation between the true and measured value. To exclude sensor errors and values outside of the operational conditions of a wind turbine, the data is filtered with the following conditions (table 4.1).

$4 \leq$	Wind speed	≤ 25 [m/s]
$0 \leq$	Wind direction	≤ 360 [°]
$263 \leq$	Temperature	≤ 308 [K]

Table 4.1: Filter conditions for wind speed, wind direction and temperature

Using the conditions stated in table 4.1, results in a data reduction of 22%. Out of these 22% it can be assumed that the biggest part of the data is dismissed due conditions outside of the operational conditions of the turbine and the remaining data is excluded because of sensor errors.

Steady state conditions

One of the main assumptions of MOST is that the mean parameters do not change in time [45]. In order to verify this assumption as best as possible, the deviation of the parameters in time has to be small. Table 4.2 gives the following conditions for the change in wind speed, wind direction and temperature for a time interval of 10 minutes. When two consecutive measurements, exceed conditions stated in the table, the data point is excluded from the dataset, resulting in only stationary conditions in the dataset.

Parameter	Condition
Wind speed	$\pm 20\%$
Wind direction	$\pm 15^{\circ}$
Temperature	$\pm 0.5K$

Table 4.2: Steady state filter conditions for wind speed, wind direction and temperature

Using the following conditions led to a total reduction of 41% of the data. Together with the filter for the operational conditions and the sensor errors, a reduction of 46% is reached.

4.3.2 Tower shading

The provided data contains 10 minute averages and for each interval the KNMI selected the instruments with offered best exposure to the free flow wind direction. Not all the effects of tower shading can be eliminated using multiple sensors in different direction at each level, therefore corrections are applied to the dataset according to [57].

4.3.3 Selection of measurement height

As explained in the introduction of this chapter, the Cabauw measurements are executed on eight levels. In literature the surface boundary layer is seen as a homogeneous layer, as assumed in MOST. Resulting in no significant difference in stability estimation based on measurements from different levels as long as these measurements are within the surface boundary layer. However in reality, stratification can take place within the surface boundary layer, which mainly takes place under stable conditions. Using multiple input parameters from different levels results in significant differences between the atmospheric stability estimations by each method. A selection of the measurement height therefore has to be made, based on:

- Layers observed by wind turbine - Stratification
  Due to stratification of the Surface Boundary Layer, multiple layers with different atmospheric stabilities may develop. The research is focused on the differences between multiple methods to estimate the stability and the impact of the stability on wind turbine design. In order to get the best estimation of the impact of atmospheric stability on the wind turbine, only the layers observed by the wind turbine have to be taken into account. Therefore, in order to get the best possible estimation of the atmospheric stability observed by the wind turbine, the wind speed and temperature gradient of the hub height minus the blade length and the hub height plus the blade length have to be taken into account.

- Monin-Obukhov Similarity Theory
  The theory of Monin-Obukhov is only valid in the Surface Boundary Layer and assumes constant fluxes in this layer. Higher in the atmosphere MOST will no longer be valid and therefore the error between the theory and reality will continue to grow at higher altitudes. Making use of the lowest measurements, near to the surface, therefore will give the best estimation of the atmospheric stability according to MOST.

In order to make a selection of which measurements heights will be selected, comparison of the atmospheric stability distribution for one method with multiple measuring heights is conducted. This comparison is shown in figure 4.5. On the y-axis the probability of occurrence is displayed and on the x-axis the $100L^{-1}$ for one method with multiple measuring height inputs: First, the question remains, of which method should be used. There are multiple methods as explained, with each leading to different results. Ãňn order to make an selection of the method, to be used to determine the best measuring heights literature needs to be consulted. In the literature, the Bulk Richardson Number is most commonly used with the best results in atmospheric stability estimations and therefore will be used to determine the best measurement height, more detailed supporting arguments can be found in [11] [43] [44] [45].

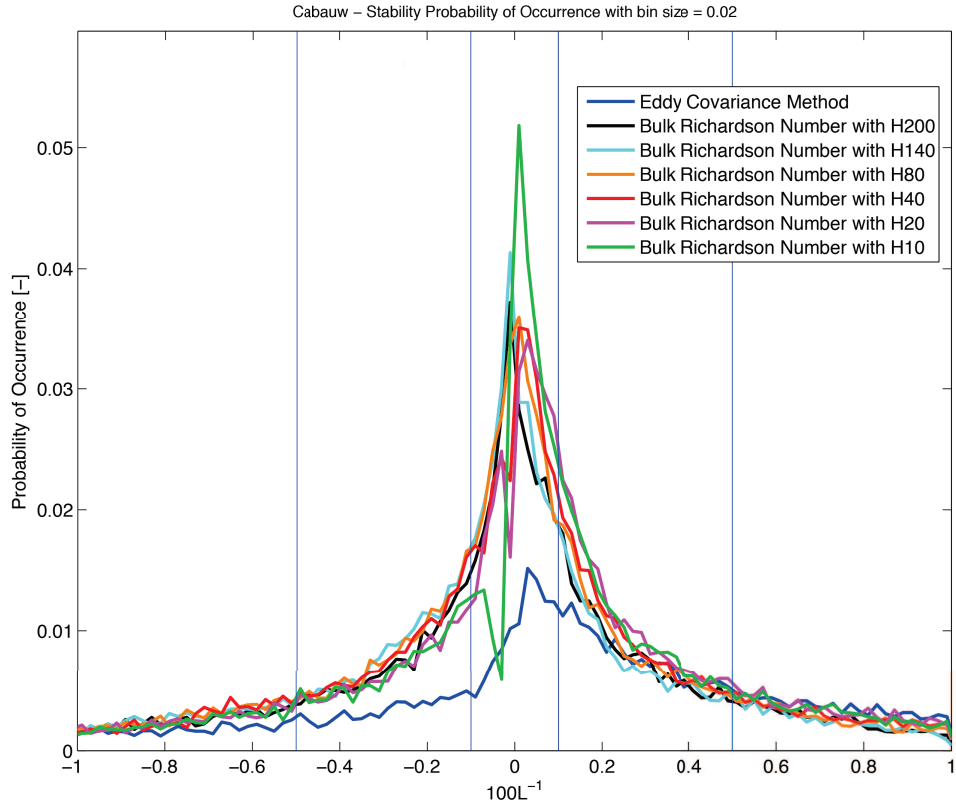

Figure 4.5: Cabauw - Probability distribution function of the Eddy Covariance Method and the Bulk Richardson Number for multiple heights 10m, 20m, 40m, 80m, 140m, 200m.

In figure 4.5, the probability distribution function of the Eddy Covariance Method and the Bulk Richardson Number for multiple heights 10, 20, 40, 80, 140, 200 meter is plotted. The Eddy

Covariance method uses high frequency sonic measurements at a height of 5 meter. For the Bulk Richardson Number Method the surface measurements together with the measurements of different heights are used to estimate the Monin-Obukhov length. It must be noted that the data used in figure 4.5 is not filtered with the Surface Boundary Layer height. The height of the Surface Boundary Layer (z_s), is assumed to be 10% of the boundary layer height (z_i). According to literature the z_i Boundary Layer height can be approximated using the following equations:

$$z_i \approx c_i \frac{u_*}{f_c} \tag{4.1}$$

$$z_s \approx 0.1 c_i \frac{u_*}{f_c} \tag{4.2}$$

where c_i is a constant varying from 0.1-0.3 depending on the stability, f_c is the Coriolis parameter depended on the latitude. For neutral homogeneous terrain the c_i is estimated to be around 0.15 [44], with decreasing values of c_i for stable and very stable conditions due to the decrease of the boundary layer height under stable conditions.

According to MOST, as explained before, the best estimation of the atmospheric stability is achieved by using the lowest measurements. However, a significant sudden drop in probability of occurrence can be observed for the lower two heights of 10 and 20 meters. This could have multiple reasons:

- The measurements at a height of 10 & 20 meters are not measured at the main tower but at a smaller mast nearby. The surroundings could influence with the measurements at these heights.
- Also, the selected bin-size could influence, the accurate measurements of real values of the parameters of interest.
- The method uses the wind speed and temperature gradient between the measurements at the surface and of the selected height. Using measurements at lower attitudes will result in a relative small difference between these measurements in comparison to the measurement differences using the surface- and measurements at higher attitudes. Due to the smaller difference, the accuracy and resolution of the measurements leads to a larger impact on the atmospheric stability estimation.

In order to prevent this phenomenon, the temperature and wind speed gradients must be higher than the measured gradients of 0-10 meters & 10-20 meters. Preferably using gradients of 0-40 meters or higher, without significant impact due to the above described phenomenon.

However, for measurements at altitudes higher than the Surface Boundary Layer height z_s, MOST can no longer be applied. A solution would be using the Surface Boundary Layer height as a filter, filtering the data points where $z_s \geq$ measurement height. This resulted in data reduction indicated in table 4.3.

Measurement height [m]	Data reduction [%]	
	with c_i=0.15	with c_i=0.25
0-40	61%	26%
0-80	96%	75%
0-140	>99%	97%
0-200	>99%	>99%

Table 4.3: Data reduction using the Surface Boundary Layer height as a filter (z_s=10% of z_i).

This resulted in a data availability of only 25% or less, depending on the c_i, when measurements higher than 80 meters are used. This is undesirable and results to a bad representation of the stability distribution. The boundary layer height z_i is only an approximation, varying for different stability conditions. The results are therefore very unreliable. It is therefore decided the Surface Boundary Layer height will not be applied as a filter by default unless otherwise indicated.

4.4 Results - KNMI met mast Cabauw

4.4.1 Overall statistics of atmospheric stability

For the Cabauw results, it is assumed that using the high frequent wind speed and temperature measurements together with the Eddy Covariance Method gives the best representation of the real atmospheric stability, because due to the high frequency temperature and wind speed measurements the heat flux and momentum flux can be determined directly.

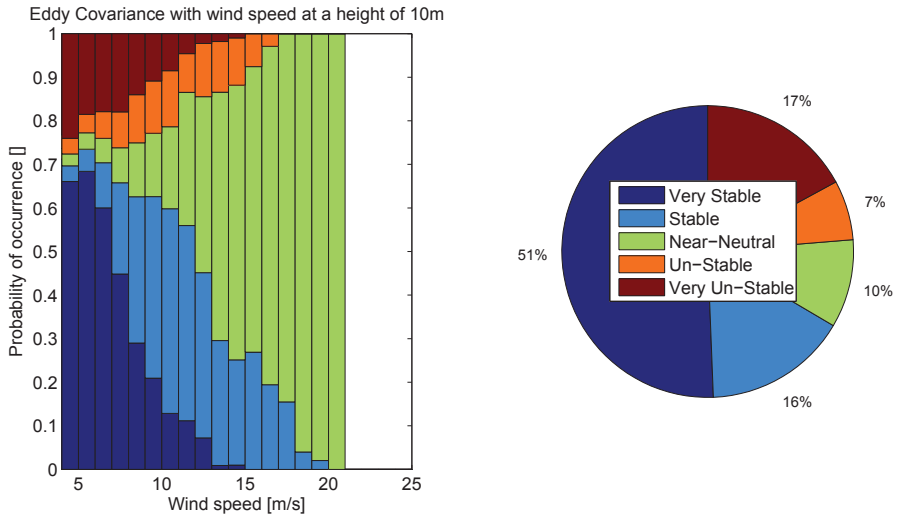

Figure 4.6: Cabauw - Eddy Covariance Method with surface measurements

Figure 4.6 shows that the conditions at the onshore KNMI met mast at Cabauw mainly consist of very stable and stable conditions. The near neutral conditions mainly take place at higher wind speeds above 15 m/s.

Very stable	$0 < L \leq 200m$	$^{100}/_{L} \geq 0.5$
Stable	$200m < L \leq 1000m$	$0.1 < {}^{100}/_{L} < 0.5$
Near Neutral	$\|L\| > 1000m$	$-0.1 < {}^{100}/_{L} < 0.1$
Unstable	$-1000m \leq L < -200m$	$-0.1 \geq {}^{100}/_{L} > -0.5$
Very unstable	$-200m \leq L < 0m$	$^{100}/_{L} \leq -0.5$

Table 4.4: Stability classification according to L and $\frac{z}{L}$ with z=100m[45].

The atmospheric stability is divided into five classes, according to the Monin-Obukhov lenght (L) and the stability parameter $\frac{z}{L} = \frac{100}{L}$. Using these five classes, mentioned in table 4.4, for the comparison of multiple methods results in the following distributions, shown in figure 4.7. In this bar diagram, the atmospheric stability estimations of the four methods are divided into five classes and are compared with the Eddy Covariance Method. From this diagram three methods distinguish from the others, the Bulk Richardson Number, Profile Method 2 and the Gradient Richardson Number give very similar distributions. However executing the comparison with the discrete classes, can give a wrong view of the reality. Therefore, a continuous display of the

stability distribution gives a better representation of the atmospheric stability and therefore it will be used also. The PDF of the stability parameter is displayed in figure 4.8.

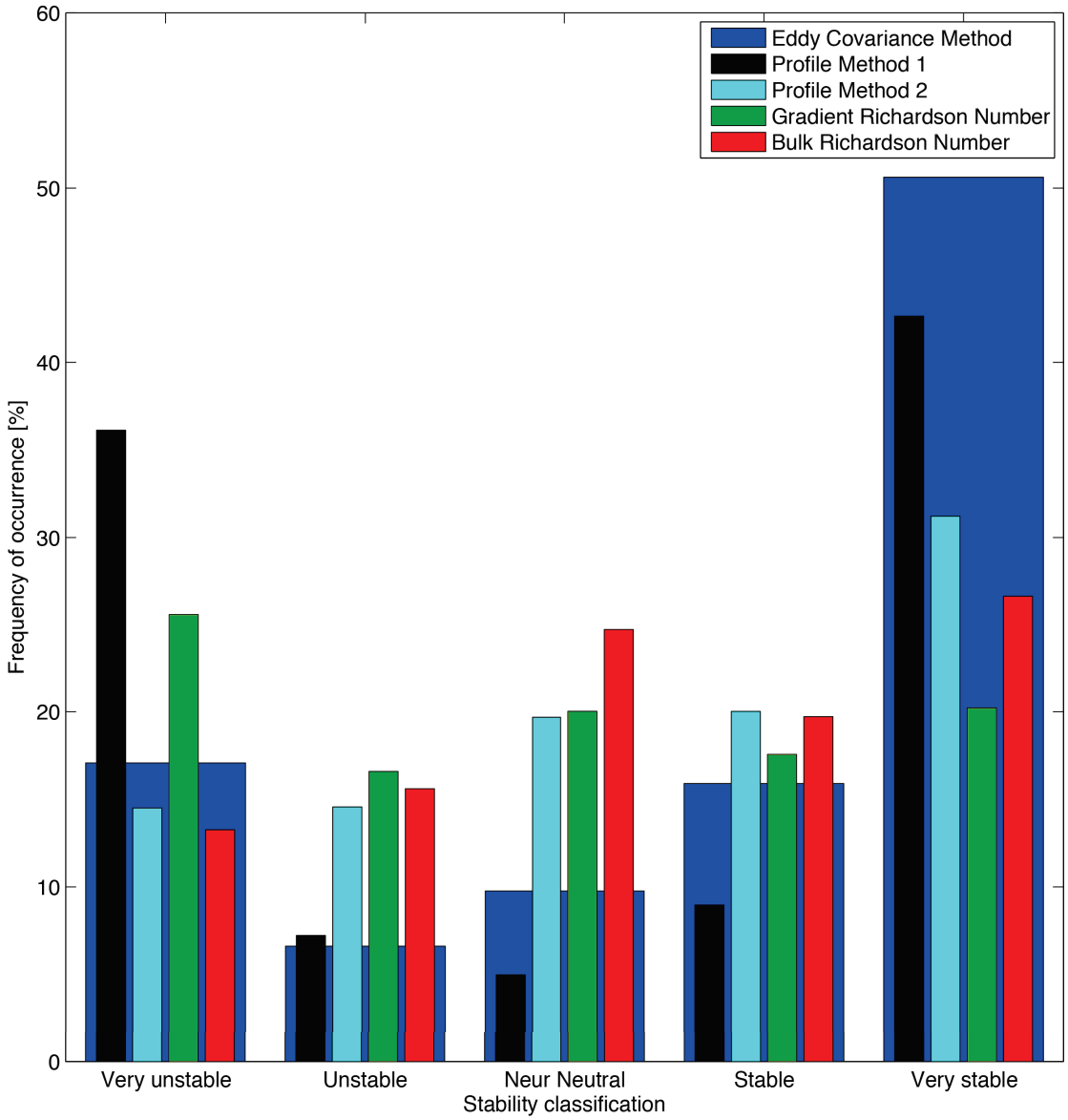

Figure 4.7: Cabauw - Comparison of Atmospheric Stability Distribution divided into five classes

From the PDF it can be observed that three methods used to estimate the atmospheric stability give very similar results with an over-prediction of neutral, stable and unstable conditions and an under-prediction of the extreme conditions. The Profile Method 1 is significantly different from the other methods, according to this method the conditions are mainly extreme, with a tendency to the prediction of very stable conditions.

Based on the BAR and PDF figures, no substantiated conclusion can be made. Mainly according to the PDF, a slight preference for the Bulk Richardson Number, Gradient Richardson Number and Profile Method 2 can be concluded. For values of the stability parameter $\|\frac{100}{L}\|$ with z = 100

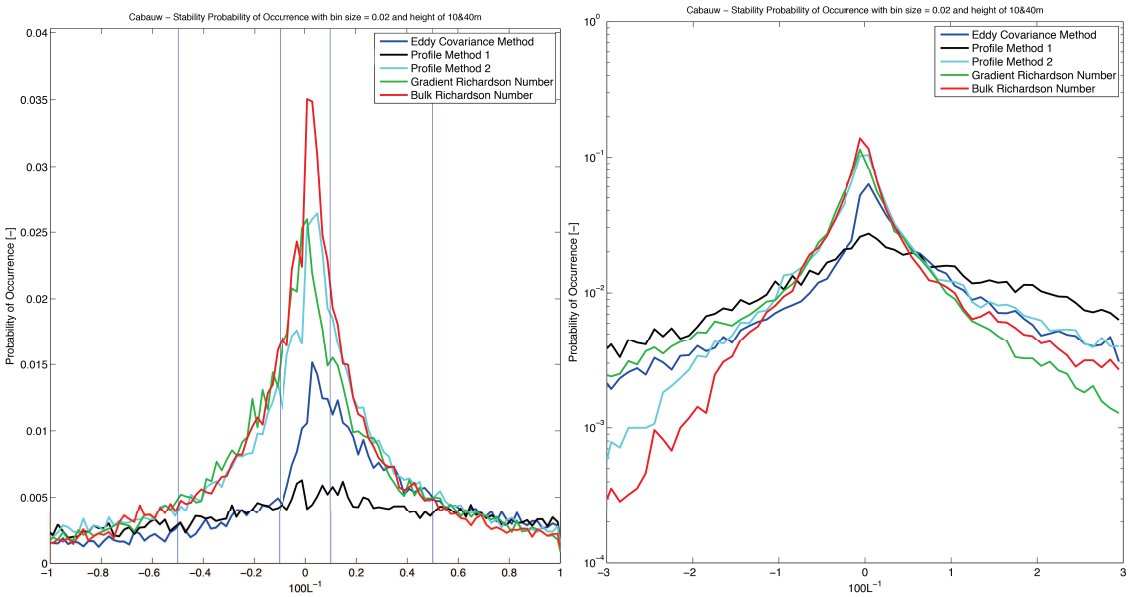

Figure 4.8: Cabauw - Comparison of Atmospheric Stability Distribution with the PDF of the stability parameter $\frac{z}{L}$. The left figure is plotted on normal scale and the right figure on semi-logarithmic scale.

m greater than 3, hardly any observations can be made, therefore small deviations of stability estimation have a significant effect on the distribution.

To obtain a better overview of the best method to determine the atmospheric stability, further research will focus on a comparison multiple levels:

- Atmospheric stability distribution per **wind speed bin**
- Atmospheric stability distribution per **hour of the day**
- Atmospheric stability distribution per **month**
- Atmospheric stability distribution per **wind direction bin**
- **Friction velocity** (u_*) per method compared to the friction velocity of the Eddy Covariance Method
- **Heat flux** ($\overline{w'\theta'_v}$) per method compared to the heat flux of the Eddy Covariance Method

4.4.2 Atmospheric stability distribution per wind speed bin

The atmospheric stability is divided into five classes and for each wind speed bin of 1 m/s the distribution of the five stability classes is represented in figures 4.6, 4.9, 4.10, 4.11 and 4.12, respectively the Eddy Covariance, the Bulk Richardson Number, the Profile Method 2, the Profile Method 1 and the Gradient Richardson Number Methods.

From these five figures a number of observations can be made:

Wind speeds below 10 m/s

According to the Eddy Covariance Method, the atmospheric stability conditions at Cabauw are mainly very stable. Less occurring are the stable and very unstable conditions for wind speeds below 10 m/s and the frequency of very stable and very unstable conditions decrease with increasing wind speed.
The Bulk Richardson Number, Profile Method 2 and the Gradient Richardson Number give very similar results for the distribution of the atmospheric stability per wind speed bin. Similar to the results of the bar graph.
Looking more closely at the figures, results in the conclusion that the frequency of occurrence for very unstable and unstable conditions is the lowest according to the Bulk Richardson Number. The frequency of occurrence for the very unstable and unstable conditions according to the Profile Method 2 and finally to the Gradient Richardson Number are increase compared to the Bulk Richardson Number. These three methods however give too low indications for very stable and stable conditions according to the Eddy Covariance Method.
The Profile Method 1 indicates that for wind speeds below 10 m/s, only very stable and very unstable conditions occur. Comparing the Profile Method 1 with the Eddy Covariance Method results in an over-prediction of the unstable conditions.

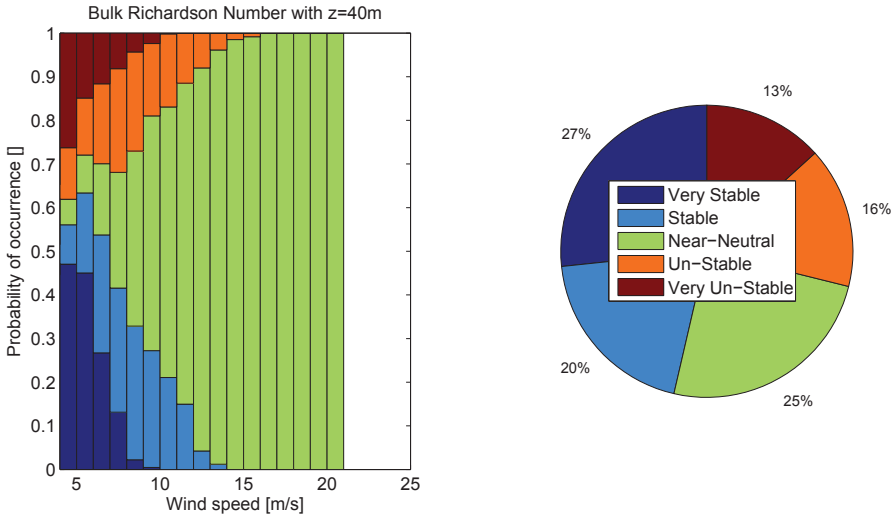

Figure 4.9: Cabauw - Bulk Richardson Number with speed and temperature measurements at height of 40m.

Above wind speeds of 10 m/s

According to the Eddy Covariance Method the atmospheric stability distribution consist mainly of near neutral and stable conditions for wind speeds above 10 m/s.
According to the Bulk Richardson Number and the Profile Method 2, the atmosphere consist almost entirely of near neutral conditions. A shift from stable to neutral conditions can be observed.
The stability distribution according to the Gradient Richardson Number consists also of unstable conditions.
For the Profile Method 1, the stability distribution above 10 m/s consist mainly of very unstable,

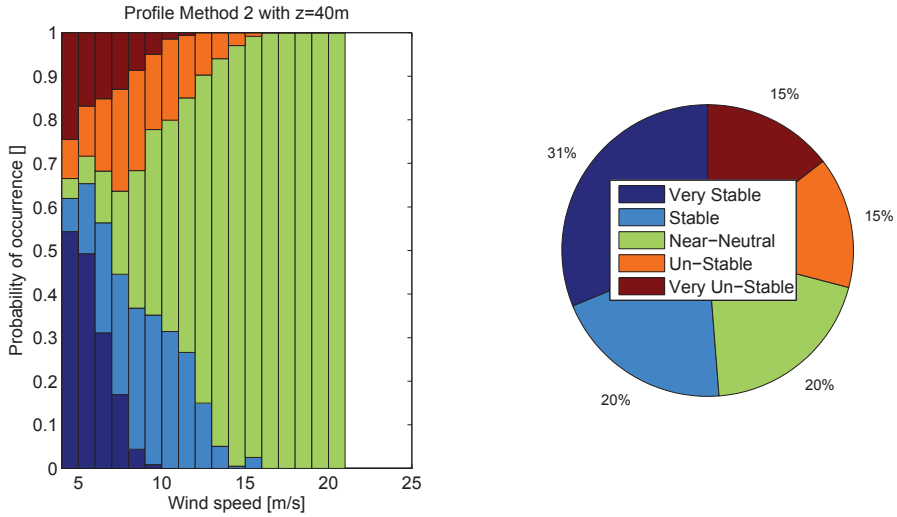

Figure 4.10: Cabauw - Profile Method 2 with speed and temperature measurements at height of 40m.

unstable and stable conditions. Almost no near neutral conditions have been observed which is not in agreement with the Eddy Covariance Method and the three other methods.

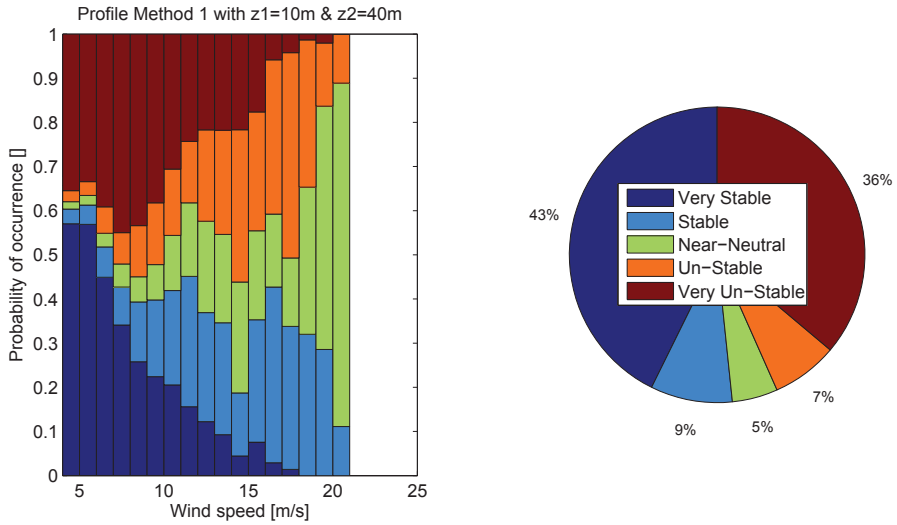

Figure 4.11: Cabauw - Profile Method 1 with speed and temperature measurements at height of 10 and 40m

From the atmospheric stability distribution per wind speed, the same conclusion can be made. The Bulk Richardson Number, Gradient Richardson Number and Profile Method 2 give very similar results. The Bulk Richardson Number and Profile Method 2 give the best results. The Gradient Richardson Number predicts more unstable conditions.
The Profile Method 1 corresponds only with the Eddy Covariance Method for low wind speed (below 5 m/s).

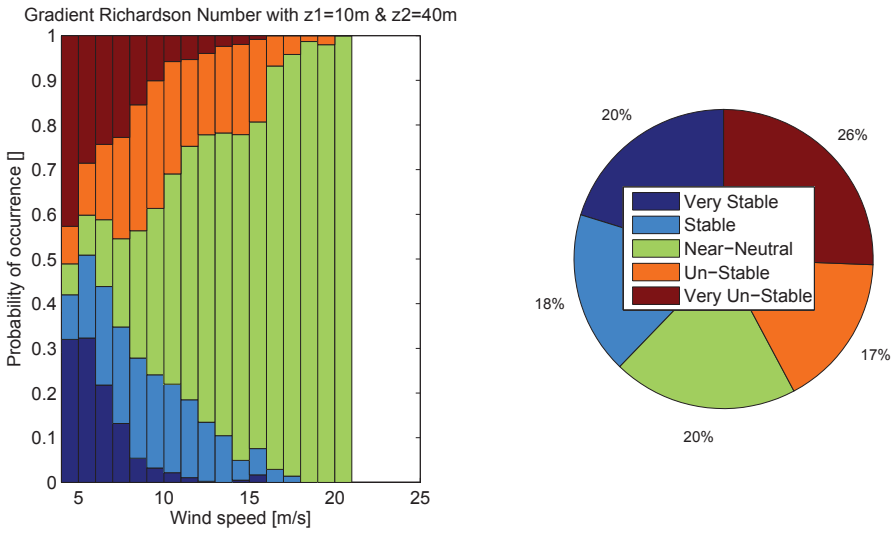

Figure 4.12: Cabauw - Gradient Richardson Number with speed and temperature measurements at height of 10 and 40m

4.4.3 Atmospheric stability distribution per hour of the day

The atmospheric stability is for each hour of the day, distributed into five stability classes, which is represented in figures 4.13, 4.14 and 4.15, for the Eddy Covariance, the Bulk Richardson Number, the Profile Method 2, the Profile Method 1 and the Gradient Richardson Number methods respectively.

From these five figures a number of observations can be made:

Night time (20:00-07:00)

According to the Eddy Covariance Method, the atmospheric stability is mainly very stable with almost no unstable and very unstable conditions during the night. Comparing this with estimation of the Bulk Richardson Number and Profile Method 2, which are very similar, the very stable conditions occur less frequently and near neutral and stable conditions occur more frequently.
The Profile Method 1, as already described before, describes the atmosphere with almost only extreme conditions and therefore corresponds badly in comparison with the Eddy Covariance Method.
The Gradient Richardson method gives an indication of around 15% unstable conditions during the night, which is an overprediction of the very unstable conditions. This results in less very stable conditions.
Overall Profile method 2 provides the best representation of the atmospheric stability distribution for night time, slightly better than the Bulk Richardson Number.

Day time (07:00-20:00)

During day time (07:00-20:00), according to the Eddy Covariance Method almost no very stable and mainly very unstable conditions occur. The distributions of the Bulk Richardson Number

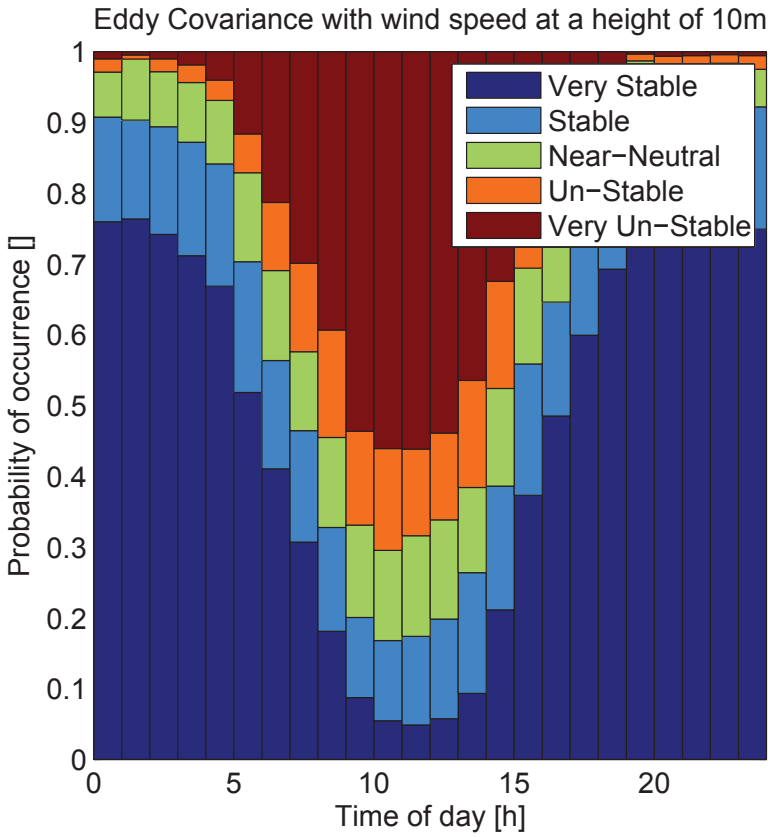

Figure 4.13: Cabauw - Hourly distribution of Eddy Covariance Method

and the Profile Method 2 are similar during the day time. Where the Profile Method 1 gives a significant over-prediction of unstable conditions. At the end the Gradient Richardson Number provides the overall the best agreement with the Eddy Covariance Method during the day.

A possible improvement of the atmospheric stability estimation could be achieved by combining Bulk Richardson Number with the Gradient Richardson Number by selecting the Bulk Richardson Number for night time (20:00-07:00) and the Gradient Richardson Number for the day time (07:00-20:00), this will be further discussed in chapter B.4.

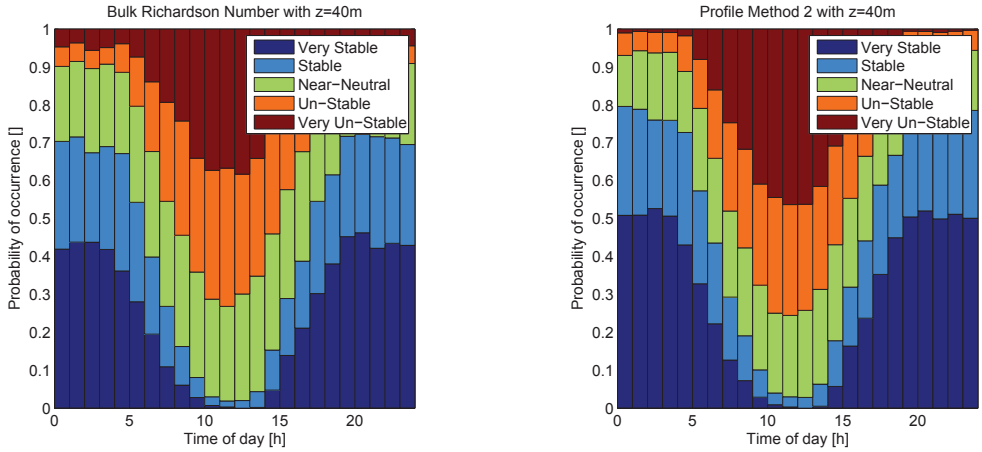

Figure 4.14: Cabauw - Hourly distribution of (left) Bulk Richardson Number and (right) Profile Method 2 with speed and temperature measurements at height of 40m.

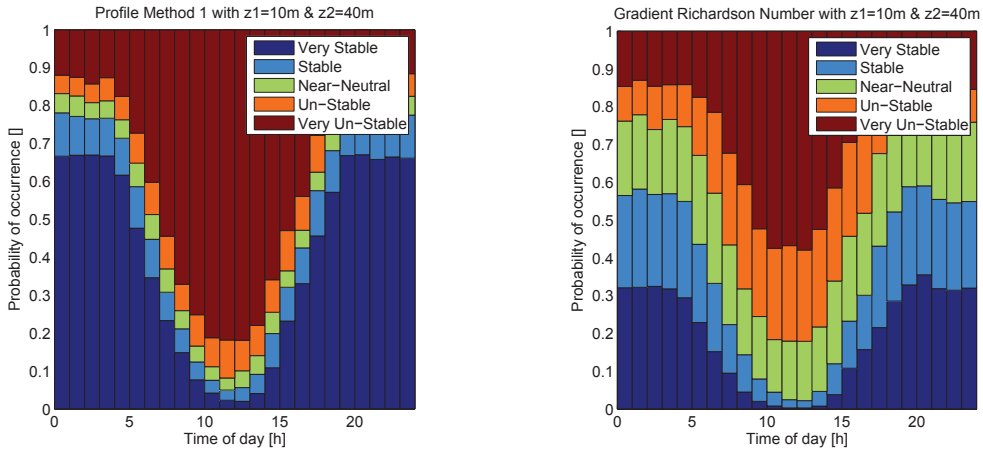

Figure 4.15: Cabauw - Hourly distribution of (left) Profile Method 1 and (right) Gradient Richardson Number with speed and temperature measurements at height of 40m.

4.4.4 Atmospheric stability distribution per month

The atmospheric stability is divided into five classes and for each month the distribution of the five stability classes is represented in figures 4.16, 4.17 and 4.18, for the Eddy Covariance, the Bulk Richardson Number, the Profile Method 2, the Profile Method 1 and the Gradient Richardson Number respectively.

From these five figures a number of observations can be made:

Unstable conditions

According to the Eddy Covariance Method small fluctuations between each month can be observed. With in the months of March, April, May and June a peak of around 30% of very unstable conditions is observed.

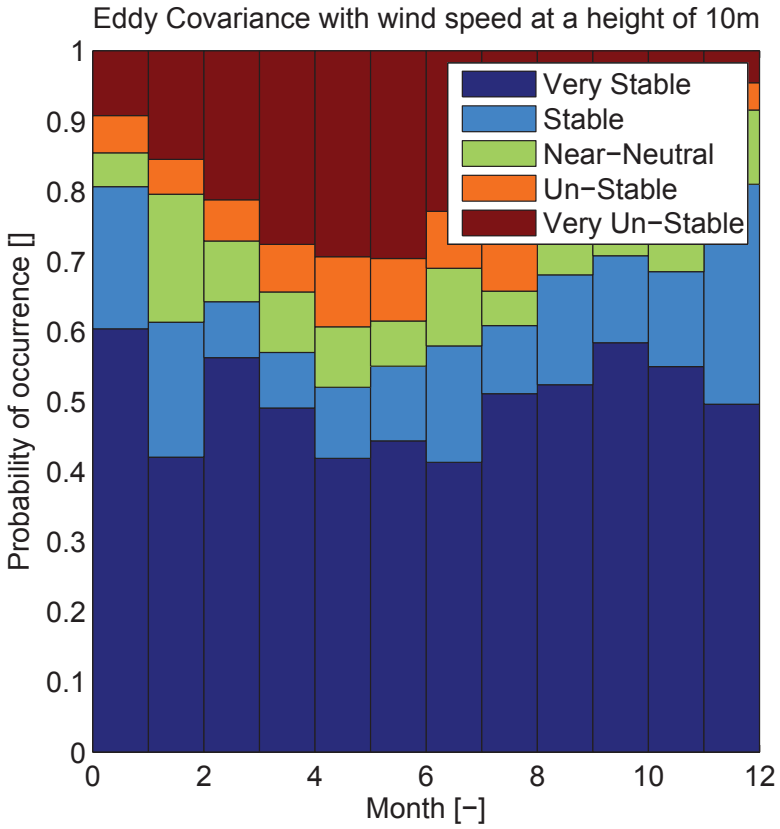

Figure 4.16: Cabauw - Monthly distribution of the Eddy Covariance Method with speed and temperature measurements at height of 10m.

The same peak of unstable conditions can be observed in the results of the Bulk Richardson Number and Profile Method 2. The Profile Method 1 and Gradient Richardson Number give a much higher estimation of the very unstable conditions, with the peak occurring in the same months. This indicates seasonal influences on the atmospheric stability, which are visible in the distribution of the unstable and very unstable conditions in figure 4.16. This agrees with the expectations, because during the summer months, the earth's temperature is higher, resulting in

heating of air near to the surface. Warm air rises and mixes with the cooler air at higher altitudes. This results in mixing of multiple layers and is seen as an unstable atmosphere.

Stable conditions

Small seasonal difference can also be observed for stable conditions, with a minimum in the months of March, April, May and June. In the same months, the unstable conditions are at its maximum.

Analyzing the monthly distribution of the stability, no significant differences could be observed influencing the conclusion of the best stability estimation method.

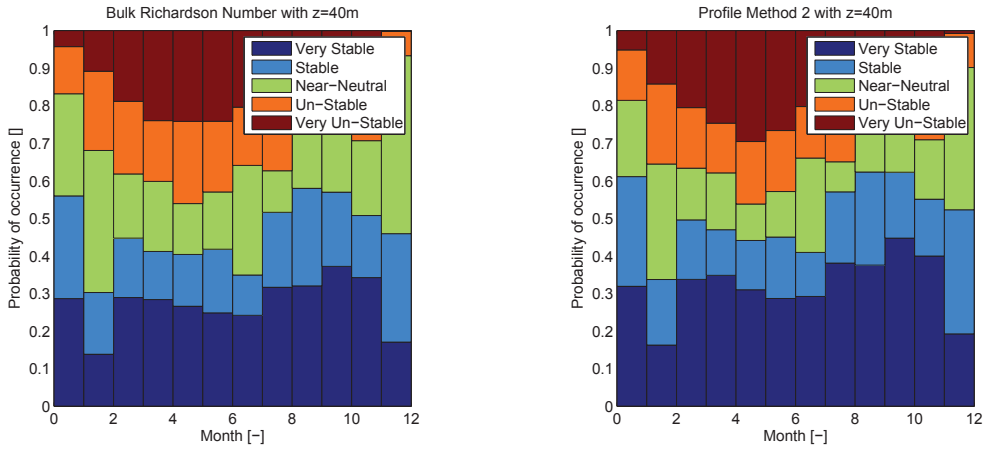

Figure 4.17: Cabauw - Monthly distribution of the (left) Bulk Richardson Number and (right) Profile Method 2 with speed and temperature measurements at height of 40m.

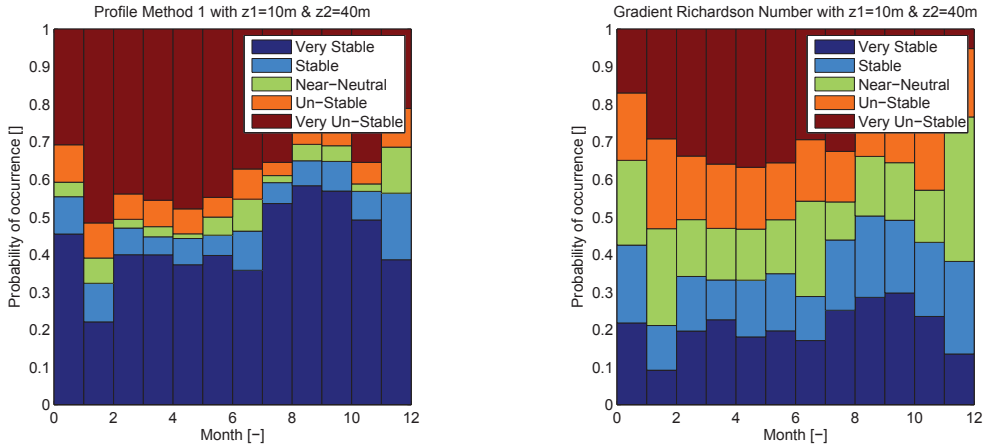

Figure 4.18: Cabauw - Monthly distribution of the (left) Profile Method 1 and (right) Gradient Richardson Number with speed and temperature measurements at height of 40m.

4.4.5 Atmospheric stability distribution per wind direction bin

The atmospheric stability is divided into five classes. For wind direction bin of 30 degrees, the distribution of the five stability classes is represented in figures 4.19, 4.20 and 4.21, for the Eddy Covariance, the Bulk Richardson Number, the Profile Method 2, the Profile Method 1 and the Gradient Richardson Number methods respectively.

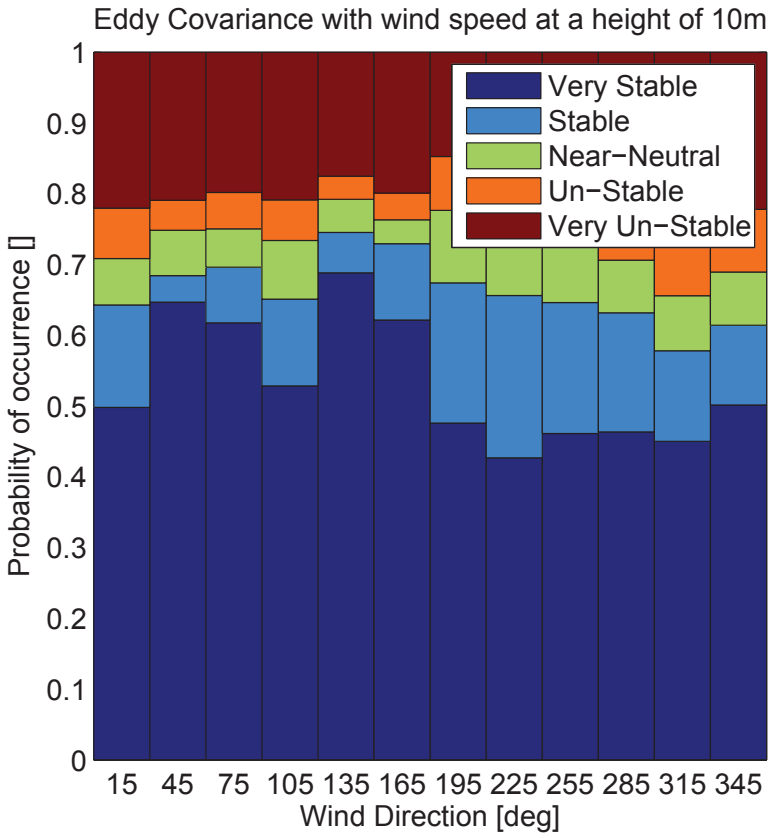

Figure 4.19: Cabauw - Atmospheric stability distribution per wind direction bin of the Eddy Covariance Method with speed and temperature measurements at height of 10m.

From these five figures the following observations can be made:

- The trend found in the previous comparisons can also be found in the figures below. The Eddy Covariance Method gives an higher frequency of occurrence for very unstable conditions and lower frequency of occurrence for unstable and neutral conditions compared to the Bulk Richardson Number, Gradient Richardson Number and Profile Method 2.

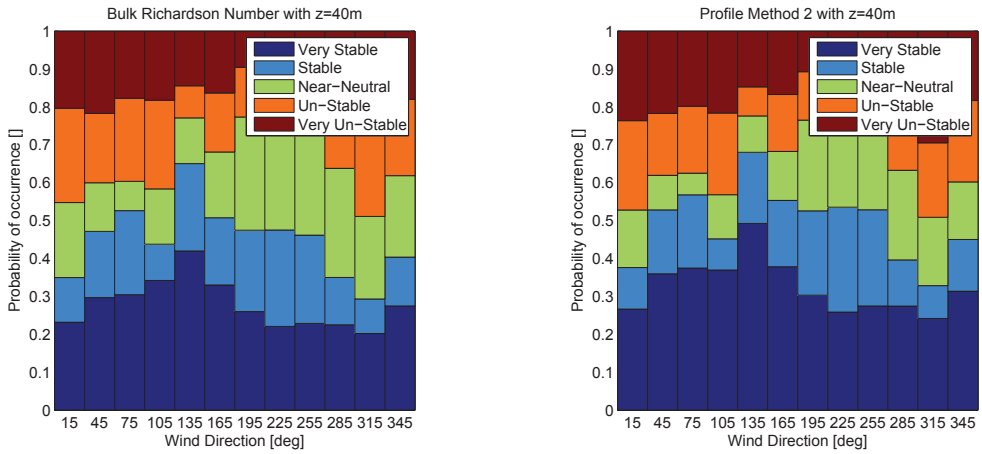

Figure 4.20: Cabauw - Atmospheric stability distribution per wind direction bin of the (left) Bulk Richardson Number and (right) Profile Method 2 with speed and temperature measurements at height of 40m.

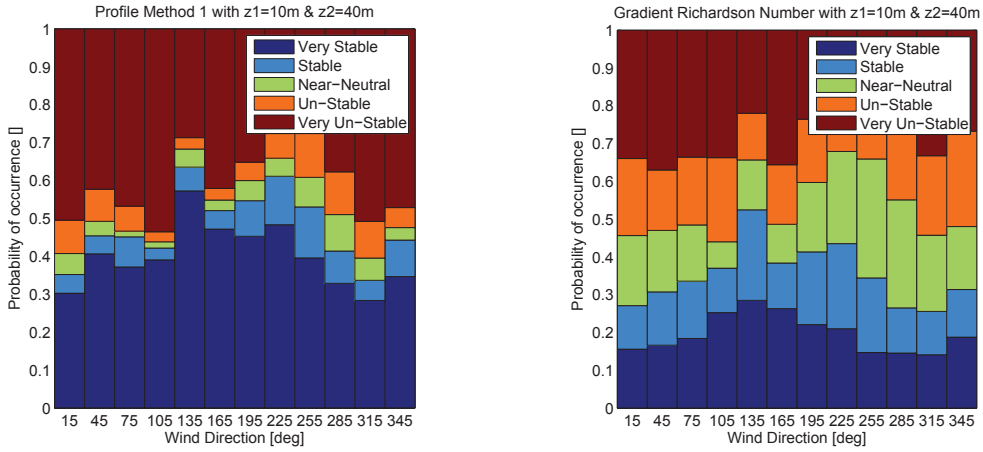

Figure 4.21: Cabauw - Atmospheric stability distribution per wind direction bin of the (left) Profile Method 1 and (right) Gradient Richardson Number with speed and temperature measurements at height of 40m.

4.4.6 Friction velocity (u_*) per method compared to the friction velocity of the Eddy Covariance Method

In the previous sections, different aspects of the atmospheric stability distribution are observed. The atmospheric stability was compared based on the Monin-Obukhov length (L).

$$L = -\frac{{u_*}^3}{\kappa \frac{g}{\theta_v} \overline{w'\theta'_v}} \tag{4.3}$$

The Monin-Obukhov length (L) is determined from friction velocity (u_*) and the heat flux ($\overline{w'\theta'_v}$). In this section, the main focus will be on the friction velocity, which is used to describe shear related motion in the air. In figures 4.22 and 4.23, eight plots are visible with a direct comparison to the friction velocity determined using the Eddy Covariance Method, of each of the four methods used in this research. The x-axis corresponds to the u_* determined by using the Eddy Covariance Method, under the assumption that is in agreement with reality. The y-axis shows the u_* determined using the other methods, respectively for each graph.

The friction velocity u_* as a result of the Profile and Richardson Number methods is determined using a logarithmic wind profile with stability correction. The friction velocity is determined to make an estimation of the atmospheric stability of the profile methods using equation 2.26 or 2.31 (section 2.4.2), depending on the method. However, the atmospheric stability estimation of the Richardson Number method does not lead directly to a estimation of the friction velocity. Therefore, the atmospheric stability estimation of the Richardson Number methods is used to determine the friction velocity using the logarithmic profile with stability corrections from the ψ functions in table 2.2 and the above mentioned equations. In appendix E.3 a routine check is executed, to check the validity of the method. Using an ideal vector of u_* with a mean of 0.5 and standard deviation of 0.1 to calculate the wind speed and temperature differences and from these the u_*. Small differences could be observed, due to the iterations steps taken in this method.

Figure 4.22 shows the comparison between each method and the Eddy Covariance Method where the Surface Boundary Layer height filter is disabled, while figure 4.22 presents the same results when the filter is activated.

Method	$Slope$	$Slope_{SBL}$	R	R_{SBL}
Profile Method 1	1.45	1.45	0.08	0.47
Profile Method 2	1.34	1.33	0.89	0.90
Gradient Richardson Number	1.42	1.35	0.13	0.55
Bulk Richardson Number	1.34	1.32	0.67	0.91

Table 4.5: Slope & Correlation R - Friction velocity (u_*) with $_{SBL}$ indicating the use of the Surface Boundary Layer height as a filter

In table 4.5, two parameters are shown. The slope between the friction velocity u_* determined using the Eddy Covariance Method and the slope determined through one of the other methodologies used in this research. The slope is determined using a Least-Squares fit and ideally approaching one for best agreement. The second parameter is the correlation R, which is a way of

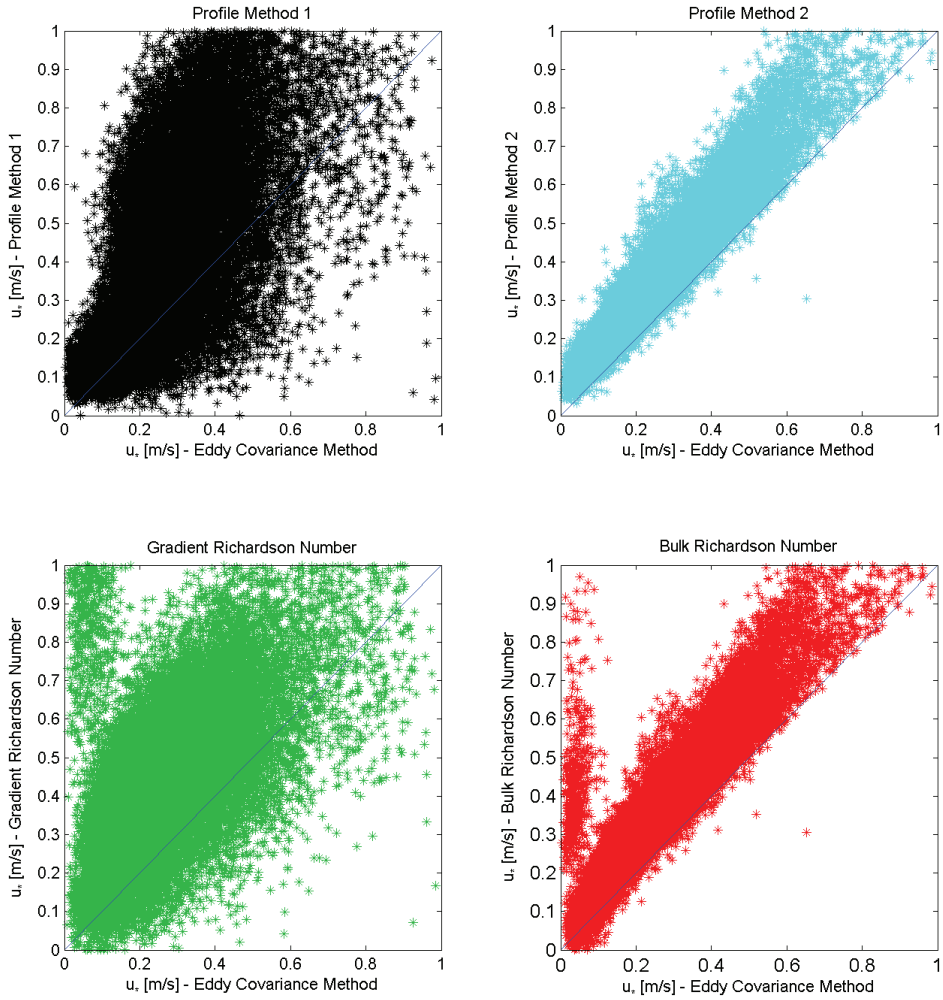

Figure 4.22: Cabauw - Comparison of Friction Velocity (u_*) without the filter for the Surface Boundary Layer height.

indicating the strength of the relation between two variables. The most appropriate method to be selected will be the one, resulting in the smallest scatter between the two variables.

Profile Method 1

From the figures above a couple of observations can be made for the first Profile Method. First of al, a slope of 1.45 can be observed, which results in a tendency to over predict the friction velocity. The overprediction of the u_* results in an overprediction of Monin-Obukhov length (L). Based on the relation between u_* and L found in equation 4.3. The overprediction of the Monin-Obukhov length results in an underprediction of the extreme conditions. However, due to the large scatter, which is clearly visible and also indicated by the correlation R of 0.08 without the

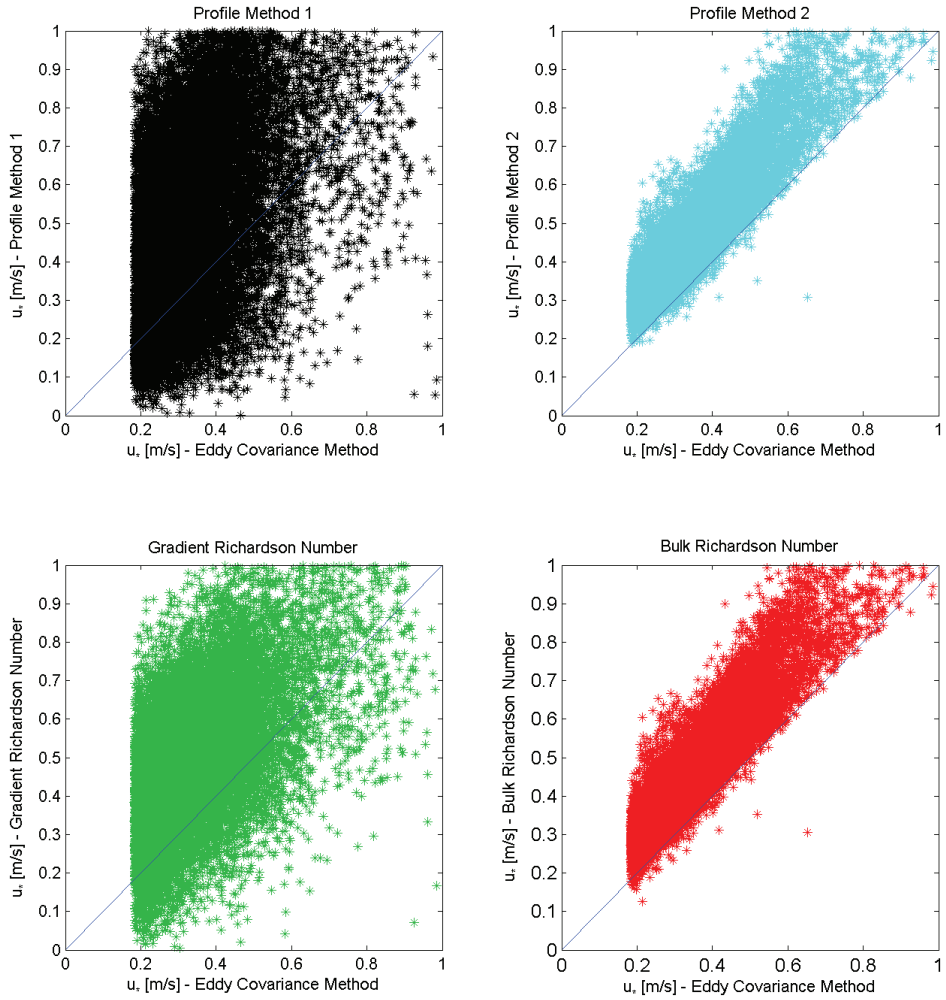

Figure 4.23: Cabauw - Comparison of Friction Velocity (u_*) with the Surface Boundary Layer height as a filter ($c_i = 0.15$ and $z_s = 10\%$ of z_i).

Surface Boundary Layer height as a filter, the slope of 1.45 has no profound effect on the overall distribution.

Therefore it can be concluded that the match between the Profile Method 1 and the Eddy Covariance Method is poor, which is in agreement with the previous findings.

Profile Method 2

For the second Profile Method an overall good agreement of the u_* can be found, with a tendency of overprediction. The slope determined by the Profile Method is around 1.33, indicating an overprediction of the friction velocity, resulting in an overprediction of the Monin-Obukhov length (L). Based on the relation between u_* and L found in 4.3, a shift from unstable and stable

conditions towards neutral conditions can be seen.
In the figure, a small scatter is visible which decreases the standard deviation and decreases the uncertainty of the stability estimation. Together with a high correlation (around 0.88) found in table 4.5, it can be concluded that the second Profile Method is most suitable to estimate the atmospheric stability based on the Cabauw data.

Gradient Richardson Number

For Gradient Richardson Number a very large scatter of u_* can be observed in figure 4.22. The largest scatter can be observed for small values of u_*, indicating the impact of measurements outside of the Surface Boundary Layer.
For the Gradient Richardson Number a tendency of overprediction is visible, resulting also in a shift from unstable and stable conditions to neutral conditions. However, due to the large scatter and low correlation of 0.13 without the Surface Boundary Layer filter (0.55 with the filter) a large uncertainty of the atmospheric stability estimation has to be expected.

Bulk Richardson Number

For the Bulk Richardson Number an overall overprediction of the u_* is clearly visible, with a slope of around 1.33. The overall overprediction results in a shift of unstable and stable conditions to neutral conditions.
The scatter is similar to the scatter of the Profile Method 2. However, for small values of u_*, a large scatter can be observed in the figure without the Surface Boundary Layer filter. Due to the big difference in correlation, between the data with and without using the Surface Boundary Layer filter (0.67 without and 0.91 with the filter), measurements outside of the Surface Boundary Layer result in a big scatter when the Richardson Number is used to determine the atmospheric stability. This corresponds to the findings of the Gradient Richardson Number.

Nevertheless the Bulk Richardson Number gives one of the closest estimations of the atmospheric stability based on the Cabauw data.

From the comparison of the u_*, it can be concluded that the Profile Method 2 and the Bulk Richardson Number are the recommended methods to estimate the atmospheric stability. Without the Surface Boundary Layer height as a filter, the results of the Profile Method 2 is the closest method. With the Surface Boundary Layer height as a filter, the Bulk Richardson Number gives a slightly better correlation in comparison to the Profile Method 2. The methods using the Richardson Number are more effected due to measurements outside the Surface Boundary Layer, than the Profile methods.

4.4.7 Heat flux ($\overline{w'\theta'_v}$) per method compared to the heat flux of the Eddy Covariance Method

As described in the previous section the Monin-Obukhov length (L) is determined from friction velocity u_* and heat flux ($\overline{w'\theta'_v}$). In this section, the main focus will be on the heat flux. In figure 4.24 and 4.25, eight plots are visible with a direct comparison of the heat flux determined with Eddy Covariance Method and one of the four methods used in this research. The x-axis shows the $\overline{w'\theta'_v}$ determined with the Eddy Covariance Method, and the y-axis shows the $\overline{w'\theta'_v}$ determined with the other methods.

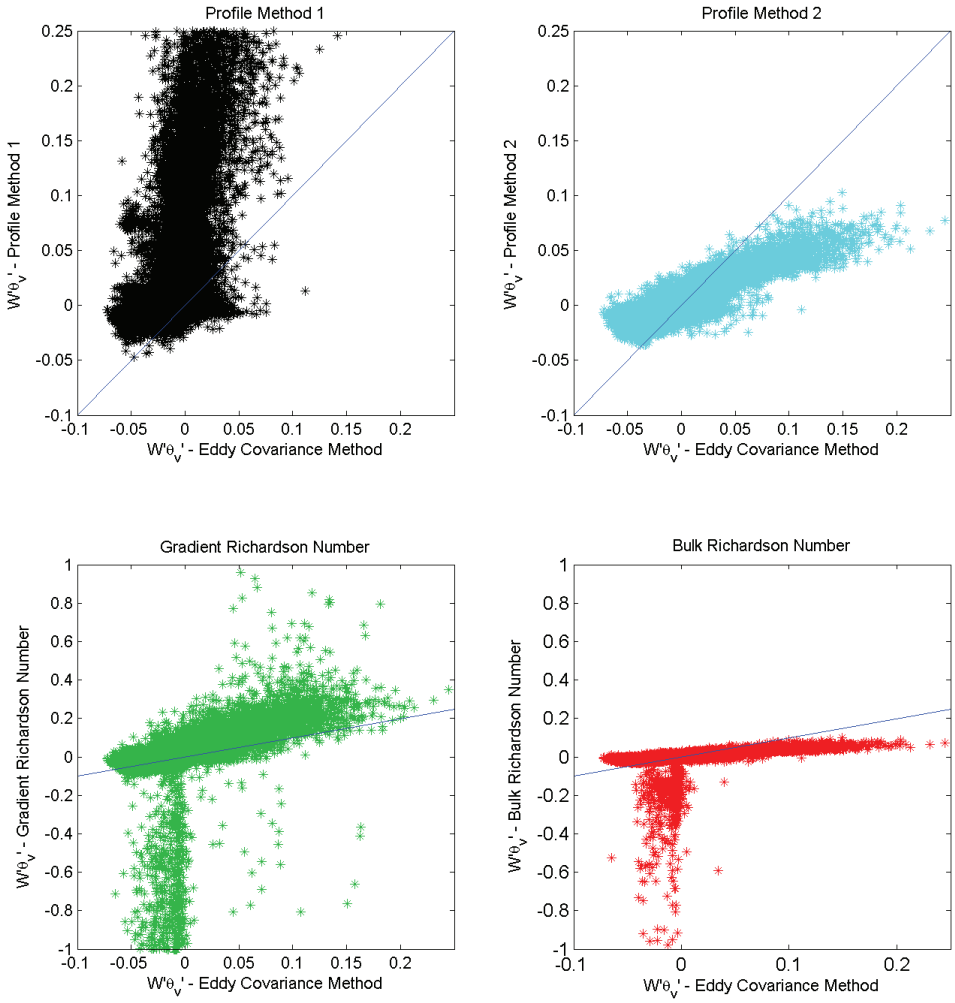

Figure 4.24: Cabauw - Comparison of Heat flux ($\overline{w'\theta'_v}$) without the filter for the Surface Boundary Layer height

The heat flux $\overline{w'\theta'_v}$ is determined in a similar manner as the friction velocity u_*, as described in section 4.4.6, by using equations 2.27, 2.28 and 2.29.

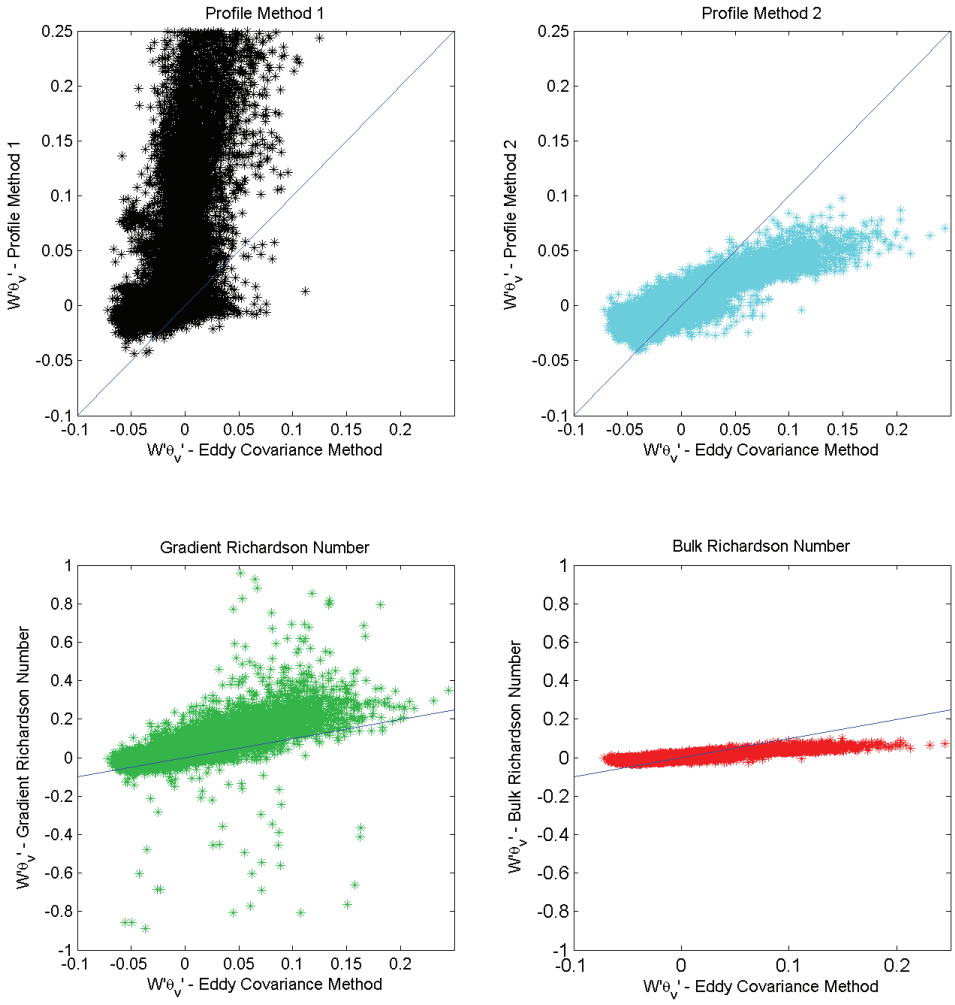

Figure 4.25: Cabauw - Comparison of Heat flux ($\overline{w'\theta'_v}$) with the Surface Boundary Layer height as a filter ($c_i = 0.15$ and $z_s = 10\%$ of z_i).

Method	$Slope$	$Slope_{SBL}$	R	R_{SBL}
Profile Method 1	3.78	4.6	0.37	0.40
Profile Method 2	0.38	0.38	0.86	0.87
Gradient Richardson Number	6.67	1.62	0.01	0.39
Bulk Richardson Number	0.38	0.31	0.02	0.88

Table 4.6: Correlation R - Heat flux ($\overline{w'\theta'_v}$) with $_{SBL}$ indicating the use of the Surface Boundary Layer height as a filter.

Profile Method 1

Looking at the heat flux estimation of the first Profile Method a significant overprediction is clearly visible with increasing error as $\overline{w'\theta'_v}$ increases. The slope of the data is around 4, indi-

cating that the heat flux prediction is on average around four times higher compared to the Eddy Covariance Method. The agreement of the heat flux is increased for negative values and values near zero of the $\overline{w'\theta'_v}$, thus for stable and near neutral conditions respectively. However, for positive values, unstable conditions, the error increases rapidly.
The overprediction of the $\overline{w'\theta'_v}$ results in an underprediction of Monin-Obukhov length (L), which based on the relation between $\overline{w'\theta'_v}$ and L found in 4.3 results in a shift from neutral to unstable conditions.

The big scatter found with the first Profile Method, is also clearly visible in the correlation of the $\overline{w'\theta'_v}$ determined using the Eddy Covariance Method shown, in table 4.6

Profile Method 2

The heat flux estimation of the second Profile Method is much closer to the heat flux estimation of the Eddy Covariance Method compared to the Profile Method 1. With a slope of 0.38, for large positive values of the heat flux, under unstable conditions, there is a tendency of underprediction. Which results in a shift from unstable to neutral conditions. For near neutral conditions respectively, there is a fairly good agreement of the heat flux. However, for negative values, which corresponds to stable conditions an increasing error is visible. In the end this results in a correlation of 0.86 without and 0.87 with the Surface Boundary Layer height as a filter.

Gradient Richardson Number

The Gradient Richardson Number heat flux estimations show a large scatter, mainly for negative values of the $\overline{w'\theta'_v}$. The estimation does not correspond to the Eddy Covariance Method results. This results in an overprediction of unstable conditions, which corresponds to the findings in the previous sections. Introducing the Surface Boundary Layer height as a filter, the scatter is significantly decreased with an increase in correlation from 0.01 to 0.39. The slope is also drastically decreased from 6.57 to 1.62. Once again showing the impact of measurements outside of the Surface Boundary Layer on the atmospheric stability estimation for methods based on the Richardson Number.

Bulk Richardson Number

The Bulk Richardson Number heat flux estimations shows large scatter for negative values, unstable conditions, similar to the findings of the Gradient Richardson Number. For stable conditions, positive values of the $\overline{w'\theta'_v}$ there is a very good agreement of both estimations. This results in a very low correlation, $R = 0.02$, when the Surface Boundary Layer filter is not used and a high correlation, $R = 0.88$ when the filter is used. Similar to the results of the Profile Method 2, the slope is around 0.38 with a decrease in slope when the SBL filter is used. A significant underprediction of the heat flux $\overline{w'\theta'_v}$ results in an overprediction of Monin-Obukhov length (L), resulting in a shift from extreme to neutral conditions.

4.5 Statistical analysis of the friction velocity (u_*) and heat flux ($\overline{w'\theta'_v}$) for multiple measurement heights

Until now, in this research a maximum measuring height of 40 meters is used, because this resulted to the most suitable indications based on a short survey. However, only available measurement heights can be used which often do not correspond with the preferred measurement height. In this section a brief analysis will be conducted, looking at the slope and correlation of the friction velocity and heat flux measurements for different heights and different methods.

In figure 4.26 and 4.27, the slope and correlation of respectively the friction velocity and heat flux are shown. The left side of the figures indicating the slope and the right side the correlation. The top two figures show the results without the Surface Boundary Layer height filter and the bottom two with.

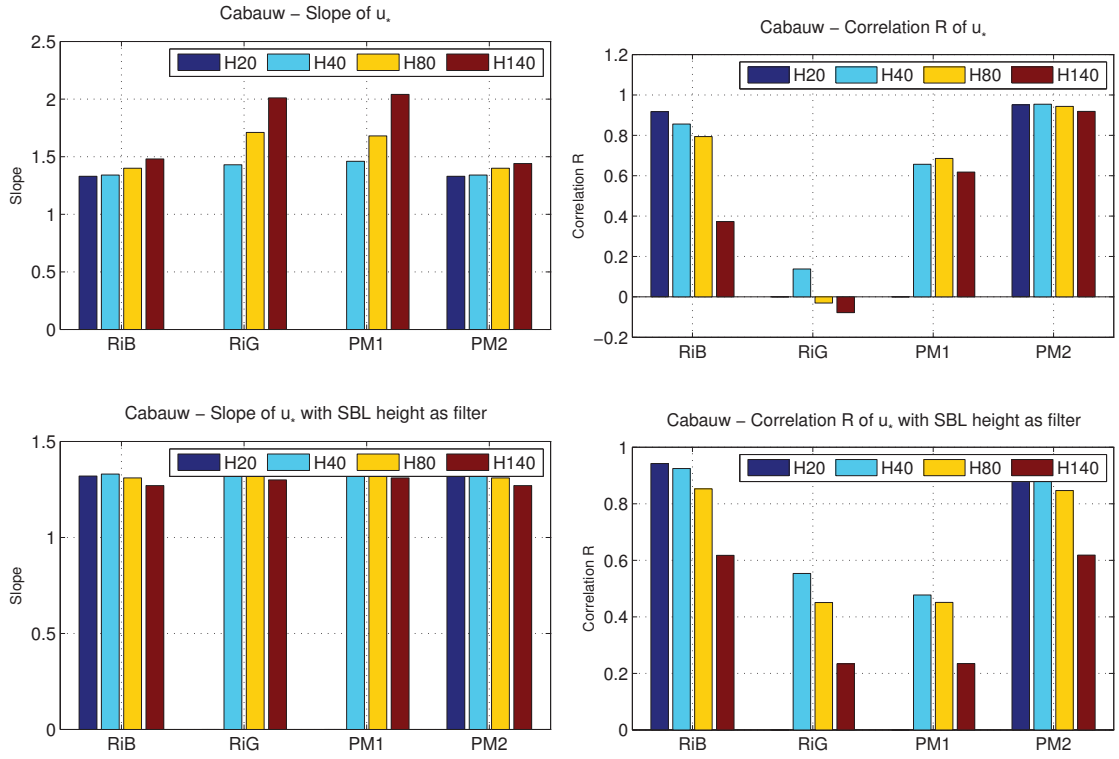

Figure 4.26: Cabauw - Slope (left) and Correlation (right) of Friction Velocity (u_*) with and without the Surface Boundary Layer height as a filter for four methods.
RiB - Bulk Richardson Number, RiG - Gradient Richardson Number, PM1 - Profile Method 1, PM2 - Profile Method 2

4.5.1 Friction velocity

An over-prediction of the friction velocity for all methods can be observed, with significant differences between results using different measurement heights for both the Gradient Richardson Number and Profile Method 1. For these methods, a measurement height of 20 meters resulted in unrealistic atmospheric stability estimations, therefore the results are excluded from the plots.

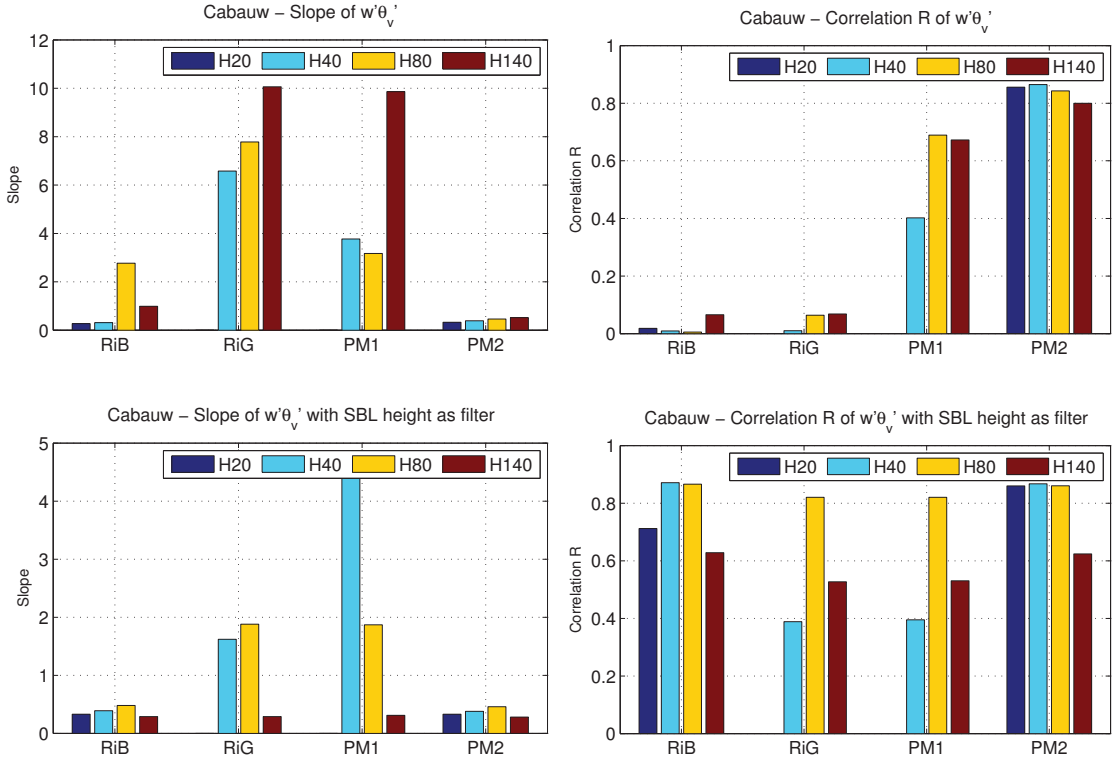

Figure 4.27: Cabauw - Slope (left) and Correlation (right) of Heat flux $(w'\theta'_v)$ with and without the Surface Boundary Layer height as a filter for four methods.
RiB - Bulk Richardson Number, RiG - Gradient Richardson Number, PM1 - Profile Method 1, PM2 - Profile Method 2

The profile Method 2 and Bulk Richardson Number giver very similar results, with a slope of around 1.4 for all measurement heights.

The correlation of the friction velocity for both the Gradient Richardson Number and Profile Method 1 is very low. For the Gradient Richardson Number without the Surface Boundary Layer filter the correlation is in some cases even negative. The correlation for the Bulk Richardson Number is strongly depended on the measurement height. The highest correlation can be found using a height of 20 meters and the lowest using 140 meters. This supports the findings in previous sections, that especially the Richardson Number methods are significantly influenced when the measurements are outside of the Surface Boundary Layer. It could, however, be a result of different conditions at different levels in the atmosphere. Comparing the correlation of the friction velocity using different measurement height for the Profile Method 2, results in very consistent and correlation values.

4.5.2 Heat flux

Similar to the results of the friction velocity, the results of the Gradient Richardson Number and Profile Method 1 show high scatter using different heights. For the Bulk Richardson Number and Profile Method 2, a significant underprediction of the heat flux can be observed, with a slope of around 0.4 (depended on method and measurement height).

Due to the large differences between the results using different measurements heights it can be concluded that the Gradient Richardson Number and Profile Method 1 are not recommended methods to estimate the atmospheric stability.

The second Profile Method is in terms of correlation but also in terms of slope much more consistent in the results, mainly for the heat flux. The Richardson Number methods requires the Surface Boundary Layer filter in order to provide acceptable correlations. Depended on the height this will however result in significant data reductions.

If we look at both the friction velocity and the heat flux of the Bulk Richardson Number and Profile Method 2 a small trend can be observed. The slope improves using higher measurements heights, while the correlations decrease with increasing height. In the determination of the atmospheric stability, the preference is given to moderate heights.

4.6 Summary & Conclusions based on the Cabauw data

In this chapter, atmospheric stability analysis is executed using five methods applied on the 2011 Cabauw data. Before the analysis could be executed, two filter types were selected to handle the data correctly. First, all extreme values and sensor errors were removed from the dataset. Secondly the steady state check is executed. MOST requires stationary flow and the steady state filter removes data points for which the deviation from previous values exceeds certain conditions, as explained in section 4.3.1.

Four of the five methods to determine the atmospheric stability are based on MOST, which is only valid in the Surface Boundary Layer. The height of the top measurement must not exceed the Surface Boundary Layer height, otherwise this results in large scattering of the friction velocity and heat flux. However, depending on the height of the top measurement a large data reduction is possible, resulting in a bad representation of the stability distribution. Therefore a maximum measurement height of 40 meter is selected to ensure a minimum distortion of the stability estimation outside of the Surface Boundary Layer, when the filter is not applied in the dataset. In the last section 4.5, a short statistical analysis is executed using multiple measurement heights, exceeding the previous stated 40 meters to validate results in a larger range of heights and verify the assumptions.

For each method a brief summary will be given:

- **Profile Method 1**

  The Profile Method 1, based on the Cabauw data, shows a tendency to over predict unstable conditions. For the determination of the friction velocity and heat flux, large scattering was found, especially for unstable conditions. The tendency to unstable conditions and large uncertainty of the estimation is also found in multiple papers of Sathe [45][46], where they did an analysis, based on the wind profile corrections.
  Based on the findings in this research and in literature it can be concluded that the Profile Method 1 is not a recommended method to estimate the atmospheric stability.

- **Profile Method 2**

  Based on the Cabauw data, it is found that the Profile Method 2 has a tendency to predict near neutral condition and underpredict extreme conditions. The scattering of the friction velocity and heat flux estimated with the Profile Method 2 is smaller, resulting in a better overall agreement. The previous section showed that the Profile Method 2 is very consistent in the estimation of the friction velocity and heat flux. For different measurement heights small differences in results were observed. A small preference goes to moderate heights, around 40-60 meters. The tendency towards neutral conditions and small scattering of the friction velocity and heat flux agrees with the findings in multiple papers of Sathe [45] [46] at OWEZ. Based on the findings in this research and in literature it can be concluded that the Profile Method 2 is a recommended method to estimate the atmospheric stability.

- **Gradient Richardson Number**

  It is found that the Gradient Richardson Number has a tendency towards near neutral and unstable conditions. Similar to the results of the Profile Method 1, a large scatter of the friction velocity and heat flux can be found. Adding the Surface Boundary Layer filter results in large reduction of the scatter. The large scatter corresponds to findings in multiple papers of Sathe [45] [46]. Based on the findings in this research and in literature it can be concluded that the Gradient Richardson Number is not a recommended method to estimate the atmospheric stability.

- **Bulk Richardson Number**

  The results of the Bulk Richardson Number are very similar to the Profile Method 2, because they both use the same temperature and wind speed measurements to determine the atmospheric stability, resulting in a tendency towards near neutral conditions and underprediction of extreme conditions for the Bulk Richardson Number.

  A large scatter was found for both the friction velocity and heat flux, especially for unstable conditions. Based on the Cabauw data, it seems that both methods based on the Richardson Number are greatly influenced by measurements outside of the Surface Boundary Layer. By adding the Surface Boundary Layer filter a large reduction of the scattering is achieved and finally results in the best overall agreement of the atmospheric stability distribution using a measurement height of 40. However, using measurements of different heights leads to a significantly different results and the Surface Boundary Layer filter is required for a low scatter.

  The research of Sathe [45] [46] at OWEZ showed similar results. Large scatter for the Bulk Richardson Number without the Surface Boundary Layer filter and the overall best method when the Surface Boundary Layer filter is used. The results of the Bulk Richardson Number and the Profile Method 2 were very similar to each other, which also corresponds to the findings of the current work presented in this thesis. The research of Lange et al. [36] showed direct comparing the Bulk and Gradient Richardson Number, resulting in a good approximation of the wind profile for the Bulk Richardson Number and with a large error using the Gradient Richardson Number under stable conditions. In the research of Peña [43] a direct comparison of the Monin-Obukhov length for Eddy Covariance Method and the Bulk Richardson Number, resulting in a high correlation using a limited range. Based on the findings in this research and in literature it can be concluded that the Bulk Richardson Number is a recommended method to estimated the atmospheric stability, however the impact of measurement outside the Surface Boundary Layer have to be taken into account by applying a suitable filter.

The following preliminary conclusions could be made based on the Cabauw data:

1. Significant differences between four atmospheric stability methods are observed, with very high scatter for some methods. Therefore the selection of the **measurement height, filters and method** is of **utmost importance for the quality** of the atmospheric stability estimation.

2. The best results are obtained with Bulk Richardson Number (with 0-40 meter measurements) using the Surface Boundary Layer filter. However, the Profile Method 2 gives similar results and is more consistent using different heights. Also the quality of the second Profile Method is not dependent on the Surface Boundary Layer filter. Therefore the Profile Method 2 gives the overall best results in the estimation of the atmospheric stability.

3. Methods based on the Richardson Number are strongly influenced by measurements outside of the Surface Boundary Layer, resulting in very high scatter of both the friction velocity and heat flux estimations. However, using the Surface Boundary Layer filter results in a large reduction of the data, which perhaps leads to a incorrect atmospheric stability distribution.

4. Possible improvement for the distribution of the atmospheric stability is a combination of the Bulk Richardson Number and the Gradient Richardson Number, based on time or wind speed. The Gradient Richardson Number has a small tendency to unstable conditions, during the day or for low wind speed the Gradient Richardson Number gives a better agreement.

4.7 Additional classification systems

The main focus of this thesis is discussed in previous sections. As an extension in this section, two additional classification systems will be compared to Eddy Covariance Method using a sonic anemometer at a height of 5 meters: the Pasquill-Gifford Method and Large-Eddy Simulation.

4.7.1 Pasquill-Gifford Method

As described in section 2.5.1 the Pasquill-Gifford Method uses basic meteorological data to estimated the atmospheric stability. According to the Pasquill-Gifford Method the atmospheric stability is distributed into seven classes.

A	Extremely unstable
B	Moderately unstable
C	Slightly unstable
D	Neutral
E	Slightly stable
F	Moderately stable
G	Extremely stable

Table 4.7: Pasquill-Gifford Classification system)

In figure 4.28, the distribution per wind speed bin and yearly distribution is shown for Cabauw based on the Pasquill-Gifford Method. It can be observed that 67% of the time the atmospheric conditions are near-neutral according to Pasquill-Gifford Method, with only slightly more than 25% stable and very stable. Almost no very unstable and unstable conditions can be observed.

Comparing these results with the results of the Eddy Covariance Method, in figure 4.6, it can be seen that there is a significant overprediction of near neutral conditions and underprediction of stable and unstable conditions. This is mainly because according to the Pasquill-Gifford Method the conditions are almost always near-neutral with wind speeds above 6 m/s at a height of 10 meters, except during the day with very high insulation. The overprediction of near-neutral conditions corresponds with results found in literature [54]. Comparing the distributions of the Pasquill-Gifford and the Eddy Covariance Method show that they are not in agreement with each other.

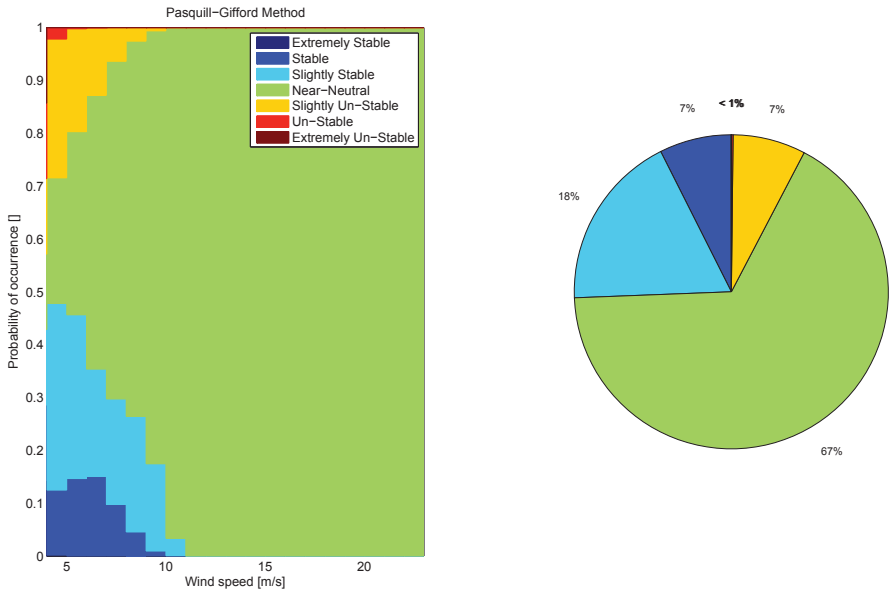

Figure 4.28: Cabauw - Pasquill Gifford Method

Besides the poor agreement of the distribution, the Pasquill-Gifford Method can not be applied to offshore locations. This is because the Pasquill-Gifford uses the insulation of the sun, the cloud coverage and the coupled heating of the surface. However, this is not applicable for offshore locations, due to the high heat capacity and mixing of layers the water surface temperature fluctuates gradually. This will result in an overprediction of near-neutral when the Pasquill-Gifford Method is used.

Because of the above mentioned two reasons, it was decided not to proceed with the Pasquill-Gifford method.

4.7.2 Large-Eddy Simulation

In this subsection, a comparison of the atmospheric stability determined with the LES model and sonic measurements at Cabauw will be executed using a weather model of the Royal Dutch Meteorological Institute (KNMI) with the pressure gradient, initial conditions and lateral forcing as input of the LES model. Measurements of multiple meteorological sites throughout the Netherlands including the Cabauw met mast are used as input for the KNMI weather model.

Within the LES model the Monin-Obukhov length (L) is determined at surface level. Comparing the atmospheric stability with the sonic measurements is executed in two ways. First, by divid-

ing the Monin-Obukhov length in discrete classes according to table 4.4 and using a PDF for continuous comparing.

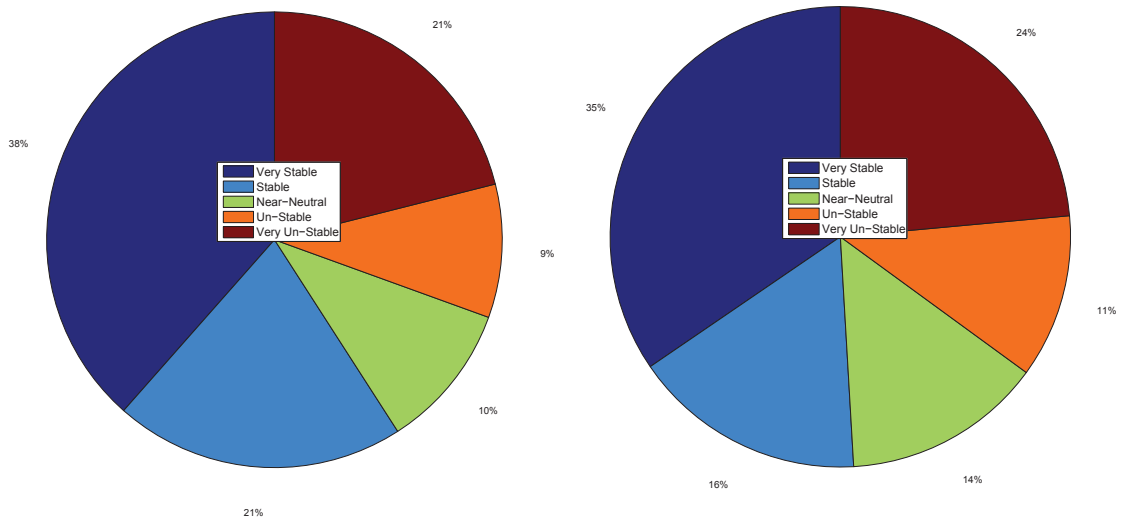

Figure 4.29: Cabauw - Atmospheric stability distribution of the (left) Eddy Covariance Method and (right) LES model

It can be observed that the distributions in figure 4.29 and 4.30 are very similar. In terms of the overall distribution only very small differences can be seen with a maximum deviation of 5%. From figure 4.30, it can be observed that the stable and very stable conditions are under predicted by the LES model. The neutral and unstable conditions are therefore overpredicted.

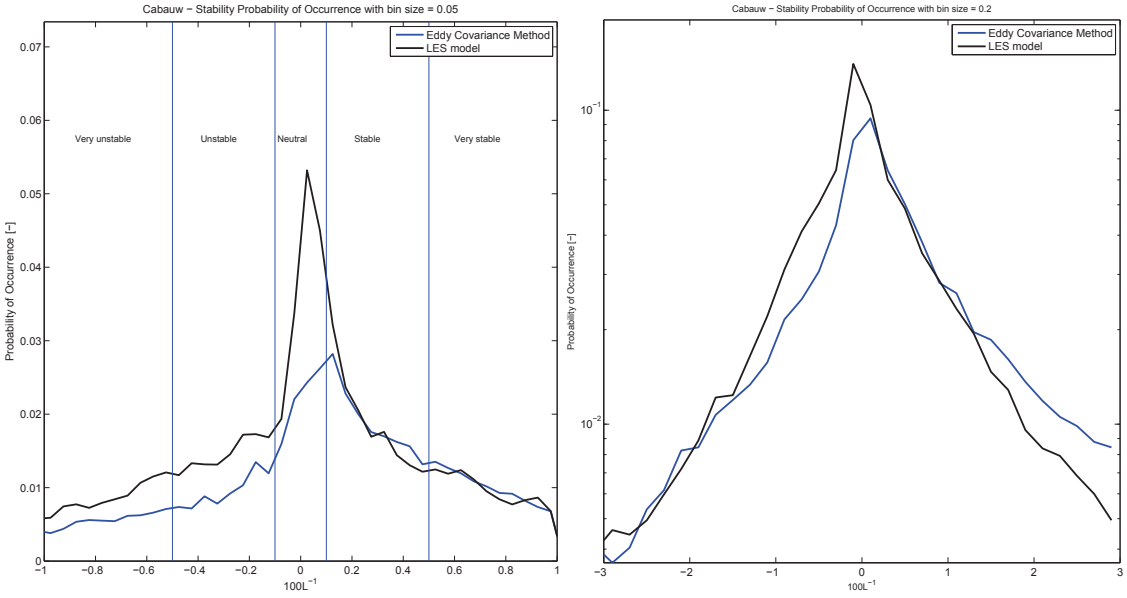

Figure 4.30: Cabauw - PDF comparing the Eddy Covariance Method and LES model

The atmospheric stability estimation of the LES model and the Eddy Covariance Method are very close to each other. The results are more accurate than the Profile Method 2. One of the reasons for which the results are so close to each other, is that the LES model uses a weather model which uses as input of the Cabauw met mast data. It is therefore unclear how good the atmospheric stability estimation will work when the same method is used at a different location.

An additional advantage of the use of the LES model is that one can directly determine the wind profile from the output. Therefore, the use of the LES seems promising, but further research is required. The atmospheric stability estimation on a different location can be investigated and a comparison of the wind profile would be possible. Further investigation could give insight and determine whether, if measurement campaigns on the specific location are still required and whether a LES model can be used.

Chapter 5

Atmospheric stability analysis - Lindenberg Boundary Layer Measurement Tower

5.1 Introduction

The German Weather Service (DWD), similar to the KNMI, has multiple meteorological measurement programs. The Lindenberg Boundary Layer Measurement Tower is part of this program, located near Lindenberg-Falkenberg about 65 kilometre Sout-East of Berlin. The basic installation was completed in 1998 with gradually expansion of the measurement equipment over the years. The site houses several measurement systems, as can be seen in figure 5.1, and it is surrounded by rural landscape consisting of crop-lands, meadows, forest and lakes.

The Lindenberg site consisting of small 10 meter tower, a main tower of 99 meters, measurements of vertical soil moisture & temperature profiles and radiation & turbulent fluxes. The main tower is equipped with sensors to measure wind speed, wind direction, temperature and humidity at heights of 10, 20, 40, 60, 80 and 98 meter. Equiped also with sonic measurement equipment at heights of 2, 50 and 90 meter. In order to ensure minimum influence of the tower structure on the data, the main tower has three booms on each level, pointing approximately towards North, South and West, mounted on a lattice construction.

The basic meteorological data are measured at the small 10 meter mast, and the pressure is measured in the vicinity with the help of a pressure sensor. The radiation and soil measurements (surface temperature etc.) are located approximately 120 meter South of the small mast. The flux measurements are performed using omni-directional sonic anemometer thermometers. The sonic measurement equipment at the tower are mounted at booms pointing approximately towards the South (191°).

The Lindenberg Boundary Layer Measurement Tower data were obtained from ICDC, CliSAP/ KlimaCampus, University of Hamburg from January 1 to December 31, 2010.

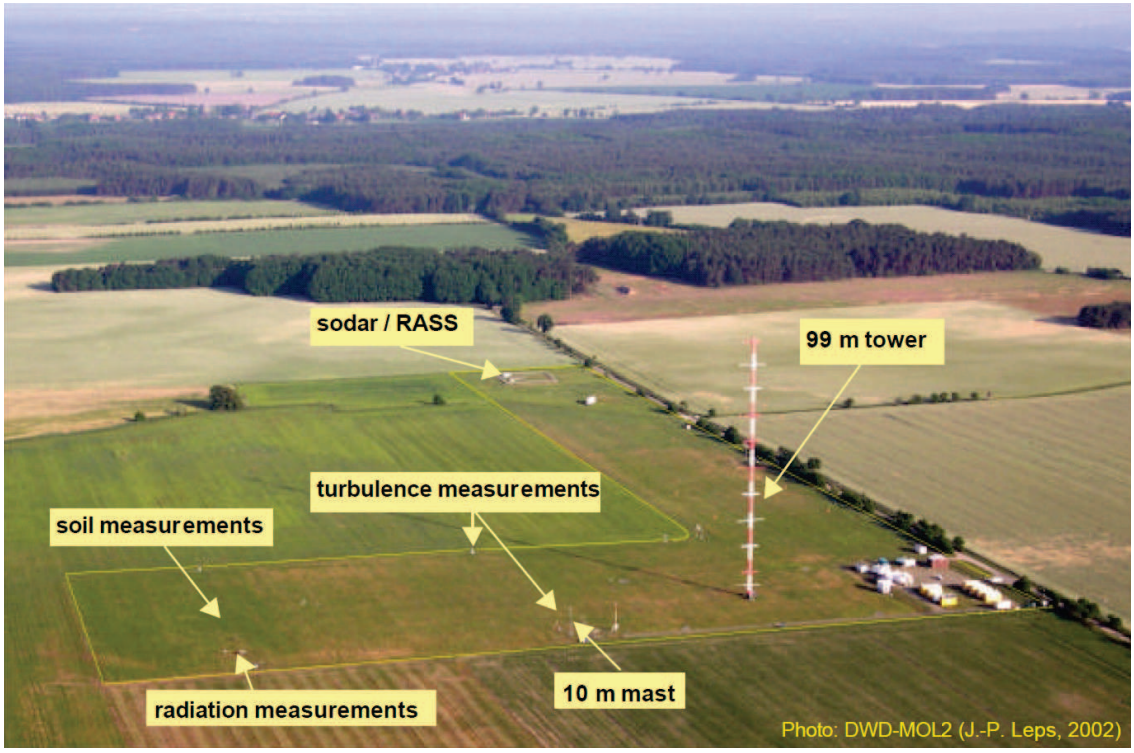

Figure 5.1: Lindenberg-Falkenberg Field Site.

5.2 Data processing

Before the atmospheric stability can be determined from the given data, a couple of factors have to be taken into account.

- Data filtering
- Tower shading
- Selection of measurement height

5.2.1 Data filtering

Data filtering is of utmost importance for the validity of the data and research. The Lindenberg data is therefore, similar as explained in chapter 4.3.1 filtered using two filters.

- Operational conditions & sensor errors
- Steady state conditions

Both filters are extensively explained in the chapter 4.3.1 and therefore will not be explained in detail. Using both filters on the Lindenberg data resulted in a reduction of data of around 54%, which can be divided into a reduction 46% due to the operational conditions filter and 18% of the steady state conditions filter, with a small overlap when both filters are used.

5.2.2 Tower shading

At each level, three sensors pointing approximately North, South and West are used to ensure minimum influence of the tower structure on the data. However, sonic measurements are only measured at one boom pointing South (191°). Therefore the sonic measurement data is influenced by the tower structure for wind directions from the sector 330°-50° [1]. This data therefore will be filter, resulting in a slight revised operational conditions filter compared to the filter used with the Cabauw data.

$4 \leq$	Wind speed	≤ 25 [m/s]
$50 \leq$	Wind direction	≤ 330 [°]
$263 \leq$	Temperature	≤ 308 [K]

Table 5.1: Filter conditions for wind speed, wind direction and temperature.

5.2.3 Selection measurement height

In chapter 4, it is observed that measurements outside of the Surface Boundary Layer have significant effect on the results of the atmospheric stability estimation. As a result of this observation a measurement height of 40 meters is selected for the methods based on MOST.

[1] Derived from personal communication with Mr. U. Rummel at the German Weather Service (DWD)

5.3 Results - Lindenberg Boundary Layer Measurement Tower

In this chapter, the Lindenberg data is used to analyse the behaviour of multiple methods to estimate the atmospheric stability and execute a comparison with the Eddy Covariance Method based on sonic measurements at three heights. The main difference between the Lindenberg and Cabauw data is that at Cabauw only sonic measurements at a height of 5 meters are available.

5.3.1 Overall statistics of atmospheric stability

For the overall statistics of Lindenberg, the distribution per year of multiple methods is compared to the Eddy Covariance Method, assuming that the Eddy Covariance Method gives the best representation of the real atmospheric stability.

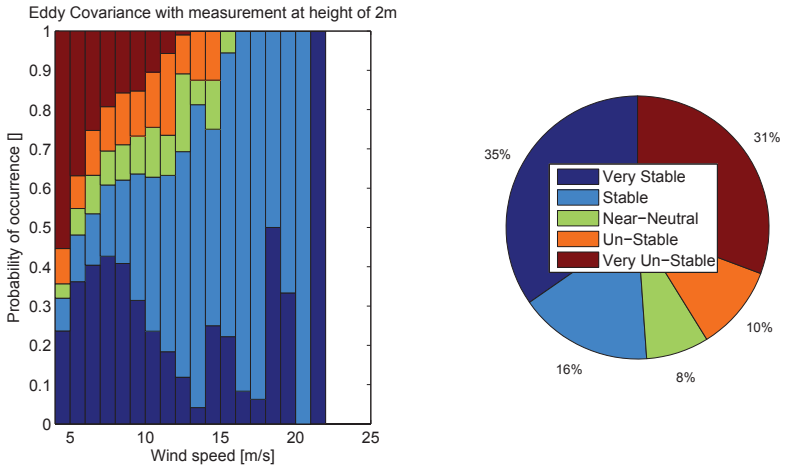

Figure 5.2: Lindenberg - Eddy Covariance Method with sonic measurements at a height of 2m.

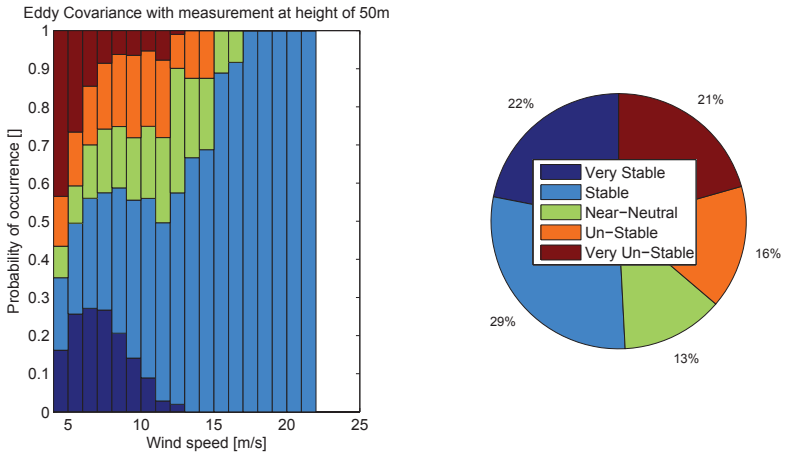

Figure 5.3: Lindenberg - Eddy Covariance Method with sonic measurements at a height of 50m.

Figures 5.2, 5.3 and 5.4, at heights of 2, 50 and 90 meters respectively, show the stability distribution according to the Eddy Covariance Method divided into five classes. On the left side, the

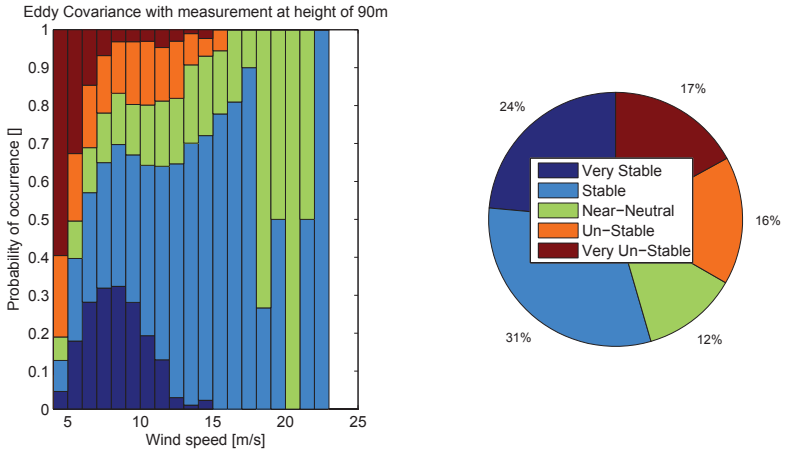

Figure 5.4: Lindenberg - Eddy Covariance Method with sonic measurements at a height of 90m.

stability per wind speed bin is shown and on the right side the yearly distribution. The specification of the five classes can be found in table 4.4 in section 4.4.1. A number of observations can be made.

- Large differences, up to 15% can be observed between the distributions determined using the Eddy Covariance Method at different heights. This is opposing to the assumption made by Monin-Obukhov that the momentum and heat fluxes are constant in the Surface Boundary Layer. It can be partly explained by the fact that the sonic measurements at times are outside of the Surface Boundary layer.
  The Eddy Covariance Methods at three heights shows that the extreme conditions, that is very unstable and very stable, decrease with increasing height and that leads to the corresponding increase of near neutral conditions.

From figures 5.5 and 5.6 the following observations can be made:

- The four methods, Profile Method 1 & 2, Gradient & Bulk Richardson Number give very similar results with respect to the near neutral conditions. For very unstable and very stable the difference however is almost 20%.
  For very unstable conditions, an over prediction of all four methods is clearly visible in figures 5.6 and 5.5. For the Profile Method 1 and the Gradient Richardson Number this can lead to an over prediction of 30% or more. The stability estimations of the Profile Method 2 and Bulk Richardson Number are much closer to the Eddy Covariance Method, especially for very unstable and very stable conditions. Preliminary results show therefore a preference for the Profile Method 2 and Bulk Richardson Number, similar to the results found in Cabauw and in the literature analysis presented in chapter 2.

- Both the Profile Method 2 & Bulk Richardson Number give a close approximation of the stability when compared to the Eddy Covariance Method. The distribution calculated by both methods are the closest to the conditions found with the Eddy Covariance Method near the surface.

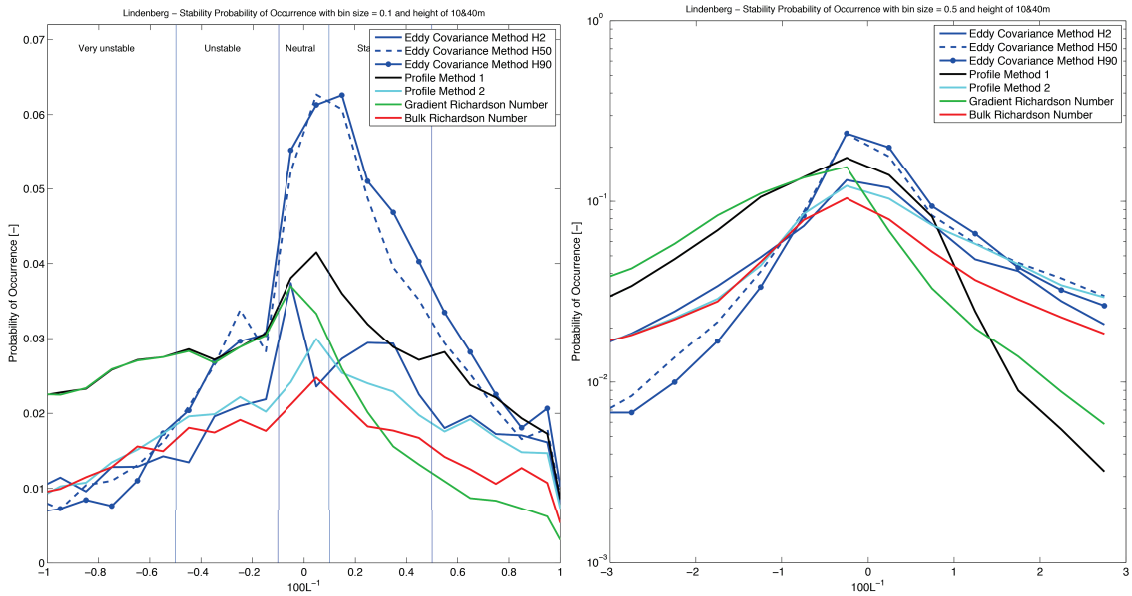

Figure 5.5: Lindenberg - Comparison of Atmospheric Stability Distribution with the PDF of the stability parameter $\frac{z}{L}$. The left figure is plotted on normal scale and the right figure on semi-logarithmic scale.

Similar to the analysis executed on the Cabauw data, a comparison on multiple levels is executed to obtain a better overview of the best method to determine the atmospheric stability. The comparison is mainly conducted against the Eddy Covariance Method at 50 meters, which will be discussed in this chapter. The measurement height of 50 meters is selected, because of two reasons. First, the previous results showed that sonic measurements near the surface leads to more extreme conditions and therefore higher measurements give a better representation of the conditions observed by the wind turbine. Secondly, MOST is only applicable within the Surface Boundary Layer and therefore the measurement height of 50 meters will be better compared to the one at 90 meters. A total overview of the Lindenberg results can be found in appendix C.2.

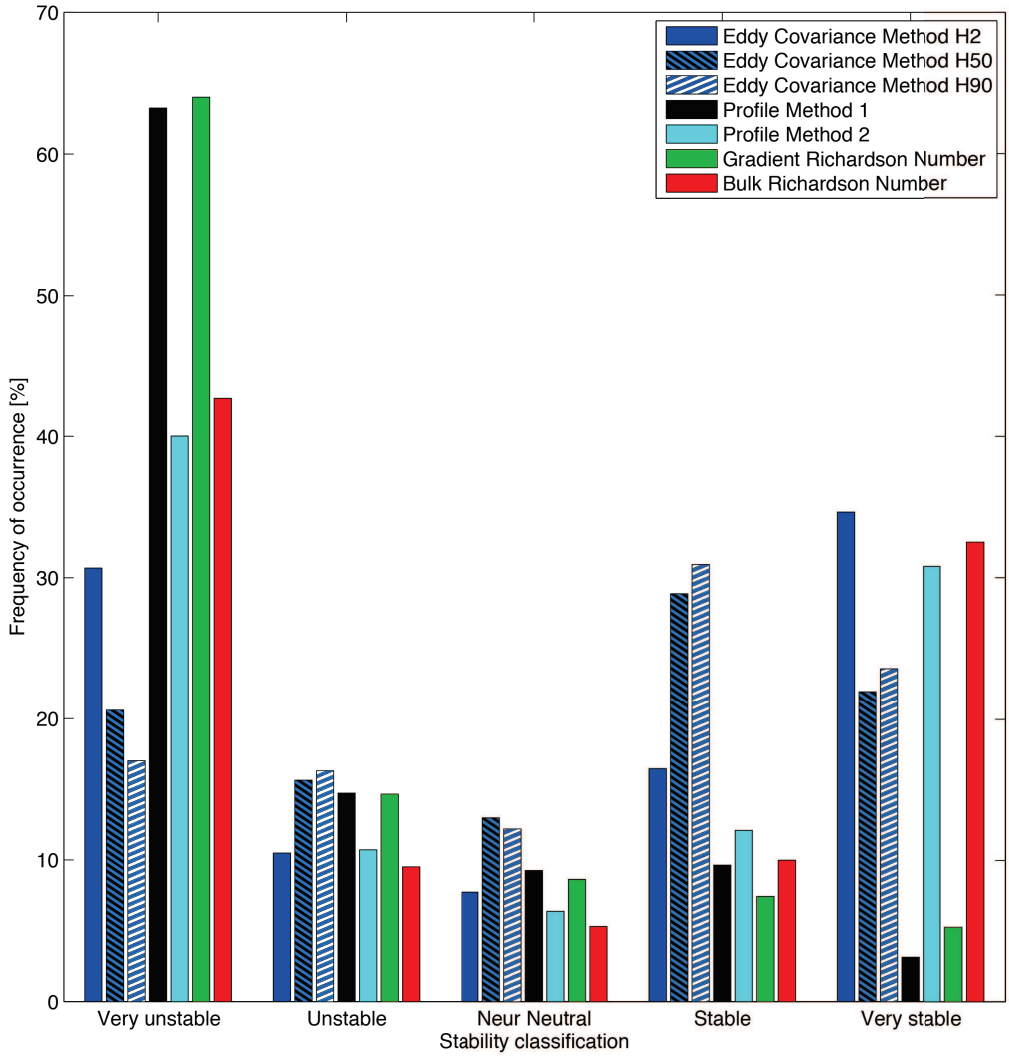

Figure 5.6: Lindenberg - Comparison of Atmospheric Stability Distribution divided into five classes.

5.3.2 Atmospheric stability distribution per hour of the day

The comparison of the atmospheric stability for each hour of the day, distributed into five stability classes, showed some differences compared to the results found at Cabauw. The majority agreed well with the results found at Cabauw. For example, most appropriate method was the Profile Method 2 demonstrating the highest accuracy when compared to the Eddy Covariance Method at Cabauw.

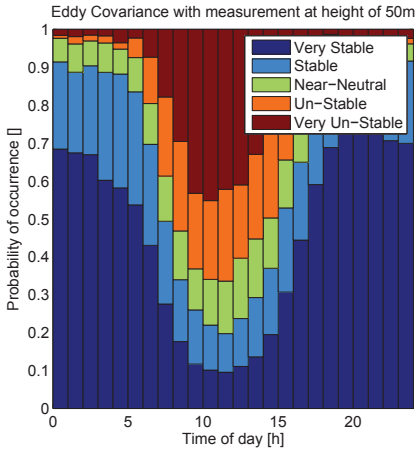

Figure 5.7: Lindenberg - Hourly distribution of Eddy Covariance Method at a height of 50m.

However, based on the Cabauw data, a possible improvement of the atmospheric stability estimation could be achieved by combining Profile Method 2 with the Gradient Richardson Number, by selecting the Profile Method 2 for night time and the Gradient Richardson Number for the day time. A closer look at the Lindenberg data, figures 5.7 and 5.8 revealed that the Gradient Richardson Number gives a significant overprediction of unstable conditions during the day. Therefore, combining the Profile Method 2 and the Gradient Richardson Number did not result in an improvement of the stability estimation.

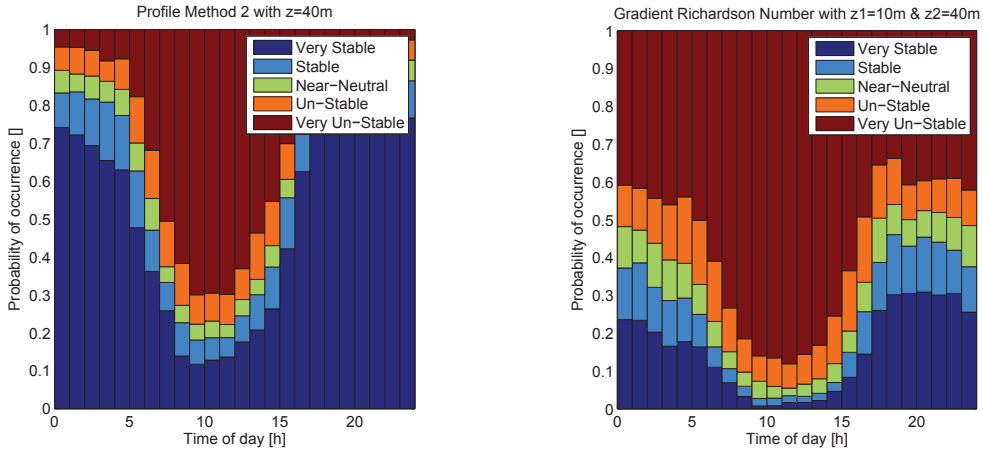

Figure 5.8: Lindenberg - Hourly distribution of (left) Profile Method 2 and (right) Gradient Richardson Number.

5.3.3 Friction velocity (u_*) per method compared to the friction velocity of the Eddy Covariance Method

Different aspects of the atmospheric stability distribution are observed. The atmospheric stability was compared based on the Monin-Obukhov length (L). The Monin-Obukhov length (L) is a function of the friction velocity (u_*) and heat flux $(\overline{w'\theta'_v})$. In this section, a comparison of the friction velocity of each method with the friction velocity determined using the Eddy Covariance Method. Firstly, a direct comparison of the friction velocity determined by the Eddy Covariance Method using multiple measurement heights. The x-axis of the left figure 5.9 shows the u_* determined with the Eddy Covariance Method at a height of 2 meters and the y-axis shows the u_* determined with the Eddy Covariance Method at a height of 50 meters. The right figure uses the u_* determined with the Eddy Covariance Method at a height of 50 meters on the x-axis and on the y-axis a height of 90 meters.

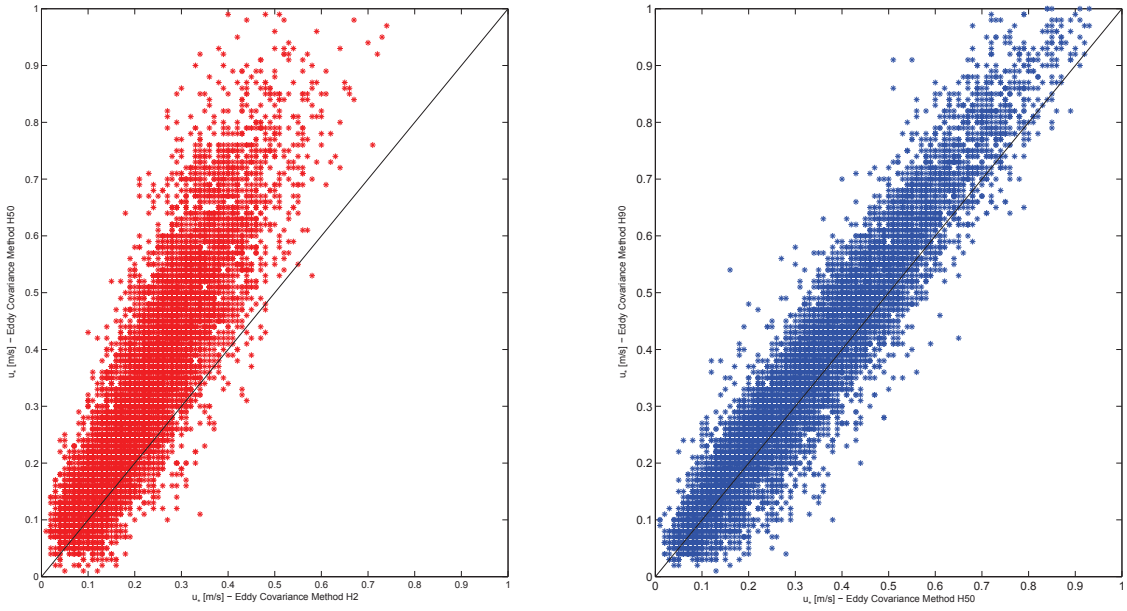

Figure 5.9: Lindenberg - Comparison of u_* determined with the Eddy Covariance Method on the left at a height of 2 and 50 meters and on the right at a height of 50 and 90 m.

From this figure a trend of increasing u_* with height is clearly visible, which is unexpected. By definition $u_* = 0$ at the top of the Boundary Layer [53]. However, the increase in friction velocity with height reflects the non-uniform (disturbed) fetch conditions in the surroundings. Due to varying vegetation of agricultural areas, forests and villages the friction velocity could increase with height.[2], which is often expressed by kinks in the wind profiles.

Next the friction velocity of each method is compared to the Eddy Covariance Method at a height of 50 meters in figures 5.10 and 5.11. Figure 5.10 shows the comparison when the Surface Boundary Layer height filter is deactivated and figure 5.11 when this filter is activated.

In table 5.2, two parameters are shown for the three heights of the Eddy Covariance Method. The slope between the friction velocity u_* determined using the Eddy Covariance Method and

[2]Derived from personal communication with Mr. U. Rummel at the German Weather Service (DWD)

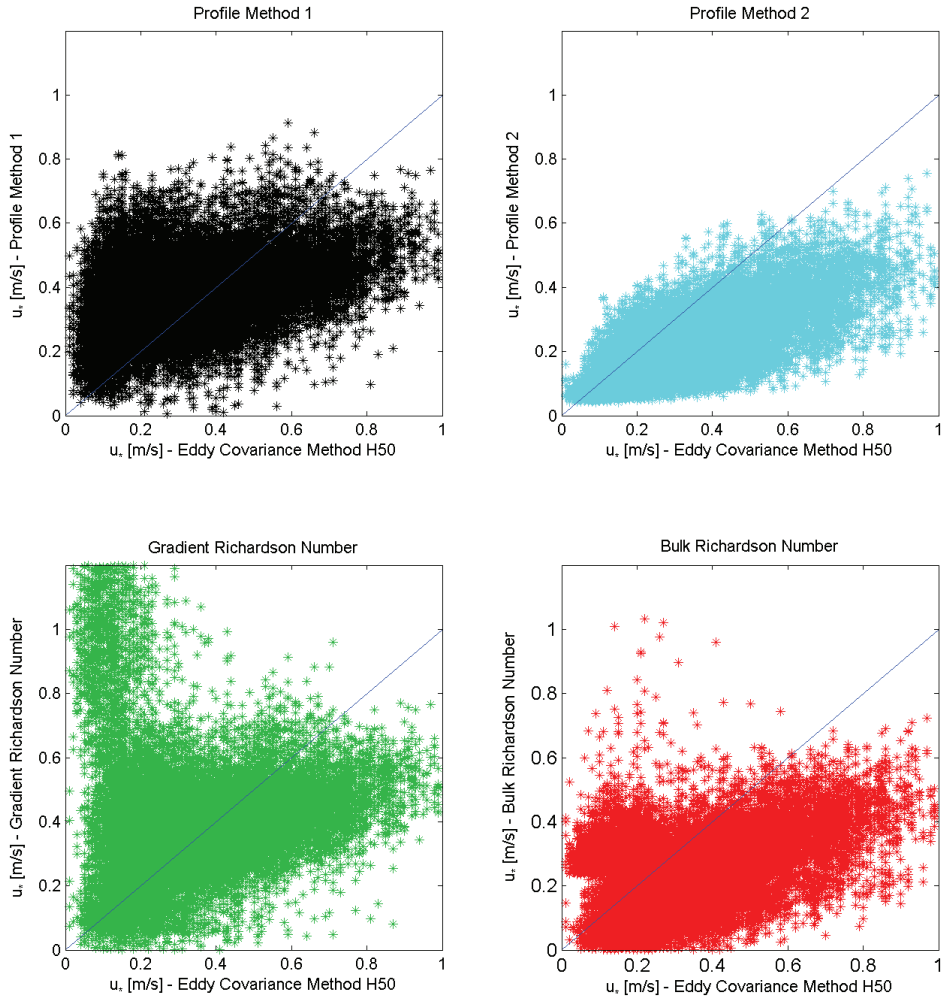

Figure 5.10: Lindenberg - Comparison of Friction Velocity (u_*) with sonic measurements at 50m without the filter for the Surface Boundary Layer height.

one of the other methods used in this research. The second parameter is the correlation R, which indicates how closely the two variables match.

- **Profile Method 1**

  In figures 5.10 and 5.11 a small underprediction of the friction velocity can be observed compared to the Eddy Covariance Method. This corresponds to a slope of 0.90, found in table 5.2. The underprediction results in a overprediction of the Monin-Obukhov length (L) and based on the relation between u_* and L found in 4.3, a shift from unstable and stable conditions to neutral conditions can be seen.

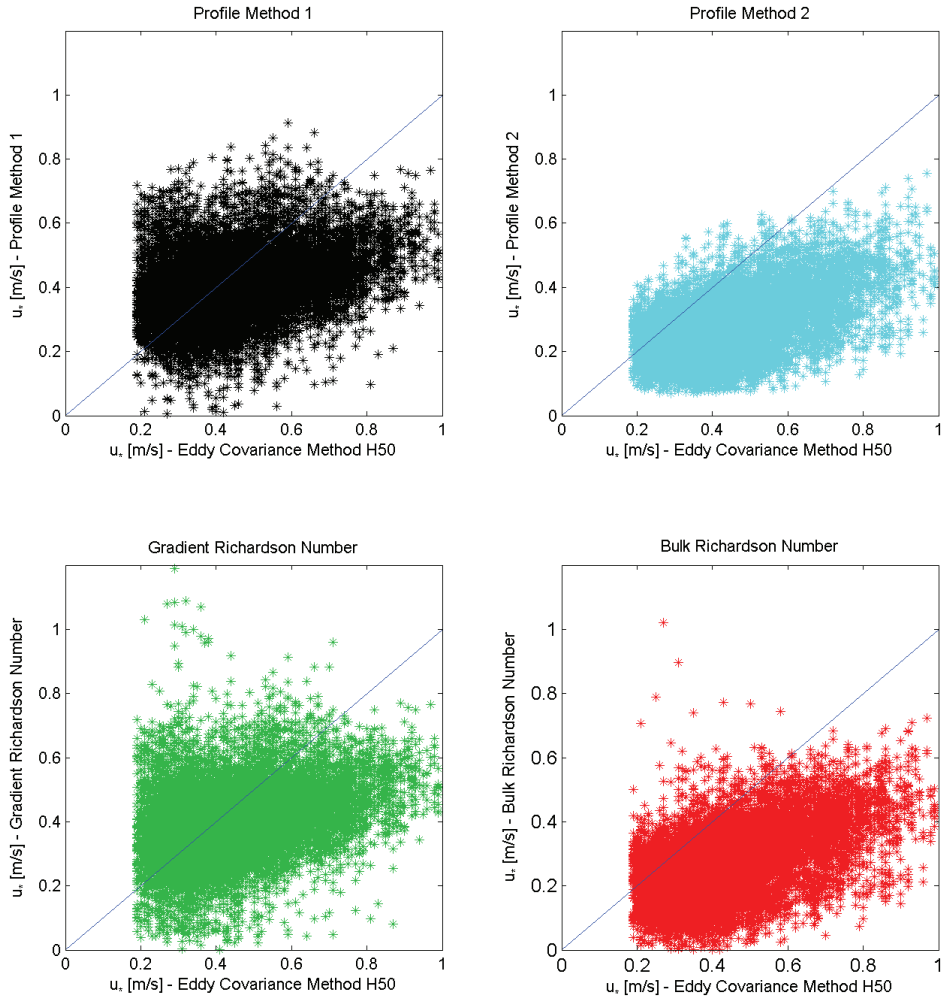

Figure 5.11: Lindenberg - Comparison of Friction Velocity (u_*) with sonic measurements at 50m and with the Surface Boundary Layer height as a filter ($c_i = 0.15$ and $z_s = 10\%$ of z_i).

A large scatter for the Profile Method 1 can be observed, resulting in a low correlation R of 0.3 depending on height and filters that are used.

The results of table 5.2 show that comparing with the Eddy Covariance Method at lower altitudes results in an overprediction and at higher altitudes an underprediction of the friction velocity u_*. The correlation between the u_{*EddyC} and u_{*PM1} is for each case similar. It can be concluded that the Profile Method 1 with measurement at a height of 10 and 40 meters agrees well with the Eddy Covariance Method at 50 meters height, based on the comparison of the friction velocity.

- **Profile Method 2**

  For the second Profile Method an underprediction of the friction velocity can be found compared to the Eddy Covariance Method at 50 meters. This underprediction of the friction velocity results in a shift from unstable and stable conditions to neutral. The scatter however, is significantly smaller than that in the first Profile Method, which also can be found in table 5.2. Resulting in a correlation R of around 0.56-0.74 for the second Profile Method, compared to an R of 0.3 for the first Profile Method 1.

  Looking at the results of table 5.2, it can be seen that the Eddy Covariance Method gives the best prediction. For lower altitudes an small overprediction of the friction velocity u_* can be seen and at higher altitudes an underprediction. The correlation found between the u_{*EddyC} and u_{*PM1} is for each case similar.

  The results of table 5.2 also show that the Eddy Covariance Method at 2 meters provides the closest results when compared to the Profile Method 2 with measurement at the surface and 40 meters. Higher up in the atmosphere, Profile Method 2 tends to under predict the friction velocity.

- **Gradient Richardson Number**

  The results of the Gradient Richardson Number method are very similar to the results of the first Profile Method. The trend, slope of the data, has a good correspondence with the results of the Eddy Covariance Method at all heights. However, the scatter especially when the Surface Boundary Layer height is not used as filter is very high. A negative correlation factor R of -0.13 was found for some cases.

  Again the results of table 5.2 show that comparing the Eddy Covariance Method at lower altitudes results in an overprediction of the u_* and at higher altitudes an underprediction.

  It can be concluded therefore, that the trend of the Gradient Richardson Number Method with measurement at a height of 10 and 40 meters corresponds the best with the Eddy Covariance Method at 50 meters height, based on the comparison of the friction velocity However, still results in a large uncertainty. Using the Surface Boundary Layer height as a filter, increases the correlation significantly. Measurements outside of the Surface Boundary Layer result in a big scatter when the Richardson Number is used to determine the atmospheric stability.

- **Bulk Richardson Number**

  For the Bulk Richardson Number also an underprediction of the friction velocity can be found compared to the Eddy Covariance Method at 50 meters. This results in a shift from unstable and stable conditions to neutral. The results are very similar to the results of Profile Method 2, however with a larger scatter, especially when the Surface Boundary Layer height is not used as a filter. Using the Surface Boundary Layer height as a filter, results in a correlation increase of around 0.10.

Analyzing the results of table 5.2 shows that the Eddy Covariance Method provides the best correspondence to the results of the Eddy Covariance Method. For lower altitudes, an over-

Method	$Height_{EddyC}$ $[m]$	$Slope$	$Slope_{SBL}$	R	R_{SBL}
Profile Method 1	2	1.40	1.27	0.42	0.41
	50	0.90	0.82	0.36	0.31
	90	0.80	0.73	0.35	0.74
Profile Method 2	2	0.94	0.93	0.85	0.74
	50	0.60	0.60	0.74	0.56
	90	0.54	0.53	0.74	0.55
Gradient Richardson Number	2	1.47	1.27	-0.13	0.35
	50	0.94	0.82	-0.13	0.27
	90	0.84	0.73	-0.12	0.25
Bulk Richardson Number	2	0.97	0.92	0.45	0.62
	50	0.94	0.93	0.40	0.50
	90	0.56	0.52	0.40	0.48

Table 5.2: Slope & Correlation R - Friction velocity (u_*) with $_{SBL}$ indicating the use of the Surface Boundary Layer height as a filter.

prediction of the friction velocity u_* is observed and at higher altitudes an underprediction.

Analysing the results of table 5.2 also shows that the Eddy Covariance Method at 2 meters corresponds the best with the Bulk Richardson Number with measurement at the surface and 40 meters. This is similar to the results of the second Profile Method.

In general the following can be concluded from the comparison of the friction velocity calculations:

- Looking at the friction velocity, Profile Method 2 and Bulk Richardson Number give the best results compared to the Eddy Covariance Method at multiple heights. The trend of the Bulk Richardson Number is slightly better compared to the Profile Method 2, however the correlation is significantly lower.
- From table 5.2 and figure 5.9 a trend of increasing u_* with increasing of the measurement height can be observed.

5.3.4 Heat flux ($\overline{w'\theta'_v}$) per method compared to the heat flux of the Eddy Covariance Method

In this section, the heat flux will be the main focus. The first step in the analysis is a direct comparison of the heat flux determined by the Eddy Covariance Method at different heights, visible in figure 5.12. This is a comparison of the heat flux determined with Eddy Covariance Method at a height of 50 meters and with the four methods presented in this research. In figures 5.13 and 5.14, eight plots are visible, with the x-axis showing the $\overline{w'\theta'_v}$ determined with the Eddy Covariance Method, and the y-axis shows the $\overline{w'\theta'_v}$ determined with the other methods.

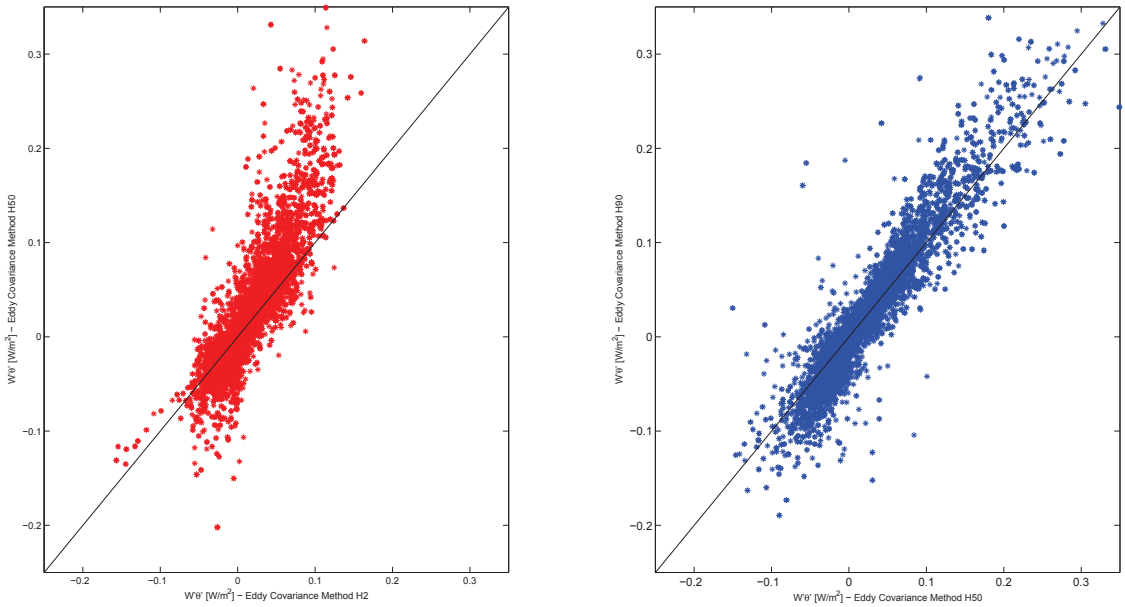

Figure 5.12: Lindenberg - Comparison of $\overline{w'\theta'_v}$ determined with the Eddy Covariance Method on the left at a height of 2 and 50 meters and on the right at a height of 50 and 90 m.

From figure 5.12 can be observed that the heat flux increases with height.

Now the comparison of each method to the Eddy Covariance Method can be executed. Table 5.3 concludes the trend and correlation comparisons of the four methods compared to the Eddy Covariance Method at three heights.

- **Profile Method 1**

  Looking at the heat flux estimation of the first Profile Method an overprediction is clearly visible with an increasing error with increasing $\overline{w'\theta'_v}$. The overprediction of the $\overline{w'\theta'_v}$ results in an underprediction of Monin-Obukhov length (L), which based on the relation between $\overline{w'\theta'_v}$ and L found in 4.3 results in a shift from neutral to unstable conditions.

  The results of table 5.3 show that compared to the Eddy Covariance Method at lower altitudes results in an overprediction of the heat flux $\overline{w'\theta'_v}$ and at higher altitudes an underprediction. Also based on the comparison of the heat flux, it can be concluded that Profile

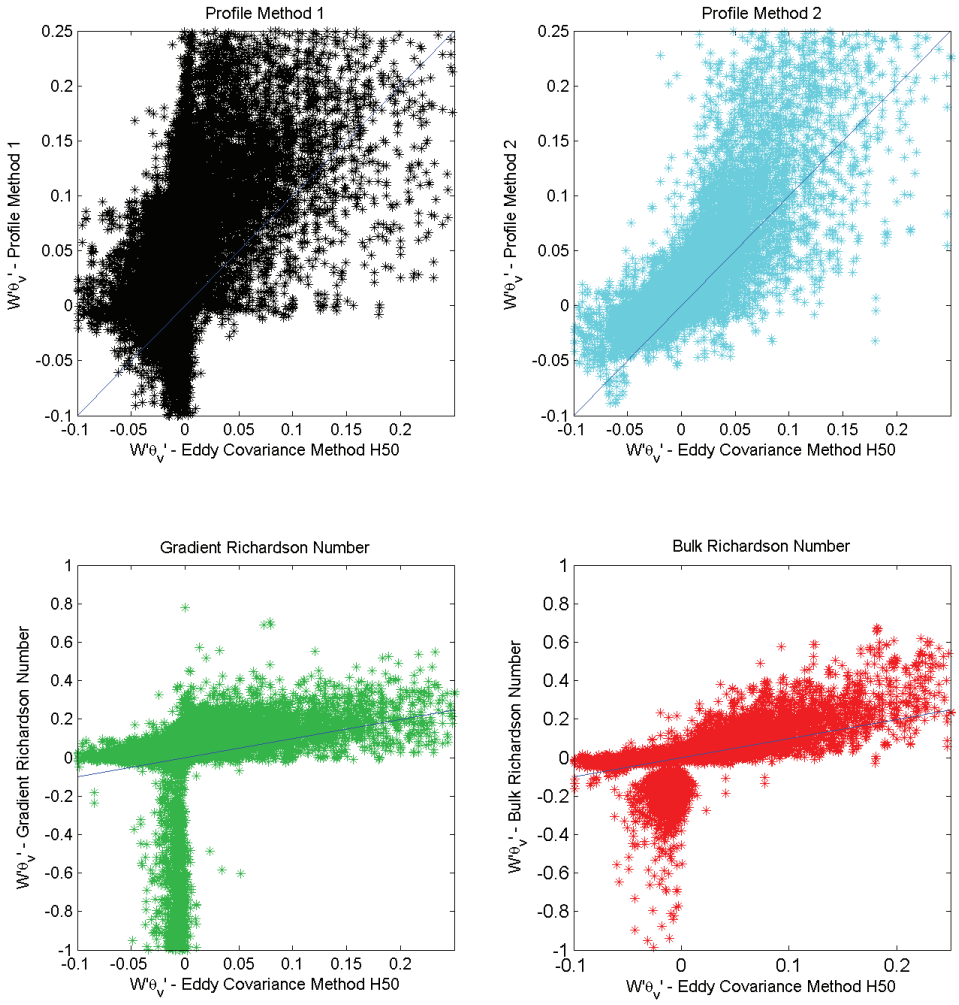

Figure 5.13: Lindenberg - Comparison of Heat flux ($\overline{w'\theta'_v}$) with sonic measurements at 50m without the filter for the Surface Boundary Layer height.

Method 1 using measurement at a height of 10 and 40 meters corresponds the best with the Eddy Covariance Method at 50 meters height.

- **Profile Method 2**

Figures 5.13 and 5.14 show an overprediction of the heat flux for both cases, with and without the Surface Boundary Layer height filter. The scattering is lower compared to the scattering of the first Profile Method, resulting in a correlation of around 0.80. Comparing the Profile Method 2 with the Eddy Covariance Method at a lower altitude, results in a significant overprediction of the heat flux. At a higher altitude, Profile Method 2 provides the lowest error when compared to the Eddy Covariance Method.

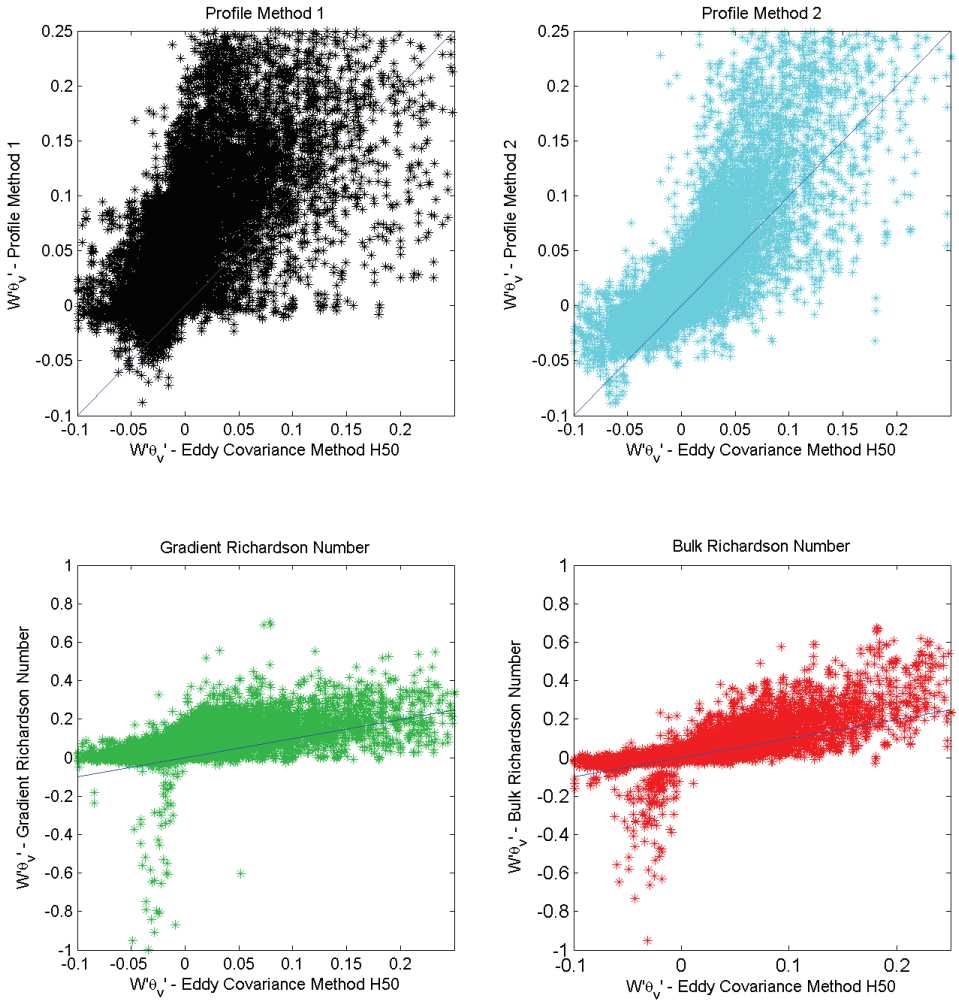

Figure 5.14: Lindenberg - Comparison of Heat flux ($\overline{w'\theta'_v}$) with sonic measurements at 50m and with the Surface Boundary Layer height as a filter ($c_i = 0.15$ and $z_s = 10\%$ of z_i).

- **Gradient Richardson Number**

The Gradient Richardson Number heat flux estimations show a large scatter. Similar to the results at Cabauw, mainly for negative values of the $\overline{w'\theta'_v}$, the estimation does not correspond with the Eddy Covariance Method. The Surface Boundary Layer height filter, reduces the scatter significantly which results in an correlation increase from 0.12 to 0.5. The slope without the Surface Boundary Layer height filter, is significantly better compared to the 1.86 with the Surface Boundary Layer filter. This is because the first is not representing the trend, due to the large scatter around zero. This clearly shows the impact of measurements outside of the Surface Boundary Layer on the atmospheric stability estimation for methods based on the Richardson Number.

Method	$Height_{EddyC}$ $[m]$	$Slope$	$Slope_{SBL}$	R	R_{SBL}
Profile Method 1	2	2.00	2.38	0.68	0.74
	50	1.09	1.30	0.59	0.66
	90	0.81	0.95	0.53	0.62
Profile Method 2	2	2.23	2.29	0.86	0.87
	50	1.28	1.34	0.83	0.82
	90	1.02	1.05	0.78	0.79
Gradient Richardson Number	2	2.08	3.81	0.15	0.57
	50	1.11	1.86	0.12	0.5
	90	0.84	1.37	0.10	0.47
Bulk Richardson Number	2	2.36	2.77	0.48	0.59
	50	1.34	1.52	0.44	0.56
	90	1.07	1.18	0.40	0.53

Table 5.3: Slope & Correlation R - Heat flux ($\overline{w'\theta'_v}$) with $_{SBL}$ indicating the use of the Surface Boundary Layer height as a filter

- **Bulk Richardson Number**

  The Bulk Richardson Number also shows a large scatter for negative values of the heat flux, for stable conditions. By using the Surface Boundary Layer height as a filter, the slope is around 1.5 which indicates an overprediction of the heat flux, resulting in a shift to unstable conditions. The correlation is slightly lower compared to the correlation found with Profile Method 2.

The second Profile Method gives the closest representation compared to the Eddy Covariance Method based on the heat flux. The slope varies from 2.3 to 1.0 at 5 to 90 meters respectively, with a correlation R of around 0.8, significantly higher compared to the correlations found with the other methods.

5.4 Statistical analysis of the friction velocity (u_*) and heat flux ($\overline{w'\theta'_v}$) for multiple measurement heights

Until now, measurements with a maximum height of 40 meters are used to determine the stability with MOST at Lindenberg. The selection of the maximum measurement height is based on two important issues. First, the methodologies use the difference at two different heights, a smaller the difference in height results in a smaller absolute temperature difference. The temperature sensors have a certain accuracy, as the difference becomes smaller the impact of the sensor accuracy increases. Secondly, as has often been described, these methods make use of MOST which is only valid in the Surface Boundary Layer. Measuring outside the Surface Boundary Layer results in large scatter, as seen in the results of Cabauw and Lindenberg. However, the filtering of the data points, wherein the measurements outside the Surface Boundary Layer are excluded from the dataset results in very large data reduction, which is certainly not desirable.

5.4.1 Friction velocity

The slope of the Profile Method 2 and that of the Bulk Richardson Number method are around 1 compared to the Eddy Covariance Method at 2 meters. For both the Profile Method 2 and the Bulk Richardson Number an underprediction can be observed when compared to the Eddy Covariance method at higher altitudes. Profile Method 1 and the Gradient Richardson Number give an overall overprediction compared to the Eddy Covariance Method at 2 meters. Comparing both methods to the Eddy Covariance method at higher altitudes results in a slope of around 1.

The correlation of the Profile Method 1 and the Gradient Richardson Number method are low. The Gradient Richardson Number is the lowest of the two. Profile Method 2 has the highest correlation and is the most consistent. The Richardson Number methods are effected by measurements outside the Surface Boundary Layer, similarly observed at the results of Cabauw.

Overall, an increase of slope can be observed when higher altitudes are selected for the methods using MOST. However, due to the correlation decreases with height, a maximum measurement height of around 40-60 meters is recommended to be used.

5.4.2 Heat flux

The heat flux estimated by all methods gives an overpredicted when compared to the Eddy Covariance Method at a height of 2 meters. When compared to the Eddy Covariance Method at higher altitudes, this results in smaller over- & underpredictions. Lowering the measurement altitude results in better predictions of the heat flux for all methods without the Surface Boundary Layer filter.

The slope of the Profile Method 2 and that of the Bulk Richardson Number are very similar again. Therefore, the correlation is the determining factor. Similar to the findings above the Profile Method 2, gives more consistent and better correlations compared to the Bulk Richardson Number.

Remarkably, the correlation of the heat flux increases when a higher measurement height is used and for the friction velocity the correlation declines when higher measurements are used.

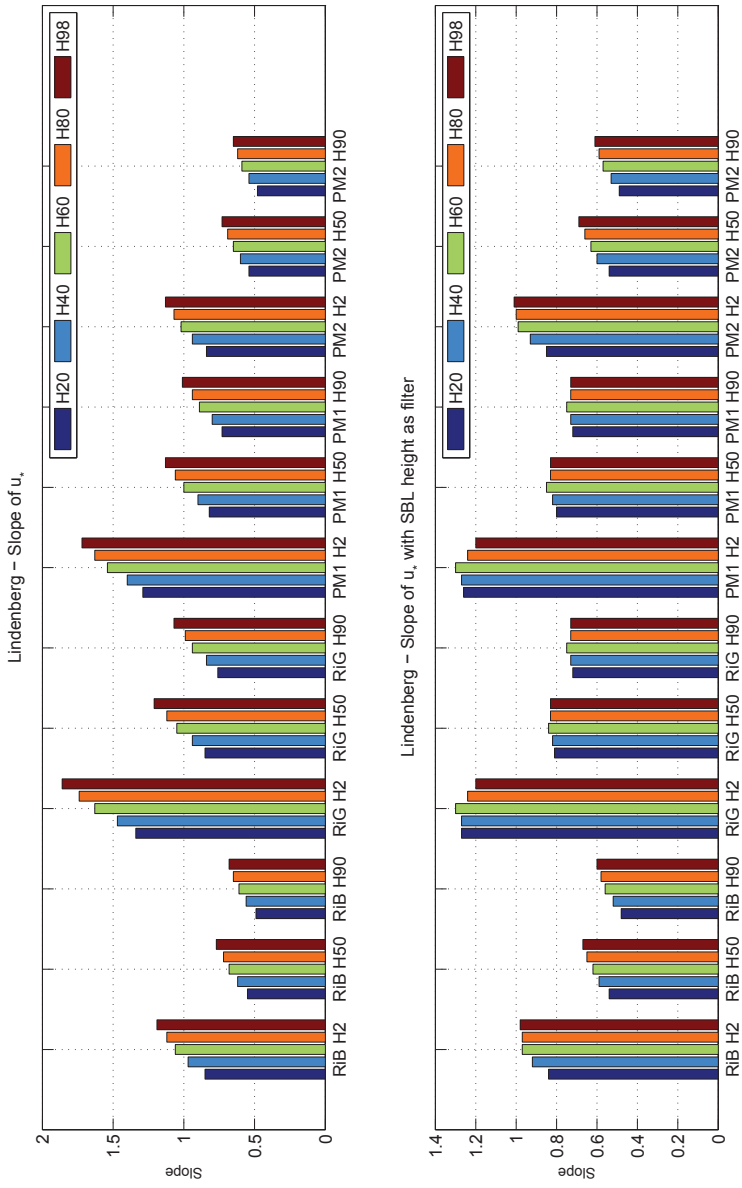

Figure 5.15: Lindenberg - Slope of Friction Velocity (u_*) with and without the Surface Boundary Layer height as a filter for four methods.
RiB - Bulk Richardson Number, RiG - Gradient Richardson Number, PM1 - Profile Method 1, PM2 - Profile Method 2
H2 - compared to the Eddy Covariance Method at 2m, H50 - compared to the Eddy Covariance Method at 50m, H90 - compared to the Eddy Covariance Method at 90m

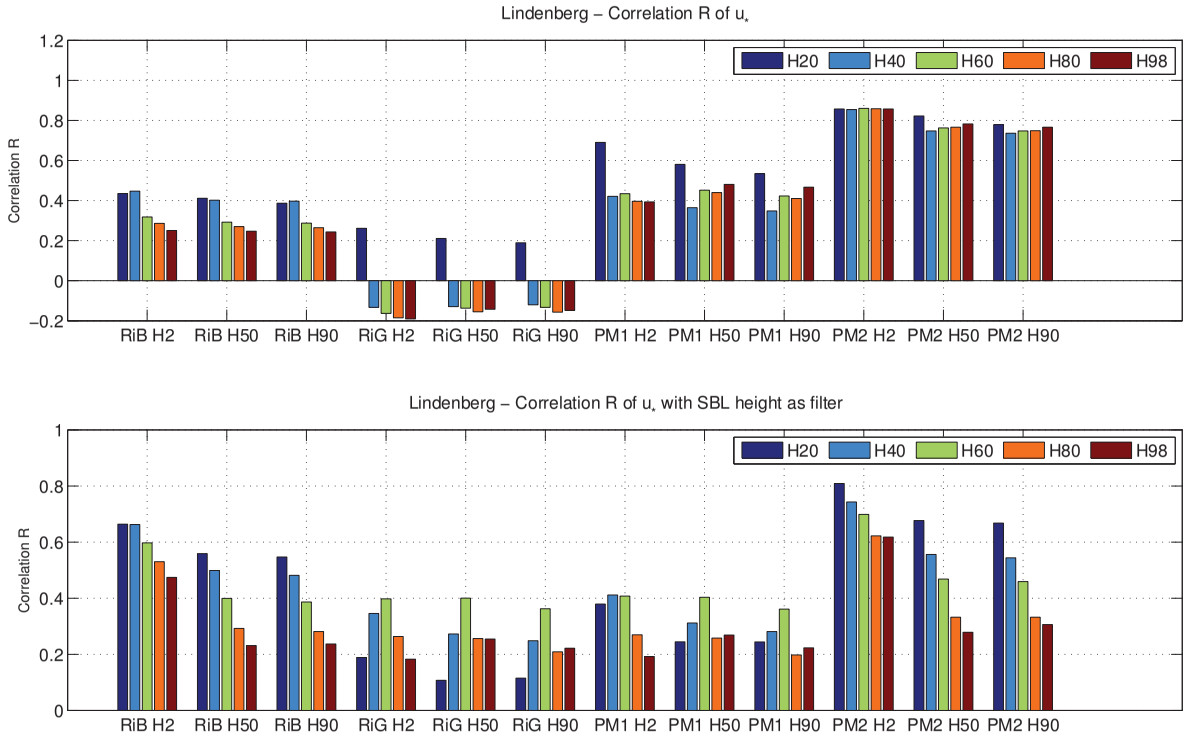

Figure 5.16: Lindenberg - Correlation of Friction Velocity (u_*) with and without the Surface Boundary Layer height as a filter for four methods.
RiB - Bulk Richardson Number, RiG - Gradient Richardson Number, PM1 - Profile Method 1, PM2 - Profile Method 2
H2 - compared to the Eddy Covariance Method at 2m, H50 - compared to the Eddy Covariance Method at 50m, H90 - compared to the Eddy Covariance Method at 90m

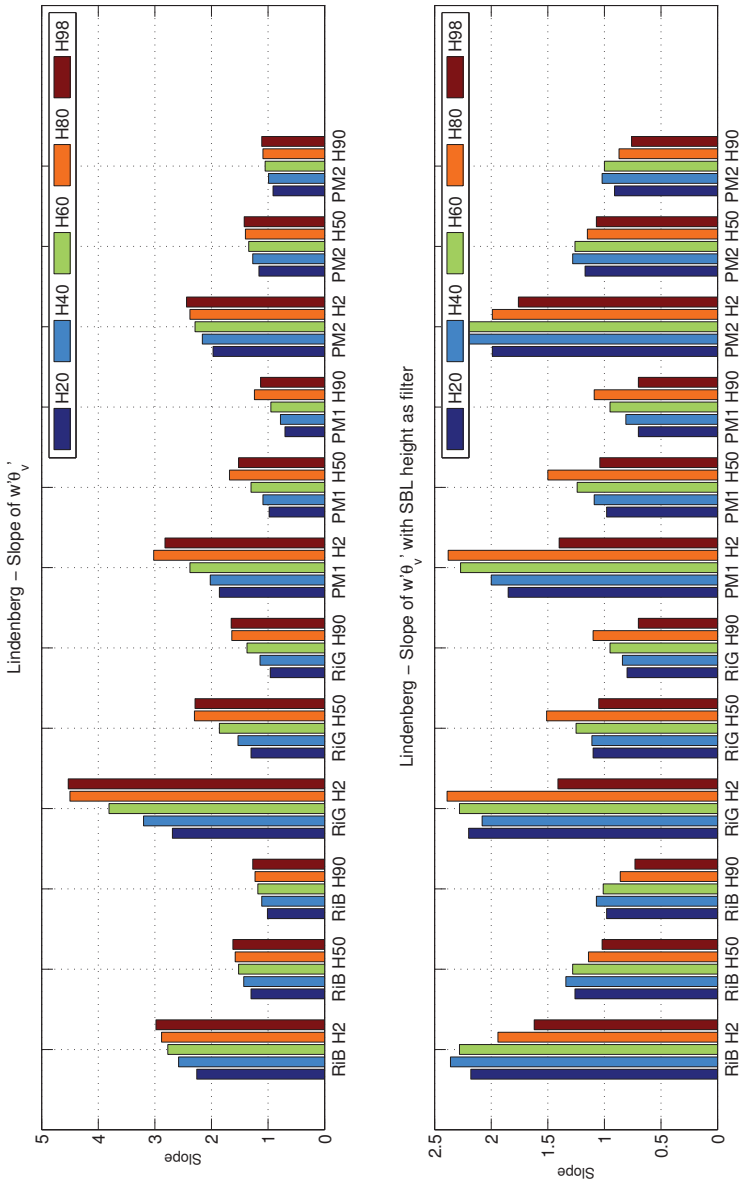

Figure 5.17: Lindenberg - Slope of Heat flux ($\overline{w'\theta'_v}$) with and without the Surface Boundary Layer height as a filter for four methods.
RiB - Bulk Richardson Number, RiG - Gradient Richardson Number, PM1 - Profile Method 1, PM2 - Profile Method 2
H2 - compared to the Eddy Covariance Method at 2m, H50 - compared to the Eddy Covariance Method at 50m, H90 - compared to the Eddy Covariance Method at 90m

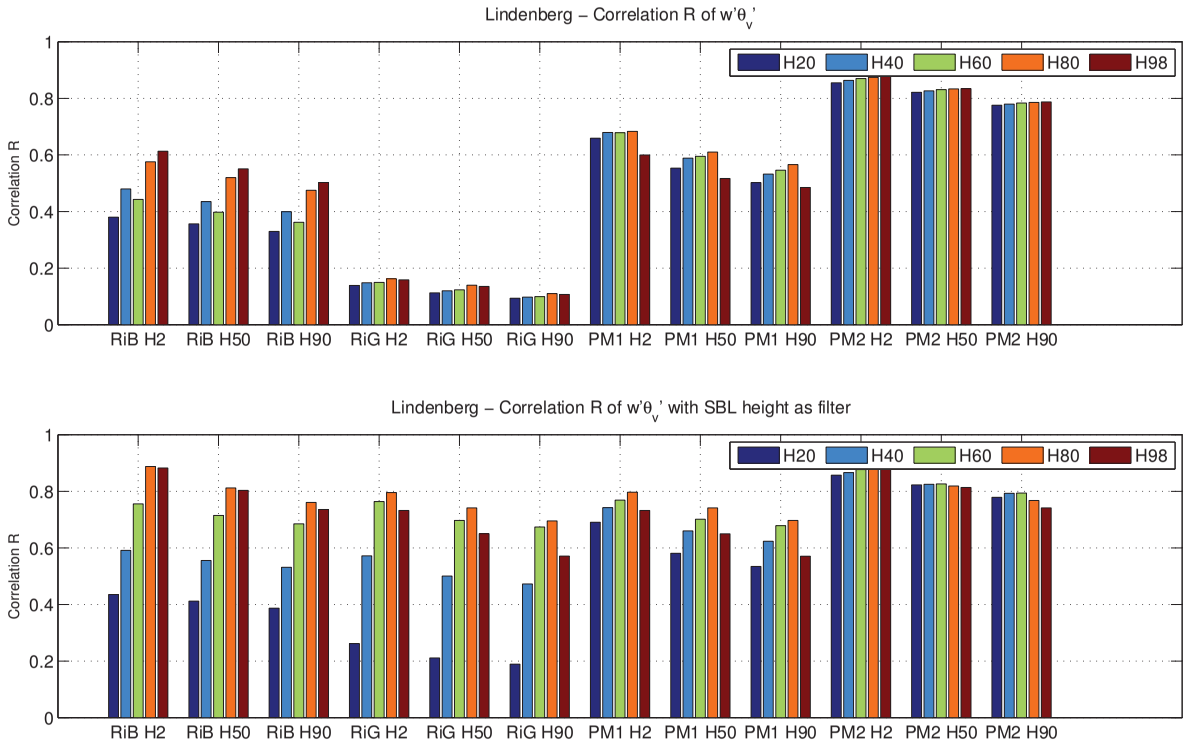

Figure 5.18: Lindenberg - Correlation of Heat flux $(\overline{w'\theta'_v})$ with and without the Surface Boundary Layer height as a filter for four methods.
RiB - Bulk Richardson Number, RiG - Gradient Richardson Number, PM1 - Profile Method 1, PM2 - Profile Method 2
H2 - compared to the Eddy Covariance Method at 2m, H50 - compared to the Eddy Covariance Method at 50m, H90 - compared to the Eddy Covariance Method at 90m

5.5 Summary & Conclusions based on the Lindenberg data

In this chapter atmospheric stability analysis was executed with five methods using the 2010 Lindenberg data. Before the analysis could be completed, two filter types are used to handle the data correctly. First, all extreme values and sensor errors were removed from the dataset and second the steady state check was executed. MOST requires stationary flow and the steady state filter removes data point where the deviation from previous values exceeds certain conditions, explained in full in section 4.3.1.

Large differences could be observed between the stability, friction velocity and heat fluxes at different heights using the Eddy Covariance Method at 2, 50 and 90 meters. Extreme conditions decreased in intensity with height and therefore increasing near neutral conditions with height. Two methods based on MOST, Profile Method 2 and Bulk Richardson Number, give significantly better results than the others. The results of these two methods are similar, providing a high accuracy approximation of the atmospheric stability when compared to the Profile Method 2. These results were closely followed by the Bulk Richardson Number, with more inconsistent results using different maximum measurement heights.

By using the Surface Boundary Layer filter, when measurement exceed the height of the Surface Boundary Layer an improved stability estimation was achieved, especially for the Richardson Number methods. However, the large data reduction has to be taken into account, which will be done in chapter 6.

Analyzing the friction velocity, Profile Method 2 and Bulk Richardson Number method lead to the closest agreement with the near surface conditions computed by the Eddy Covariance Method at a height of 2 meters. When compared to higher altitudes of 50 and 90 meters, an underprediction of the friction velocity was observed. The heat flux of Profile Method 2 and Bulk Richardson Number corresponds the closest with the Eddy Covariance Method at 90 meters, for lower altitudes however, an overprediction was found for the heat flux.

The following preliminary conclusions could be made based on the Lindenberg data:

1. Significant differences between three measurement heights (2, 50 and 90 meters) are observed using the Eddy Covariance Method.

2. Significant differences between four atmospheric stability methods are observed, with very high scatter for some methods. Therefore the selection of the **measurement height, filters and method** is of **utmost importance for quality** of the atmospheric stability estimation.

3. The best results are obtained with the Bulk Richardson Number and Profile Method 2 (using 0-40 meters measurements). However, the Profile Method 2 gives similar results and is more consistent using different heights and also the quality of the second Profile Method is not dependent on the Surface Boundary Layer filter. Therefore, Profile Method 2 is the recommended methodology for the estimation of the atmospheric stability.

4. Methods based on the Richardson Number are strongly influenced by measurements outside of the Surface Boundary Layer, resulting in very high scatter of both the friction velocity and heat flux estimations. However, using the Surface Boundary Layer filter, results in a large reduction data which could affect the agreement with the local conditions.

5. A maximum measurement height can be recommended based on the statistical analysis of section 5.4, which showed that on average a maximum measurement height of around 40-60 meters is the most suitable, depending on which method and parameter (distribution of atmospheric stability, friction velocity and heat flux) is considered.

Chapter 6

Equivalent load calculations of a wind turbine blade root

In the introduction of this master thesis, it is mentioned that both the power production and loads are significant influenced by the assumed wind profile and turbulence intensity. Thus for accurate power and load predictions, the influence of atmospheric stability on the wind profile and turbulence intensity has to be taken into account. This chapter will focus on the impact of the atmospheric stability distributions on the loads of a wind turbine, by comparing the equivalent loads using different methods to determine the atmospheric stability distribution.

6.1 Equivalent loads and simulations

In this section a short explanation of the concept equivalent load will be explained together with how the equivalent load is determined using fatigue load simulations.

6.1.1 Equivalent loads

During the life time of a mechanical component (in this case for example the blade root of a wind turbine), it endures multiple loads with variable frequencies and amplitude. By using the equivalent load, the range of multiple loads is reduced to one equivalent load. The advantage of using the equivalent load is the comparability of different loads situations. [55]

Depending on the material, there exist a fatigue limit. This would mean when a load below this limit is applied, the life of the component is infinite, indicated by the fatigue strength F_D. Applying a load slightly higher than F_D, results in failure of the component at N_D number of cycles. Figure 6.1 shows the S-N curve with N_D indicating the fatigue limit. Left from the fatigue limit the graph has a slope $\frac{1}{m}$ and on the right it is constant. From this graph the number of cycles until failure n_i can be calculated for every load, F_i, below F_D with:

$$n_i = N_D(\frac{F_D}{F_i})^m \tag{6.1}$$

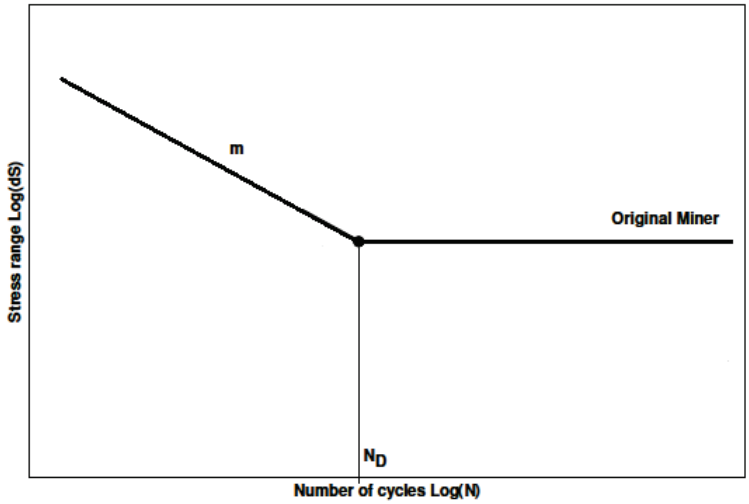

Figure 6.1: S-N diagram - Explanation of equivalent load [55]

Miner's rule indicates that if a load only occurs n_i number of cycles, below the allowed number of cycles this induces a partial damage d_i. With i indicating a load with constant amplitude and frequency. The total damage of the spectrum of loads is the sum of the partial damages of each load.

$$D = \sum_{i=1}^{n} d_i = \sum_{i=1}^{n} \frac{n_i}{N_D}(\frac{F_i}{F_D}) \tag{6.2}$$

The equivalent load or fatigue damage equivalent load, is the load with number of cycles n_{eq} where the damage is the same as the sum of the partial damages of the actual loads combined.

For a given wind speed and stability the equivalent load can be calculated by the following equation:

$$F_{EQ} = \left(\frac{\sum F_i^m n_i}{n_{EQ}}\right)^{\frac{1}{m}} \tag{6.3}$$

where F_{EQ} is the equivalent load, F_i the actual fatigue load, n_i the actual fatigue cycles and n_{EQ} is the number of equivalent cycles.

The lifetime cumulative equivalent load, F_{EQ-TOT} can be calculated, by using equation 6.3 for each wind speed and stability, $P(\zeta|_{\overline{U}})$ the probability density function of the stability at a given wind speed and $P(\overline{U})$ probability density function of the wind speed [28].

$$F_{EQ-TOT} = \sum \left(\sum F_{EQ}(\zeta|_{\overline{U}}) P(\zeta|_{\overline{U}}) \Delta\overline{\zeta} \right) P(\overline{U}) \Delta\overline{U} \tag{6.4}$$

6.1.2 Simulations

In order to determine the actual fatigue load (F_i), Holtslag [28] conducted fatigue load calculations with design simulation software (Bladed) for the blade root bending moment of a 5MW NREL reference wind turbine [31] for offshore conditions. The NREL reference turbine has a hub height of 90 meters, a blade radius of 63 meters, cut-in & out wind speed of respectively 3 and 25 m/s. For each atmospheric condition, each wind speed and stability bin, a simulation time of 600 seconds was selected. Wind speed bins of 1 m/s are considered for $\Delta\overline{U}$. The stability uses increments of 1 between $-10 < \zeta < 5$ with an increase to 0.1 between $-1 < \zeta < 1$. This is due to steep slope of turbulence and shear levels at near neutral conditions.

The results of the fatigue load calculations of Holstlag [28] for each specific condition, wind speed and stability, are used to determine the equivalent load for multiple distribution at Cabauw and Lindenberg. It has to be taken into account, that the simulations conducted by Holstlag are intended for an offshore location. This could have a small effect on the results.

6.2 Results

The results are shown in table 6.1 and 6.2 for respectively Cabauw and Lindenberg. Each table shows the equivalent load for the Eddy Covariance Method, Profile Methods and Richardson Number Methods and the deviation of each method with the Eddy Covariance Method in percentage. This is conducted for two cases, with and without the Surface Boundary Layer height as filter.

Next to equivalent load using the atmospheric stability distributions, in each table the equivalent load determined using the IEC guideline can be found. This guideline assumes only neutral conditions where the turbulence intensity is a function of the wind speed and not of the atmospheric conditions.

Method	$F_{eq10min}$ $[kNm]$	Δ_{EddyC}	$F_{eq10minSBL}$ $[kNm]$	$\Delta_{EddyCSBL}$
Eddy Covariance Method	679	-	780	-
IEC Guideline	879	29.5%	970	43.0%
Profile Method 1	751	11%	872	12%
Profile Method 2	693	2%	794	2%
Gradient Richardson Number	731	8%	820	5%
Bulk Richardson Number	699	3%	793	2%

Table 6.1: Cabauw - Equivalent load of a wind turbine blade root

In table 6.1 a couple of observations can be made based on the equivalent load estimations using multiple methods at Cabauw. An overall over-prediction of all methods can be observed when compared to the Eddy Covariance Method. With the best agreement of the Profile Method 2 and Bulk Richardson Number. Both present an overprediction of the equivalent load of around 2-3%. Similar to the results presented in chapter 4, the Profile Method 2 gives the best approximation when the Surface Boundary Layer height filter is not used, closely followed by the Bulk Richardson Number. However, when the Surface Boundary Layer height filter is used the Bulk Richardson Number estimation is slightly better.

Method	$F_{eq10min}$ $[kNm]$	$\Delta_{EddyCH2}$	$\Delta_{EddyCH50}$	$\Delta_{EddyCH90}$
Eddy Covariance Method H2	520	-	2%	2%
Eddy Covariance Method H50	510	-2%	-	-0.2%
Eddy Covariance Method H90	511	-2%	0.2%	-
IEC Guideline	684	31.6%	34.2%	34%
Profile Method 1	582	12%	14%	14%
Profile Method 2	528	2%	4%	3%
Gradient Richardson Number	606	17%	19%	19%
Bulk Richardson Number	599	15%	17%	17%
Using the Surface Boundary Layer height as a filter ($c_i = 0.15$ and $z_s = 10\%$ of z_i)				
	$F_{eq10min}$ $[kNm]$	$\Delta_{EddyCH2}$	$\Delta_{EddyCH50}$	$\Delta_{EddyCH90}$
Eddy Covariance Method H2	597	-	1%	2%
Eddy Covariance Method H50	589	-1%	-	1%
Eddy Covariance Method H90	584	-2%	-1%	-
IEC Guideline	752	27.0%	27.7%	29%
Profile Method 1	682	14%	16%	17%
Profile Method 2	625	5%	6%	7%
Gradient Richardson Number	682	15%	16%	17%
Bulk Richardson Number	631	6%	7%	8%

Table 6.2: Lindenberg - Equivalent load of a wind turbine blade root using the height filter at the bottom table.

The Surface Boundary Layer height filter resulted in an increase of the equivalent load of around 15%. This corresponds with the expectations, because when the Surface Boundary Layer height is low during very stable conditions and the load decreases under stable conditions due to the decrease of turbulence intensity.

The equivalent load of the IEC guideline shows an overprediction of 30-40%, depended on the situation. This shows the conservative results of the IEC guideline. By using load calculations with atmospheric stability estimations included, reductions of the CAPEX can be achieved. This could lead to the goal stated at the beginning of this thesis, a reduction of LCoE and increase of market share of wind energy.

The results of Lindenberg, table 6.2 are very similar to the results of Cabauw. What can be observed is that the deviation is the lowest when compared to the Eddy Covariance Method near the surface. Also, the deviation of the Bulk Richardson Number method is significantly increased compared to the deviation found at Cabauw. This could be due to the measurements. At Cabauw the surface temperature is measured at a height of 10 centimeters, whilst at Lindenberg the surface temperature itself is measured which could result in small deviations.

6.3 Conclusions & Discussions

Analyzing the results of the equivalent load showed that the Profile Method 2 and the Bulk Richardson Number are in good agreement with the Eddy Covariance Method. These results correspond with the results found in previous chapters. The significant differences between the

atmospheric stability distributions found with the Eddy Covariance Method at three heights at Lindenberg resulted in a maximum equivalent load deviation of 2.1%.

The impact of the Surface Boundary Layer height filter on the yearly equivalent load is significant. An increase of around 15% could be observed, which showed that using the filter results in a poor representation of the atmospheric stability distribution. For both the Richardson Number methods the filter significantly decreases the deviation. Therefore, the Surface Boundary Layer height filter can be activated when only for specific timesteps the atmospheric stability has to be determined. However, for overall yearly distributions, for example for fatigue calculations of a wind turbine, it is not recommended to activate the the Surface Boundary Layer height filter, due to the poor representation of the atmospheric stability distribution.
It has to be taken into account that both MOST and the equivalent load simulations assume conditions within the Surface Boundary Layer. The shear and turbulence intensity outside of the Surface Boundary Layer are different which could result in differences of both the stability estimation and equivalent load calculations. This shows the importance of the extension of the wind profile, TI description outside of the Surface Boundary Layer.

Chapter 7

Conclusions, Recommendations & Guideline

In the literature study in chapter 3, multiple analyzes are discussed, for example a direct comparison of one method with sonic measurements,assumed to be the closest to reality. Multiple methodologies are compared to each other, without having a direct comparison on the stability. Overall it could be concluded that atmospheric stability and flux estimations of the Bulk Richardson Number are in good agreement with the Eddy Covariance Method.

In existing literature methodologies have not always been compared to each other consistently. This has resulted in sometimes inconclusive findings.regarding the better estimation of the atmospheric stability. Therefore in this research, five methodologies are directly compared on multiple levels using three datasets (Cabauw, Lindenberg and Høvsøre. The analyzes of the last location can be found in appendix D) The summarized conclusions, recommendations and finally an appropriate guideline to determine the atmospheric stability can be found in this chapter.

7.1 Conclusions

From the research executed on three datasets, significant differences in distribution, friction velocity and heat flux could be observed between multiple methodologies and measurement heights. The selection of the methodology, measurement height and filters are therefore of utmost importance for the quality of the atmospheric stability estimation.

Using the sonic measurements together with the Eddy Covariance Method near surface, resulted in the estimation of more extreme conditions. The estimation of the atmospheric stability with the Eddy Covariance Method at higher altitudes resulted in a decrease of extreme conditions. These fluctuations of momentum and heat fluxes within the Surface Boundary Layer are in conflict with the assumption of constant fluxes within the Surface Boundary Layer according to Monin-Obukhov Similarity Theory. Therefore can be concluded that the Monin-Obukhov Similarity Theory does not give a detailed representation of the conditions in reality, it is only a simplification of truth to reduce the complexity of measurements and process.

Analysis of the atmospheric stability distributions using a maximum measurement height of 40 meters shows a good agreement of the atmospheric stability using the Bulk Richardson Number and Profile Method 2. The statistical analysis of the friction velocity and heat fluxes in section 5.4, showed that the Profile Method 2 gives more consistent results at different heights. In addition the quality of the atmospheric stability estimation of Profile Method 2 is not dependent on the Surface Boundary Layer filter, as found in this research and literature [45]. Therefore, the Profile Method 2 can be recommended for the estimation of the atmospheric stability for Onshore locations.

From the statistical analysis of the friction velocity and heat flux, no direct conclusion about the measurement height can be made. The statistical analysis showed a decrease of the correlation of friction velocity with increasing measurement height and also a decrease of the correlation of the heat flux with decreasing measurement height. Measurements at higher altitudes could be outside of the Surface Boundary Layer and therefore decrease the correlation. The decrease of the correlation of the heat flux with decreasing measurement height, is due to the fact that the temperature difference is decreasing. The accuracy of the temperature measurements, has therefore a larger influence on the atmospheric stability estimation, resulting in the scattering of the momentum and heat fluxes. On average a maximum measurement height of around 40-60 meters gives the most suitable results, depending on which method and parameter (distribution of atmospheric stability, friction velocity and heat flux) is considered.

Various distributions found by different methodology's are used to compare the impact on the bending moment of the blade root of a wind turbine, by considering the equivalent loads. Differences in equivalent load vary from 1-2% between the Eddy Covariance Methods at different heights up to around 15% for the Profile Method 1 and Gradient Richardson Number. The equivalent load comparison showed that the results of the Profile Method 2 give the best agreement with the Eddy Covariance Method. From the equivalent load calculations it also can be concluded that an improvement can be achieved when the atmospheric stability is taken into account, in comparison with the IEC guidelines, with potential CAPEX reductions.

If we look at the estimation of the friction velocity and heat flux, it can be concluded that methods based on the Richardson Number are strongly influenced by measurements outside of the Surface Boundary Layer, resulting in very high scatter of both the friction velocity and heat flux estimations. Using the approximation of the Surface Boundary Layer height and filtering the timesteps when the measurement height is outside of the Surface Boundary Layer, results in a large data reduction. The resulting distribution could not be in agreement with the local conditions, however it has to be taken into account that equivalent load calculations assume typical conditions of the Surface Boundary Layer (shear and turbulence intensity).

7.2 Recommendations & Further work

The research shows that especially both the Bulk Richardson Number and Profile Method 2 give a good approximation of stability, friction velocity and heat flux. However around 1980, the meteorological institutes and researchers started investigating the momentum and heat fluxes with the Eddy Covariance Method [2]. Thereby in meteorology nowadays, the Eddy Covariance Method with high frequent sonic measurements is exclusively used, though in the wind energy sector the methodologies based on MOST are still used, with corresponding uncertainties.

During the years the size of wind turbines, hub height and blade length, is gradually increasing

[7] and therefore often exceeding the Surface Boundary Layer. Further research is needed to investigate the atmospheric stability outside of the Surface Boundary Layer. More specifically:

- The translation of the atmospheric stability conditions near the surface to conditions outside of the Surface Boundary Layer.
- The extension of wind profile and turbulence intensity outside of the Surface Boundary Layer.
- The investigation of differences between the impact of atmospheric stability within and outside of the Surface Boundary Layer.

Next to the methodologies based on MOST, other methodologies have been compared to the Eddy Covariance Method. The results of the Large-Eddy Simulations are very promising. The atmospheric stability estimation of the LES model and the Eddy Covariance Method are very close to each other for Cabauw. Additional research is required, to investigate the determination of the stability distribution on different locations.

The Bulk Richardson Number and the Profile Method 2 gave very similar results for the three onshore locations used in this research. For the Bulk Richardson Number the parametrization is of utmost importance, shown in appendix F.2.1. The literature study in chapter 2 showed that the Bulk Richardson Number performs very well for offshore conditions and therefore it can be recommended that in the future similar analysis using data from an offshore met mast is executed.

7.3 Guideline

In order to determine the atmospheric stability for a certain location, a number of different methodologies are available, varying from Pasquill-Gifford (discussed in section 2.1) to methodologies based on the Monin-Obukhov Similarity Theory (discussed in section 2.4). Each methodology has different inputs and in this chapter a guideline will explain the recommended way of how to determine the atmospheric stability using Profile Method 2.

The guideline will be divided into three main parts, each with a couple subsections.

- Measurement data - Met Mast
  - Parameters
  - Frequency
  - Height
- Filters
  - Data filtering
    - Operational conditions & sensor errors
    - Steady state conditions
  - Tower shading
  - Surface Boundary Layer height
- Methodology: Profile Method 2

7.3.1 Measurement data - Met Mast

For the determination of the atmospheric stability, the starting point is the measurement data of the met mast. The measurement data of the met mast will be divided into three sections, the parameters, measurement frequency and measurement height.

Parameters

Profile Method 2 uses five parameters: wind speed, temperature, relative humidity, atmospheric air pressure and the surface roughness. The temperature, relative humidity and pressure have to be measured at multiple levels to determine the atmospheric stability, as can be seen in table 7.1 and figure 7.1.

Parameters	Level
Wind speed [m/s]	Tower
Temperature [K]	Surface & Tower
Relative humidity [%]	Surface & Tower
Pressure [Pa]	Surface & Tower
Surface roughness [m]	Surroundings

Table 7.1: Required parameters for atmospheric stability estimation - Profile Method 2

The wind speed has only to be measured at one height in the tower. It is important that this is the same height as the tower measurement of temperature, relative humidity and pressure, due to the link of the parameters in the temperature and wind profile. Further information on the measurement height will be provided in the following section.

The relative humidity, pressure are used to determine the virtual potential temperature which is required for the Profile Method 2 to determine the atmospheric stability. The potential temperature of an air particle at pressure P is the temperature that the particle would acquire if adiabatically brought to a standard reference pressure P_0. The virtual temperature (T_v) is the temperature of dry air with the same density as the moist air at constant pressure. In both the literature [50] and this research is found that for small height difference the accuracy of the temperature measurements is of great importance. It is therefore recommended that temperature differences are measured directly by one instrument and not with two measurements at two heights separately.

The last parameter found in table 7.1 is the surface roughness, describing the surroundings of the met mast with the surface roughness length.

Frequency

Typical measurement frequency of 4 Hz is used with met mast, from which the 10-minute statistics are determined. The 10-minute average data can be used to determine the atmospheric stability.

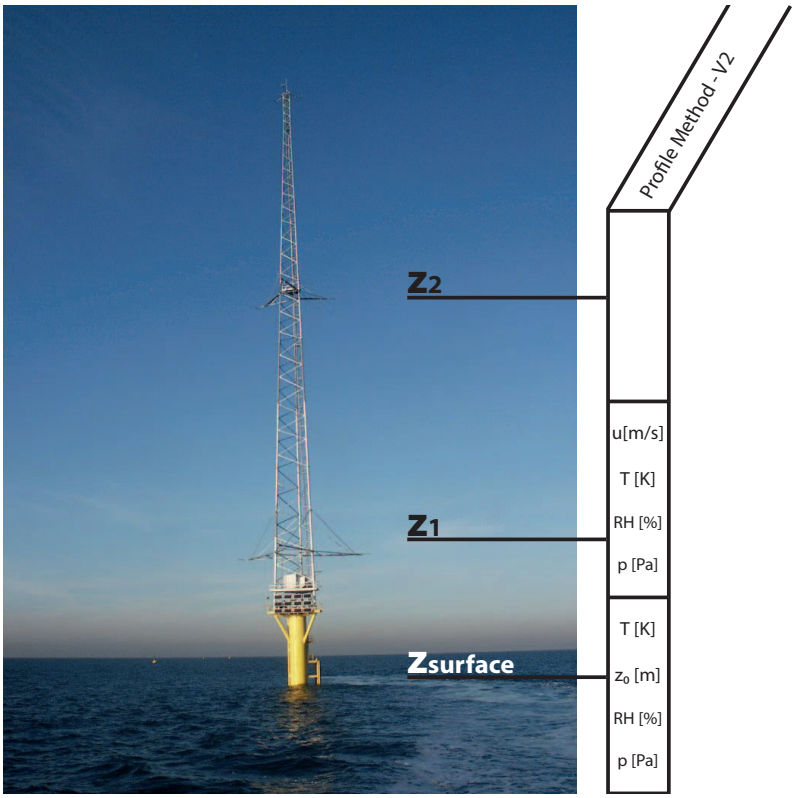

Figure 7.1: Estimation of Monin-Obukhov length with Profile Method 2, with the photograph of the OWEZ met mast [34]

Height

The measurement height is important for the estimation of the atmospheric stability. Profile Method 2 uses two measurement heights, surface measurement and tower measurement.

- Surface

  Onshore - Measurements at the surface or near the surface
  Measuring the temperature just above the surface will result in an under-prediction of the temperature difference ($\Delta\theta_v$) between both temperature measurements, which consequently will lead to an under-prediction of the stability parameter (ζ).

  Offshore - Measurement at the surface with a buoy or measurement below the surface. Due to the cool skin effect of water, using temperature measurement just below the surface will result in an on average slightly higher measured temperature, which will lead to an overprediction of the stability parameter (ζ).

- Tower
  The tower measurement or highest measurement varies per location. Each tower has different measurement heights. Depending on the tower, the measurement height has to be selected. A maximum measurement height of around 40-60 meters is recommended, because of two facts mentioned before, sensor accuracy and applicability of MOST within Surface Boundary Layer.

7.3.2 Filters

Before the atmospheric stability can be determined from a given dataset, the data first has to be filtered. Data filtering is of utmost importance for the validity of the outcome of the research. Therefore, three filters have to be applied:

- Operational conditions & sensor errors
  Use of measurement equipment can result in deviation between the true and measured value. In order to exclude sensor errors and values outside of the operational conditions of a wind turbine the data has to be filtered for operational conditions & sensor errors.
- Steady state conditions
  One of the main assumptions of MOST is that the mean parameters does not change in time [45]. In order to satisfy this assumption as best as possible, the deviation of the parameters in time has to be limited. The limits can be found in table 4.2.
- Tower shading
  Influence of tower effects on the measurement data has to be prevented. Therefore depending on the tower measurements at each level the measurement equipment with the best exposure to the free flow direction has to be selected. If not all the effects of tower shading can be eliminated using multiple sensors in different direction at each level, corrections could be applied to the dataset according to [57].

7.3.3 Methodology: Profile Method 2

After all previous steps are executed, the selection of measurement parameters, frequency, height and filters are applied, Profile Method 2 can be used to determine the atmospheric stability iteratively using the following steps:

1. Determine the friction velocity (u_*) by using equation 7.1. During the first iteration, $L = \infty$ resulting in ψ_M is equal to 0.
$$u_* = \frac{k(U_z)}{ln(\frac{z}{z_0}) - \psi_M(\frac{z}{L})} \tag{7.1}$$
2. Determine the temperature scale (θ_*) by using equation 7.2. During the first iteration, $L = \infty$ resulting in ψ_H is equal to 0.
$$\theta_* = \frac{k\delta\theta}{ln(\frac{z}{z_0}) - \psi_H(\frac{z}{L}))} \tag{7.2}$$
3. Determine the heat flux ($\overline{w'\theta'_v}$) by using equation 7.3.
$$-\overline{w'\theta'_v} = u_*\theta_* \tag{7.3}$$
4. Determine the Monin-Obukhov length (L) with equation 7.4. The first estimation of the Monin-Obukhov length can be used to get improved estimates of the u_* and θ_* (going back to step 1). Which therefore can be used to recalculate the Monin-Obukhov length. This iterative process has to be repeated until the Monin-Obukhov length does not change more than 5%.

$$L = -\frac{u_*^3}{\kappa \frac{g}{\theta_v} \overline{w'\theta_v'}} \tag{7.4}$$

where u_* is the friction velocity, κ is the Von Karman constant, g is the acceleration of gravity, θ_v is the virtual potential temperature ($\frac{g}{\theta_v}$ is the buoyancy parameter), $\overline{w}$ is the mean wind velocity, w' is the fluctuating term of the wind velocity, $\overline{\theta_v}$ is the mean virtual potential temperature and $\theta_v{}'$ is the fluctuating term of the virtual potential temperature. Together with $\overline{w'\theta_v'}$ they form the covariance wind velocity and virtual potential temperature.

References

[1] Kh. Ashrafi and Gh.A. Hoshyaripour. A Model to Determine Atmospheric Stability and its Correlation with CO Concentration. (2):186–191, 2008.

[2] M. Aubinet, T. Vesala, and D. Papale. *Eddy Covariance - A Practical Guide to Measurement and Data Analysis*. Springer Netherlands, Dordrecht, 2012.

[3] A.C.M. Beljaars. The derivation of fluxes from profiles in perturbed areas. 24(1976):35–55, 1982.

[4] A.C.M. Beljaars and F.C. Bosveld. Cabauw Data for the Validation of Land Surface Parameterization Schemes. pages 1172–1193, 1997.

[5] A.C.M. Beljaars and A.A.M. Holtslag. Flux parameterization over Land Surfaces for Atmospheric Models. *American Meteorological Society*, (march 1991), 1990.

[6] F. Beyrich and W.K. Adam. *Site and Data Report for the Lindenberg Reference Site in CEOP - Phase I*. Berichte des Deutschen Wetterdienstes, Offenbach am Main, Germany, 2007.

[7] Bosch and van Rijn. WINDSTATS.NL Statistieken over windenergie in Nederland, 2014.

[8] F.C. Bosveld. Manual Cabauw Data. 2012.

[9] British Petroleum (BP). Statistical Review of World Energy, 2013.

[10] J.A. Businger, J.C. Wyngaard, Y. Izumi, and E.F. Bradley. Flux-Profile Relationships in the Atmospheric Surface Layer, 1970.

[11] B. Cañadillas, D. Muñoz Esparza, and T. Neumann. Fluxes estimation and the derivation of the atmospheric stability at the offshore mast FINO1 . 1(December), 2011.

[12] Centraal Bureau voor de Statistiek. *Renewable energy in the Netherlands 2011*.

[13] H.A.R. de Bruin, P. Schotanus, and F.T.M. Nieuwstadt. Temperature measurement with a sonic anemometer and its application to heat moisture fluxes. 26:81–93, 1983.

[14] DEWI. DEWI GmbH - Deutsches Windenergie Institut, 2003.

[15] C.W. Edson, J.B.; Fairall. Similarity relationships in the marine atmospheric surface layer for terms in the TKE and scalar variance budgets. *Atmos. Sci.*, 55:2311–2328, 1998.

[16] European Commission. Renewable Energy : Targets by 2020.

[17] C.W. Fairall, E.F. Bradley, J.S. Godfrey, G.A. Wick, J.B. Edson, and G.S. Young. Cool-skin and warm-layer effects on sea surface temperature. *Journal of Geophysical Research*, 101:1295–1308, 1996.

[18] S.E. Frank, H.P.; Larsen. Simulated wind power off-shore using different parameterisations for the sea surface roughness. *Wind Energy*, 3:67–79, 2000.

[19] Google. Google Maps.

[20] A.A. Grachev and C.W. Fairall. Dependence of the Monin-Obukhov Stability Parameter on the Bulk Richardson Number over the Ocean. *Journal of Applied Meteorology*, pages 406–414, 1996.

[21] S.E. Gryning, H. Jorgensen, S. Larsen, and E. Batchvarova. The wind profile up to 300 meters over flat terrain. *Journal of Physics: Conference Series*, 75, July 2007.

[22] T. Heus, C. C. van Heerwaarden, H. J. J. Jonker, a. Pier Siebesma, S. Axelsen, K. van den Dries, O. Geoffroy, a. F. Moene, D. Pino, S. R. de Roode, and J. Vilà-Guerau de Arellano. Formulation of the Dutch Atmospheric Large-Eddy Simulation (DALES) and overview of its applications. *Geoscientific Model Development*, 3(2):415–444, September 2010.

[23] U. Hogstrom. Review of some basic characteristics of the atmospheric surface layer. *Boundary-Layer Meteorology*, 78(3-4):215–246, 1996.

[24] A. A. M. Holtslag. Estimates of diabatic wind speed profiles from near-surface weather observations. 29:225–250, 1984.

[25] A.A.M. Holtslag and A.P. van Ulden. *De meteorologische aspecten van luchtverontreinigingsmodellen: eindrapport van het project klimatologie verspreindingsmodellen*. Koninklijk Nederlands Meteorologische Instituut, De Bilt.

[26] M. Holtslag. Estimating atmospheric stability and correcting wind shear models accordingly. 2012.

[27] M.C. Holtslag. Exploring the Coastal Marine Atmospheric Boundary Layer. (December), 2011.

[28] M.C. Holtslag, W.A.A.M. Bierbooms, and G.J.W. van Bussel. Definition of the equivalent stability for wind turbine fatique load assessment. 2014.

[29] M.Z. Jacobson. *Fundamentals of atmospheric modeling*. Cambridge University Press, 2005.

[30] H. Jonker and P. Siebesma. A continuous Year of GPU-resident Atmospheric LES in Cabauw. 2014.

[31] J. Jonkman, S. Butterfield, W. Musial, and G. Scott. Definition of a 5-MW Reference Wind Turbine for Offshore System Development Definition of a 5-MW Reference Wind Turbine for Offshore System Development. (February), 2009.

[32] B. Kallstrand and H. Bergstrom. Mesoscale wind field modifications over the Baltic Sea. *Boundary Layer Meteorol*, 95:161–188, 2000.

[33] M. Kelly and S.E. Gryning. Long-Term Mean Wind Profiles Based on Similarity Theory. *Boundary-Layer Meteorology*, 136(3):377–390, June 2010.

[34] H.J. Kouwenhoven. User manual data files meteorological mast NoordzeeWind. (October):1–20, 2007.

[35] A. Kumar. The University of Toledo course slides: Stability Schemes.

[36] B. Lange, S. Larsen, J. Hojstrup, and R. Barthelmie. The influence of thermal effects on the Wind Speed Profile of the Coastal Marine Boundary Layer. *Boundary-Layer Meteorology*, 112(3):587–617, September 2004.

[37] B.C. Larsen. DTU Wind Energy.

[38] X. Lee, W. Massman, and B. Law, editors. *Handbook of Micrometeorology: A guide for Surface Flux Measurements and Analysis*, volume 29 of *Atmospheric and Oceanographic Sciences Library*. Kluwer Academic Publishers, Dordrecht, 2005.

[39] M. Mohan and T.A. Siddiqui. Analysis of various schemes for the estimation of atmospheric stability classification. 32(21), 1998.

[40] A.S. Monin and A.M. Obukhov. Basic laws of turbulent mixing in the surface layer of the atmosphere. 24(151):163–187, 1959.

[41] M. Motta, R. J. Barthelmie, and P. Volund. The influence of non-logarithmic wind speed profiles on potential power output at Danish offshore sites. *Wind Energy*, 8(2):219–236, April 2005.

[42] K.A. Novick, J. Walker, W.S. Chan, A. Schmidt, C. Sobek, and J.M. Vose. Eddy covariance measurements with a new fast-response, enclosed-path analyzer: Spectral characteristics and cross-system comparisons. *Agricultural and Forest Meteorology*, 181:17–32, November 2013.

[43] A. Peña and A. Hahmann. Atmospheric stability and turbulence fluxes at Horns Rev an intercomparison of sonic, bulk and WRF model data. (Sept. 2011):717–731, 2012.

[44] A. Sathe. Atmospheric stability and wind profile climatology over the North Sea - Case study at Egmond aan Zee. 2010.

[45] A. Sathe. Project Site Data - OWEZ data analysis. 2010.

[46] A. Sathe. *Influence of wind conditions on wind turbine loads and measurement of turbulence using lidars*. 2012.

[47] A. Sathe and W.A.A.M. Bierbooms. Influence of different wind profiles due to varying atmospheric stability on the fatigue life of wind turbines. *Journal of Physics: Conference Series*, 75:012056, July 2007.

[48] A. Sathe, S.E. Gryning, and A. Peña. Comparison of the atmospheric stability and wind profiles at two wind farm sites over a long marine fetch in the North Sea. (February):767–780, 2011.

[49] A. Sathe, J. Mann, T. Barlas, W.A.A.M. Bierbooms, and G.J.W. van Bussel. Influence of atmospheric stability on wind. 2012.

[50] A. Sathe, J. Mann, J. Gottschall, and M. S. Courtney. Can Wind Lidars Measure Turbulence? *Journal of Atmospheric and Oceanic Technology*, 28(7):853–868, July 2011.

[51] P. Schotanus, F.T.M. Nieuwstadt, and H.A.R. Bruin. Temperature measurement with a sonic anemometer and its application to heat and moisture fluxes, 1983.

[52] Scottish and Southern Energy. Investor presentation Foyers July 2009. (July), 2009.

[53] R.B. Stull. *Meteorology for Scientists and Engineers*. 2000.

[54] N. Sucevic and Z. Djurisic. Influence of atmospheric stability variation on uncertainties of wind farm production estimation. 0(m).

[55] D. Veldkamp. *Chances in Wind Energy, a probabilistic approach to wind turbine fatigue design*. 2006.

[56] J.W. Verkaik and A.A.M. Holtslag. Wind profiles, momentum fluxes and roughness lengths at Cabauw revisited. *Boundary-Layer Meteorology*, 122(3):701–719, October 2006.

[57] H.R.A. Wessels and Koninklijk Nederlands Meteorologisch Instituut. Distortion of the Wind Field by the Cabauw Meteorological Tower. 1983.

[58] S. Wharton and J.K. Lundquist. Assessing atmospheric stability and its impacts on rotor-disk wind characteristics at an onshore. (July 2011):525–546, 2012.

[59] J. Wieringa. An Objective Exposure Correction Method for Average Wind Speeds Measured at a Sheltered Location. *Quart. J. Roy. Meteorol. Soc.*, 102:241–253, 1976.

[60] S.S. Zilitinkevich and I.N. Esau. Resistance and heat-transfer laws for stable and neutral planetary boundary layers: Old theory advanced and re-evaluated. *Quarterly Journal of the Royal Meteorological Society*, 131(609):1863–1892, July 2005.

[61] S. Zoras, A.G. Triantafyllou, and D. Deligiorgi. Atmospheric stability and PM10 concentrations at far distance from elevated point sources in complex terrain: worst-case episode study. *Journal of environmental management*, 80(4):295–302, September 2006.

Appendix A

OWEZ

A.1 Verification of Matlab Models

For the following figures the OWEZ data from January 2007 up to and including November 2008 is used to determine the atmospheric stability. Only freestream wind data is used for figure A.1 and A.2 with wind directions between 135 and 315 degrees.

It can be seen that the frequency distribution of the analysis executed by Sathe and myself are very similar. Concluded that data handling and filtering is correct, also the programmed code for the Richardson Bulk method.

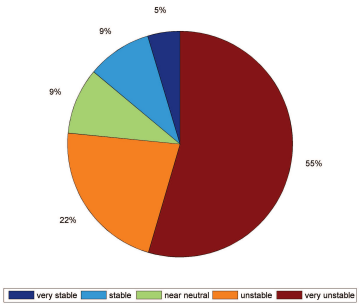

Figure A.1: Frequency distribution atmospheric stability - OWEZ data from literature [45]

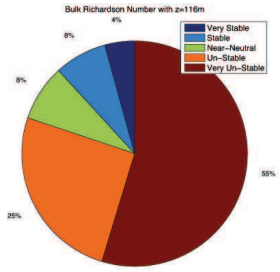

Figure A.2: Frequency distribution atmospheric stability - OWEZ data

Appendix B

KNMI Met Mast Cabauw

B.1 Verification Cabauw Sonic measurements

In this section a visual comparison of the stabiltity distribution at Cabauw is executed for the verification of the method used to estimate the stability in this research. Hereby the stability distribution found in literature is compared to the distribution found using the met mast data.

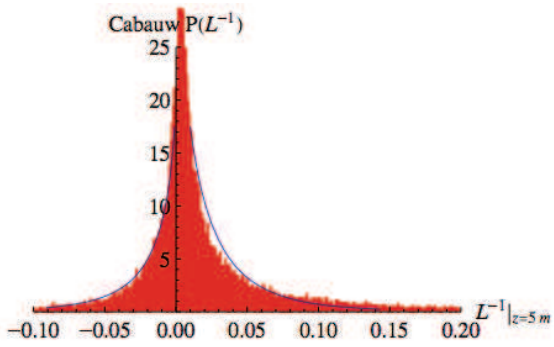

Figure B.1: Cabauw - Stability PDF according to literature [33]

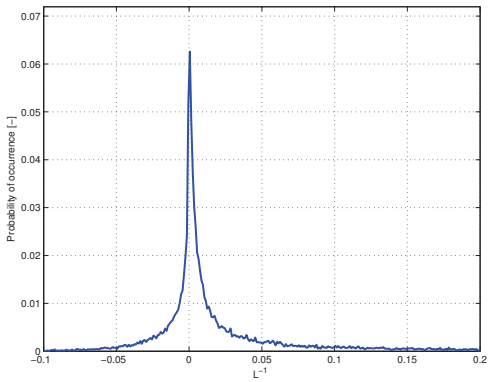

Figure B.2: Cabauw - Stability PDF based on measurements

In the paper of Kelly & Gryning [33], sonic measurement at a height of 5 meters are used to determine the atmospheric stability. The stability PDF determined by Kelly & Gryning can be found in figure B.1. Figure B.2 shows the stability PDF determined using measurement myself. Both figures show roughly the same distribution, therefore it can be concluded that method and filters used are correct.

B.2 Roughness length of surroundings Cabauw

The roughness is one of the main parameter determining the shape of the wind profile. In this section multiple papers are discussed determining the roughness length of the surroundings of Cabauw.

- Wieringa's effective roughness (z_0)
- Beljaars z_0 derived from averaged neutral wind profiles
- Bosveld

From figure B.3 and table B.1 significant differences can be observed between the roughness lengths found by these three researchers.

Direction	Roughness length Summer [m]	Roughness length Winter [m]
000-020	0.06	0.04
020-040	0.08	0.05
040-060	0.10	0.05
060-080	0.15	0.07
080-100	0.15	0.10
100-120	0.15	0.12
120-140	0.11	0.02
140-160	0.08	0.02
160-180	0.04	0.02
180-200	0.04	0.03
200-220	0.04	0.03
220-240	0.04	0.02
240-260	0.07	0.04
260-280	0.06	0.03
280-300	0.06	0.03
300-320	0.06	0.04
320-340	0.05	0.04
340-360	0.05	0.03

Table B.1: Description of roughness length surrounding Cabauw [8][4]

To analyse the impact of the found differences a small sensitivity study is executed. The second Profile Method is used to determine the atmospheric stability with various roughness lengths:

- Standard roughness of table B.1
- Standard roughness - 0.1
- Standard roughness + 0.1
- Constant roughness of 0.01 meters

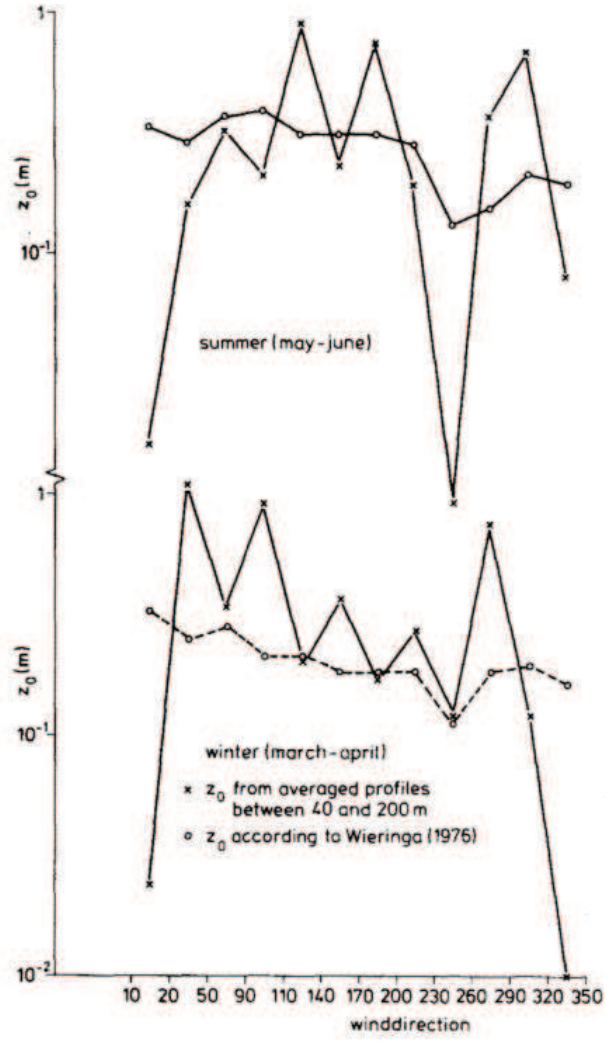

Figure B.3: Roughness lengths comparison of Wieringa's effective (z_0) [59] and Beljaars z_0 derived from averaged neutral wind profiles [3] during the summer and winter

- Constant roughness of 0.5 meters
- Constant roughness of 1 meters

Figures B.4 and B.5 show the results.

From both figures it can be concluded that the roughness length is an important parameter, because significant difference in the atmospheric stability can be seen using different roughness lengths. However an roughness increase or decrease of 0.1 is already significant when compared to the absolute roughness in table B.1. These changes result in a maximum deviation of around 1% in frequency of occurrence.

What can be observed from the figures is that an over prediction of the roughness leads to an over prediction of neutral conditions and an under prediction of unstable conditions. This corresponds with the expectations, because a roughness increase results in higher shear and more mixing of

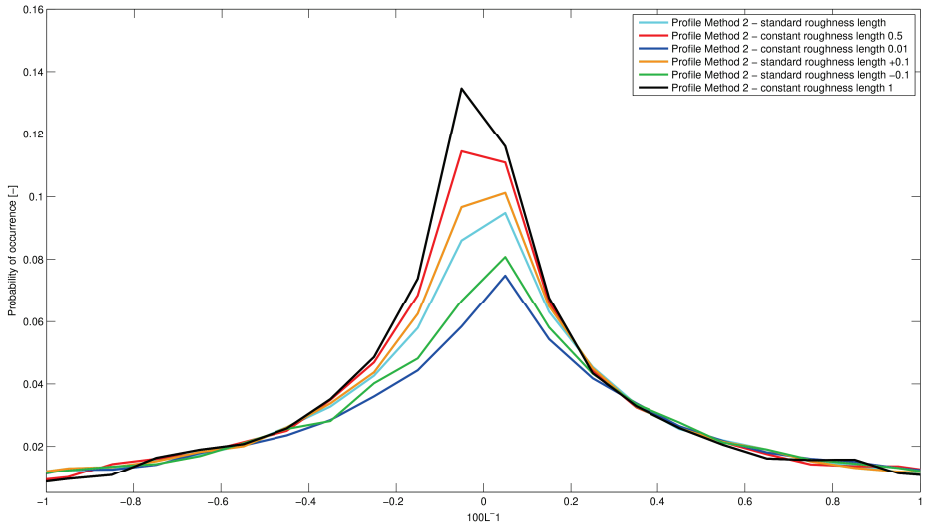

Figure B.4: Cabauw - PDF comparison for different roughness lengths

layers. Unstable conditions are then described as neutral conditions, which results in an under prediction of unstable conditions.

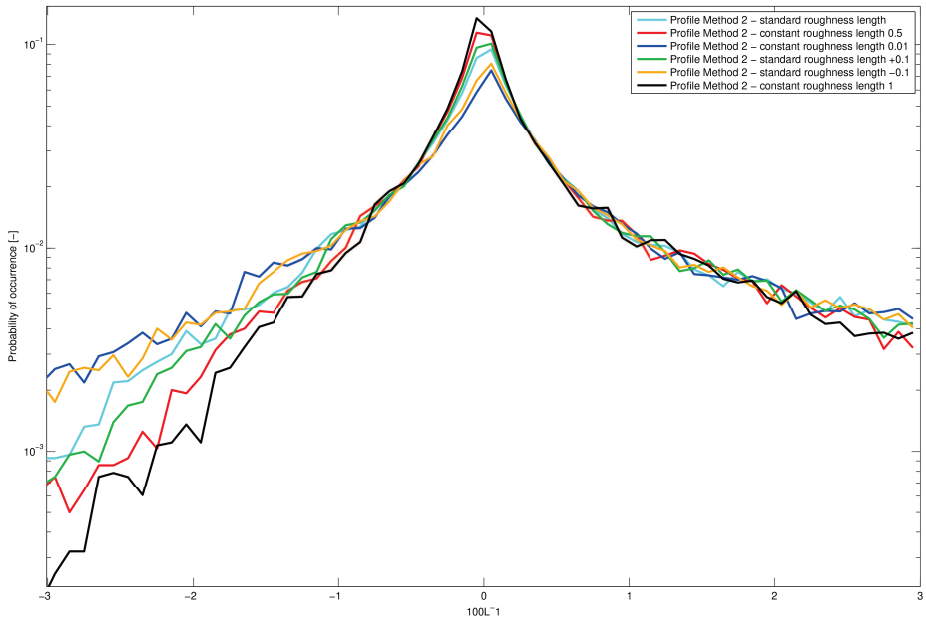

Figure B.5: Cabauw - PDF comparison for different roughness lengths on semi-logarithmic scale

B.3 Wind profile

In this master thesis multiple methodologies to estimate the atmospheric stability are directly compared to the Eddy Covariance Method. However high frequent measurement data required for the Eddy Covariance Method is not always available. Therefore in this section a comparison of atmospheric stability estimations will be executed using the wind profile. The atmospheric stability is of great influence on the wind profile and turbulence, as explained in the introduction and by comparing the predicted wind profile with a diabatic correction with the measured wind profile the quality of the atmospheric stability estimation can be analysed.

Equation 2.14 shows the logarithm profile or log law. In this equation the atmospheric stability is not taken into account, but the atmosphere is assumed to be neutral. However equation B.1 predicts the wind speed for the Surface Boundary Layer, which takes the atmospheric stability into account.

$$U_{z_2} = U_{z_1} \frac{ln(\frac{z_2}{z_0}) - \Psi_{M_2}(\frac{z_2}{L})}{ln(\frac{z_1}{z_0}) - \Psi_{M_1}(\frac{z_1}{L})} \tag{B.1}$$

It has to be taken into account that the Surface Boundary Layer height filter is used, to decrease the uncertainty of the results. However to predict the wind speed at higher altitudes, the wind profile model must be extended for the entire Boundary Layer.

The figures in this section are divided into two parts, left and right side of the figure.

- Left figure
  Shows a comparison of the four different wind profile models, predicted profile (from equation B.1), measured profile, power law and log law. With on the x-axis the stability parameter $\frac{100}{L}$ and the y-axis the ratio $\frac{U_{z40}}{U_{z10}}$ for each of the four wind profile models. The stability parameter is binned with a bin width of 0.1.
- Right figure
  Shows the ratio between the measured and predicted wind speed at 40 meters. Each point is shown in red, with the mean value in blue (averaged with a bin size of 0.1) with error bars indicating the standard deviation.

B.3.1 Observations & Conclusions

From figure B.6 it can be observed that for the Eddy Covariance the predicted profile is below the measured for unstable conditions and for stable conditions it is above the measured. The predicted profile of the Bulk Richardson Number & Profile Method 2 , respectively figure B.7 and B.8, are very similar to the measured wind profile. The Gradient Richardson Number & Profile Method 1 both give a significant under prediction of the wind speed for unstable conditions. For stable conditions the Gradient Richardson Number also gives an under prediction. The wind profile predictions of Profile Method 1 are very similar to the measured wind profile. However for both the Gradient Richardson Number & Profile Method 1 a large uncertainty can be observed, due to the large scatter of the measured and predicted wind speed.

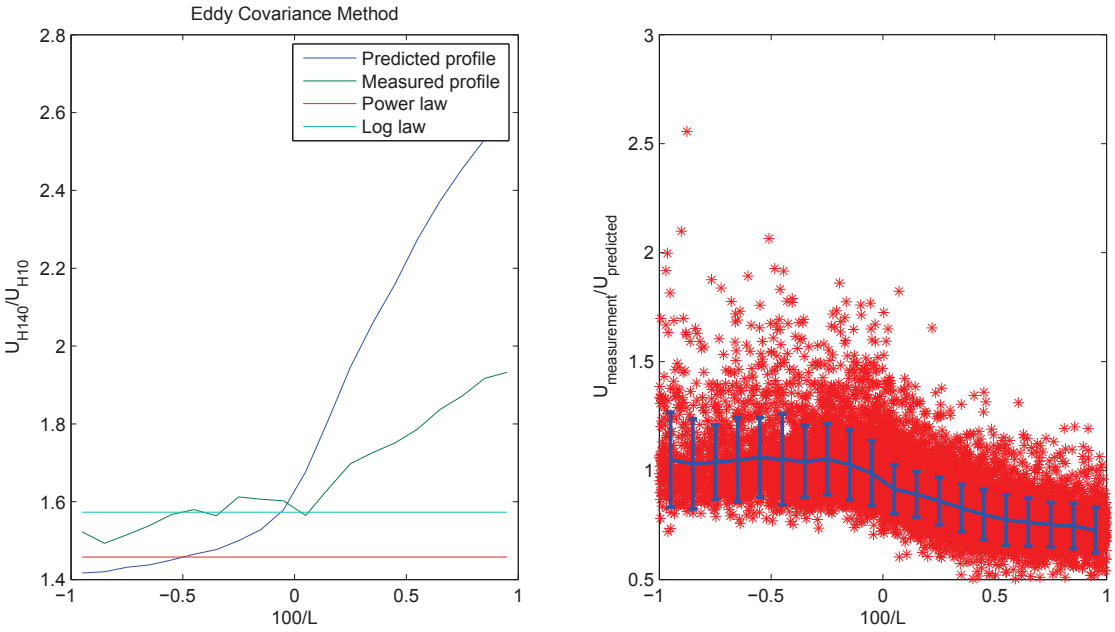

Figure B.6: Cabauw - On the left side the predicted wind profile with Eddy Covariance Method at 140 meters and on the right side the ratio of measured and predicted wind speed

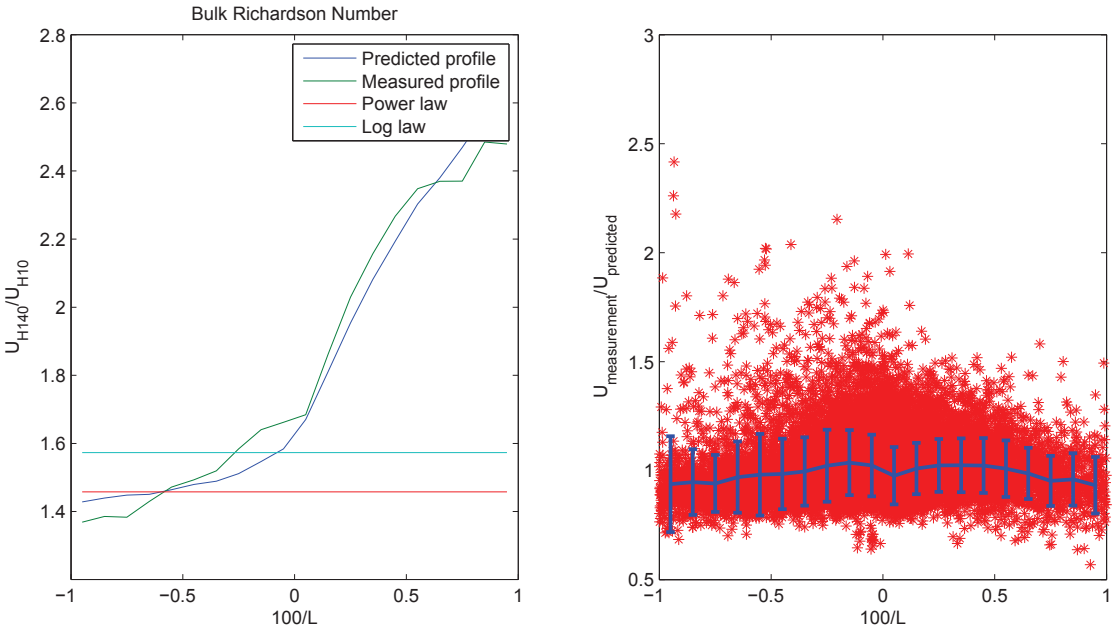

Figure B.7: Cabauw - On the left side the predicted wind profile with the Bulk Richardson Number and on the right side the ratio of measured and predicted windspeed

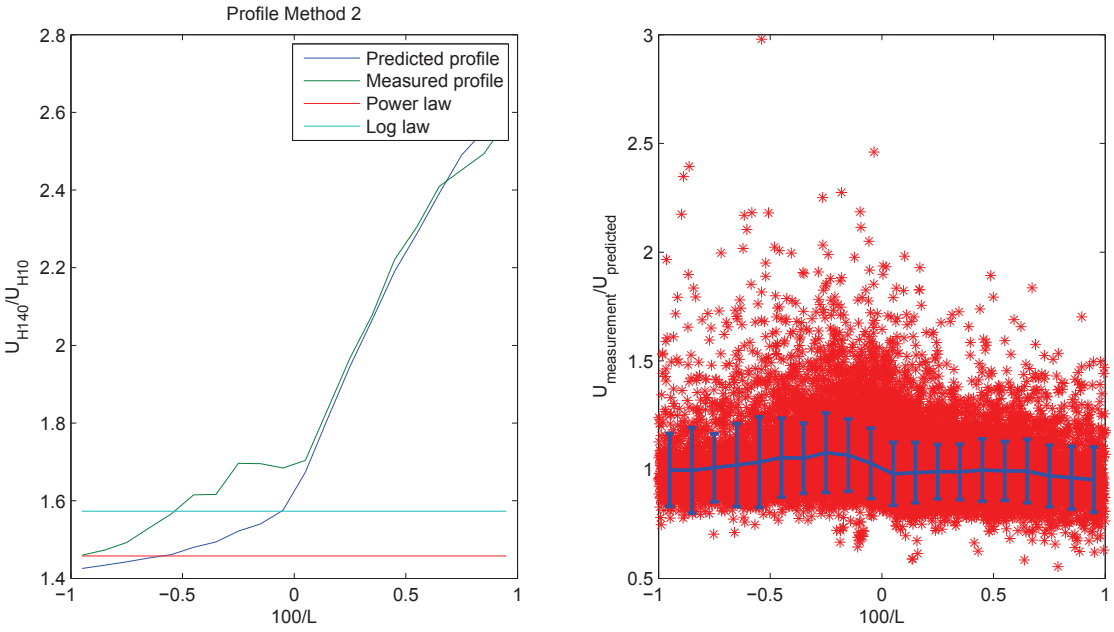

Figure B.8: Cabauw - On the left side the predicted wind profile with the Profile Method 2 and on the right side the ratio of measured and predicted windspeed

The results of the Bulk Richardson Number and Profile Method 2 are very similar. Comparing these results with the findings of Ameya Sathe shows that they are very similar. He also found that the larger scatter of the ration measured/ predicted wind speed for the Gradient Richardson Number and Profile Method 1.

In this part a prediction height of 140 meters is selected. The same analysis could be executed with a smaller height difference, 10-40 meters, this however would only results in a small increase of wind speed. A small error between the predicted wind speed and measured wind speed therefore results in big impact.

As discussed in section B.2 multiple papers discuss the roughness length around the Cabauw met mast. Unfortunately they give different values for the environment, which could have a small impact on the predicted wind profile. Next to the constant roughness deviation from reality, also seasonal variation of roughness is of influence which are not taken into account.

The results found by comparing multiple methodologies with the wind profile are similar to the results found in chapter 4. What could be observed was that the conditions found by the Eddy Covariance Method near the surface, does not represent the entire Surface Boundary Layer. The deviation between the predicted and measured wind profile using the Bulk Richardson Number and Profile Method 2 were smaller, it is therefore recommended to use the Eddy Covariance Method at more representatives altitudes for wind turbines.

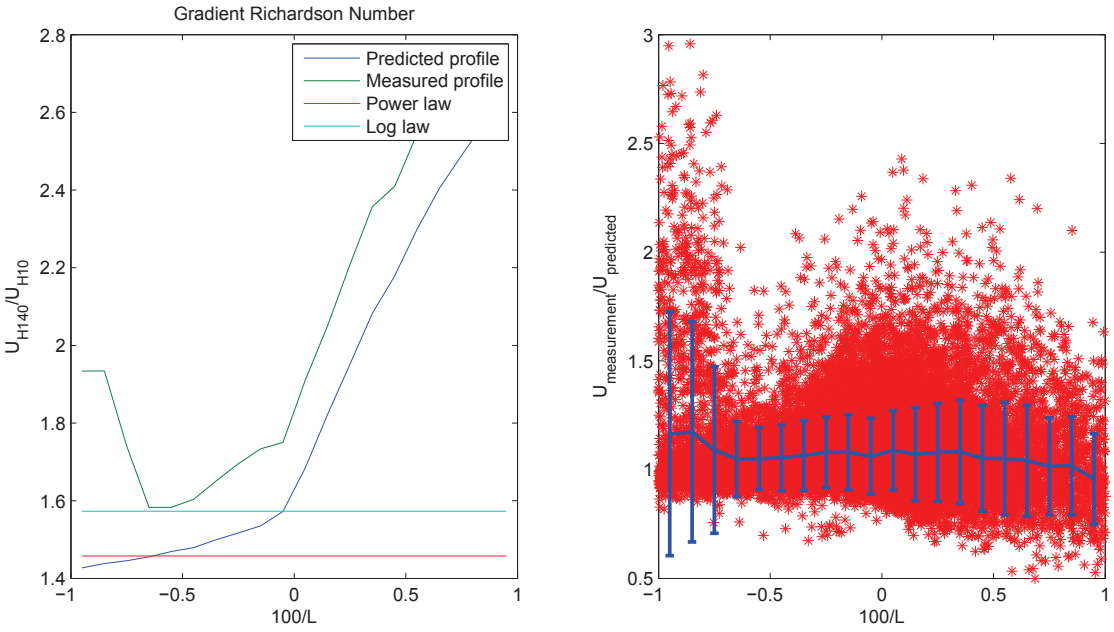

Figure B.9: Cabauw - On the left side the predicted wind profile with the Gradient Richardson Number and on the right side the ratio of measured and predicted windspeed

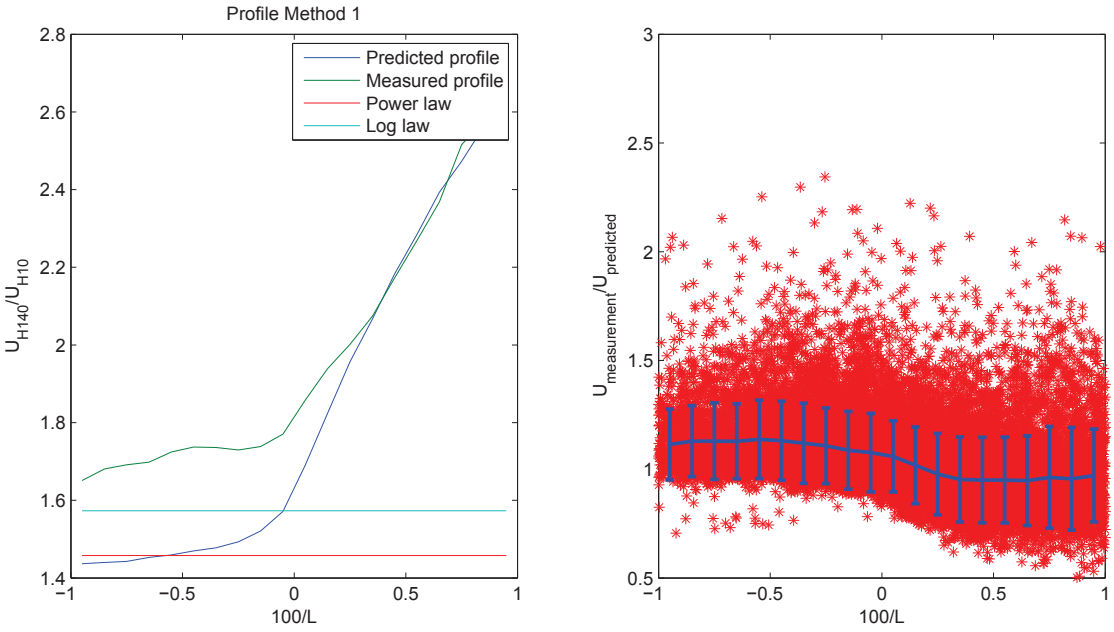

Figure B.10: Cabauw - On the left side the predicted wind profile with the Profile Method 1 and on the right side the ratio of measured and predicted windspeed

B.4 Improved Atmospheric Stability estimation with combination of multiple methodologies

By combining multiple methodologies using the wind speed or time of the day could improve the estimation of the atmospheric stability.

- Time of the day: A possible improvement of the atmospheric stability estimation could be achieved by combining Bulk Richardson Number with the Gradient Richardson Number by selecting the Bulk Richardson Number for night time (20:00-07:00) and the Gradient Richardson Number for the day time (07:00-20:00).
- Wind speed: A possible improvement of the atmospheric stability estimation could be achieved by combining Bulk Richardson Number with the Gradient Richardson Number by selecting the Bulk Richardson Number for wind speeds above 7 m/s and the Gradient Richardson Number for wind speeds below 7 m/s.

As can be deducted from a number of figures, there is a small improvement in overall distribution found by combination two methodologies using the Cabauw met mast data. However, the results of Lindenberg, shown in section 5.3.2, give no indication of possible improvements, so therefore no further investigation into possible improvements based on the multiple methods for wind speeds and time of the day.

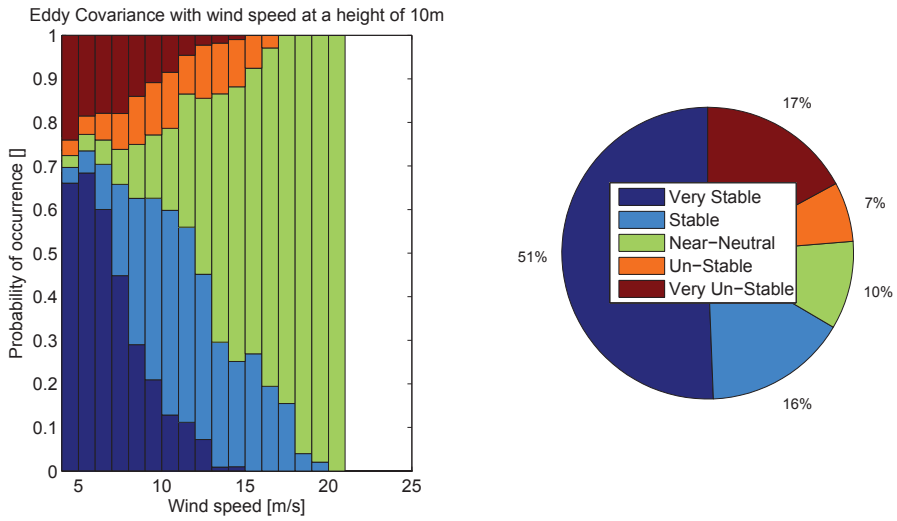

Figure B.11: Cabauw - Eddy Covariance Method with surface measurements

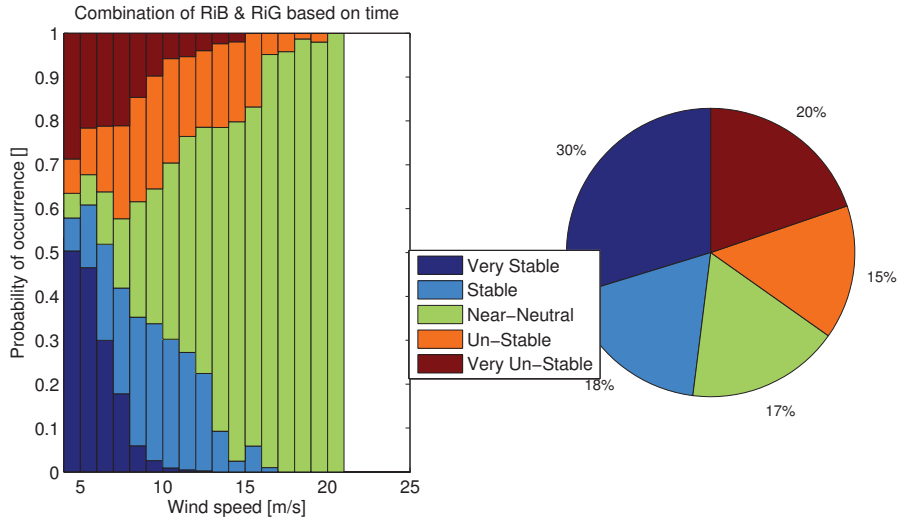

Figure B.12: Cabauw - Combination of Bulk & Gradient Richardson Number based on time

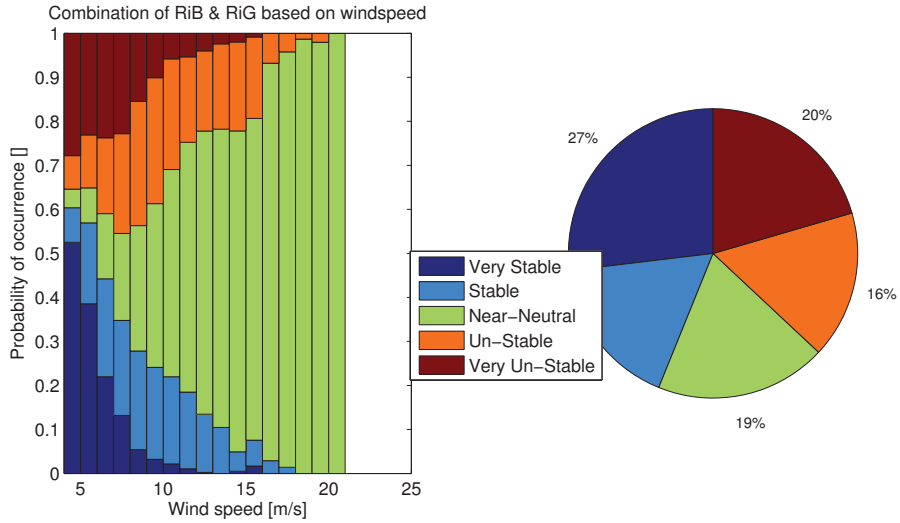

Figure B.13: Cabauw - Combination of Bulk & Gradient Richardson Number based on wind speed

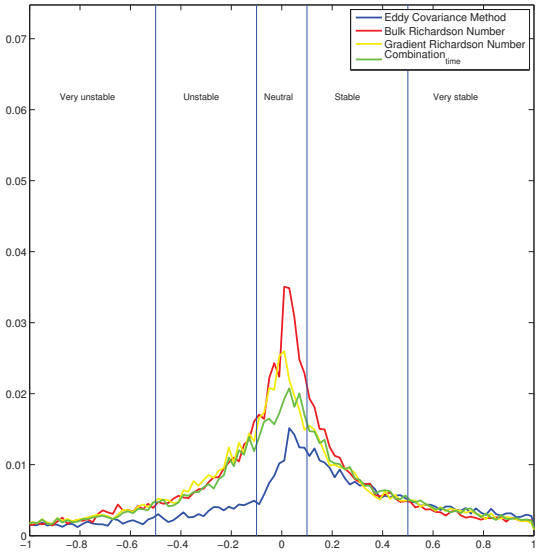

Figure B.14: Cabauw - PDF with combination of Bulk & Gradient Richardson Number based on time

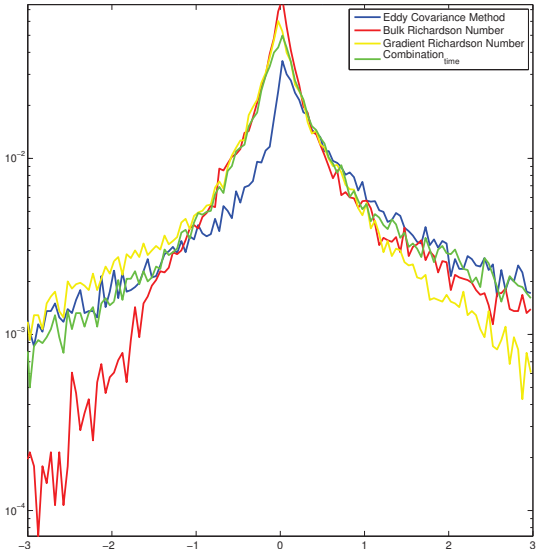

Figure B.15: Cabauw - PDF on semi-logarithmic scale with combination of Bulk & Gradient Richardson Number based on time

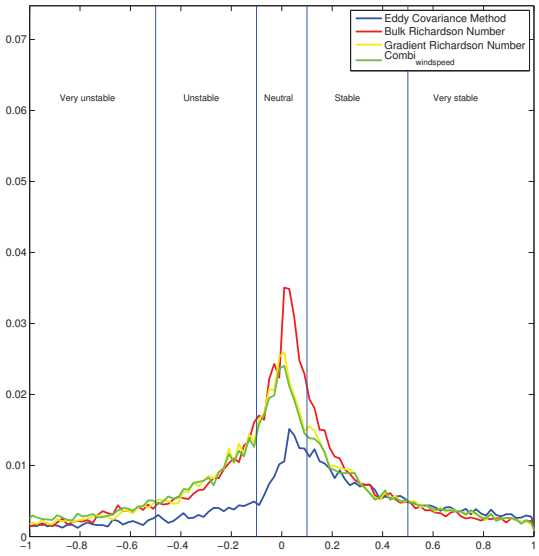

Figure B.16: Cabauw - PDF with combination of Bulk & Gradient Richardson Number based on wind speed

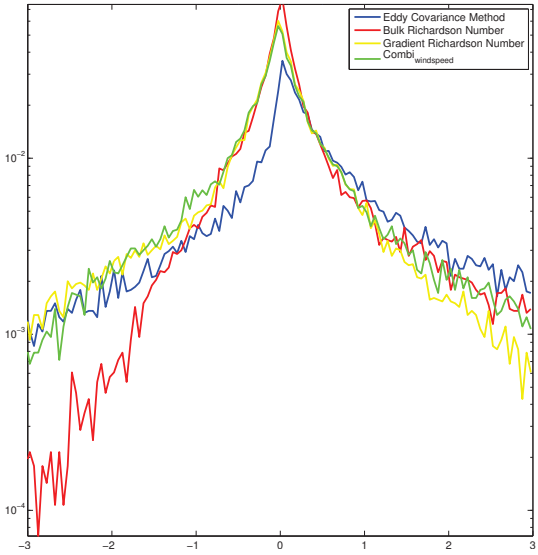

Figure B.17: Cabauw - PDF on semi-logarithmic scale with combination of Bulk & Gradient Richardson Number based on wind speed

Appendix C

Lindenberg Boundary Layer Measurement Tower

C.1 Roughness length

In literature, little information is available of the roughness surrounding Lindenberg. The terrain is often described as mainly grassland and agricultural fields in the immediate vicinity. A little bit further to the South-East a small village is situated and to the West a small forest can be found. Due to the grasslands surrounding the Lindenberg Measurement Tower the roughness in direct vicinity can therefore be described at around 0.01 m. [6]

No literature is available, discussing the roughness surrounding the Lindenberg measurement tower. To get an first estimation of the surroundings roughness around Lindenberg, the roughness length is determined using the 2010 data at Lindenberg. The sonic measurements are used to determine the Neutral conditions and filtering the other data. The data then is divided into sectors of each 30 degrees and for each moment in time the roughness is iteratively determined using the logarithmic wind profile without diabatic corrections. For each sector the lowest and highest 5% of the data are again filtered, to eliminate the extremes. In the end the mean roughness length for each sector is calculated, which can be seen in table C.1

Table 1 – Land use around the Lindenberg reference stations depending on scale

Land cover within	Falkenberg	Forest Station
100 m	Grassland	pine forest
500 m	grassland / cropland	pine forest
10 km	grassland / cropland – 60 % pine forest – 30 % open water – 5 % settlements – 5 %	grassland / cropland – 28 % pine forest – 60 % open water – 7 % settlements – 5 %

Figure C.1: Figure with overview of land use surrounding Lindenberg [6]

Direction	Roughness length [m]
000-030	0.15
030-060	0.08
060-090	0.08
090-120	0.08
120-150	0.08
150-180	0.10
180-210	0.09
210-240	0.09
240-270	0.08
270-300	0.06
300-330	0.08
330-360	0.10

Table C.1: Roughness derived from measured wind profile under neutral conditions

C.2 Results

In this section additional figures of chapter 5 can be found.

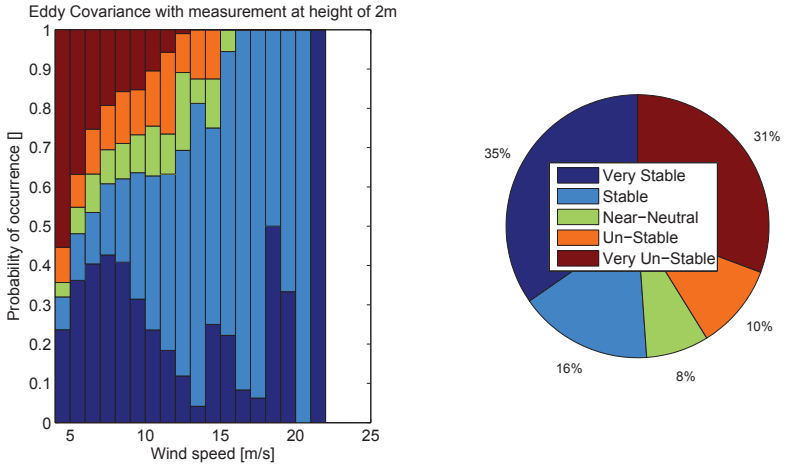

Figure C.2: Lindenberg - Eddy Covariance Method at a height of 2m

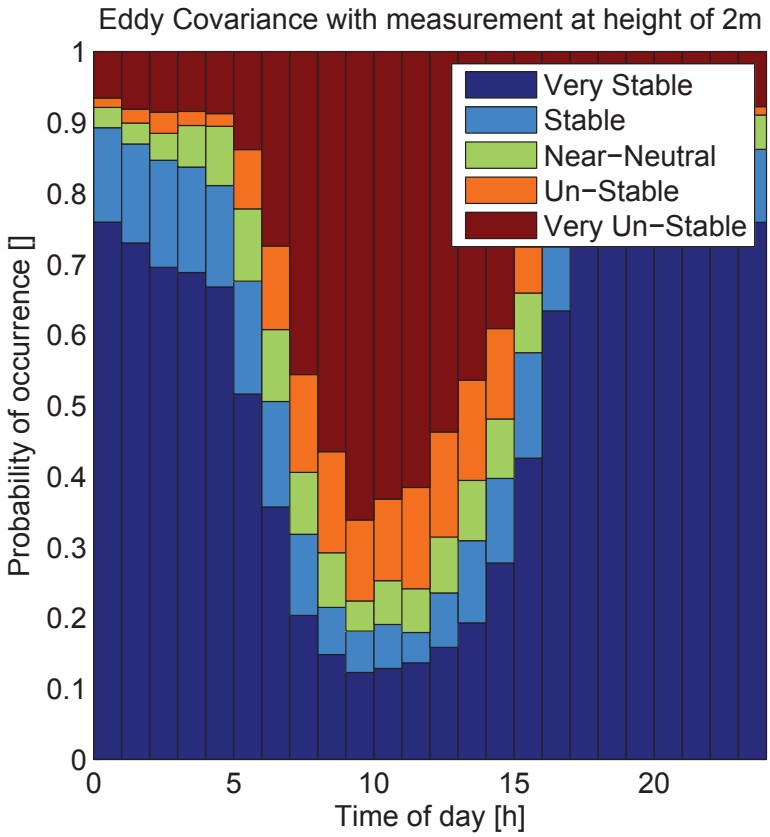

Figure C.3: Lindenberg - Hourly distribution of Eddy Covariance Method at a height of 2m

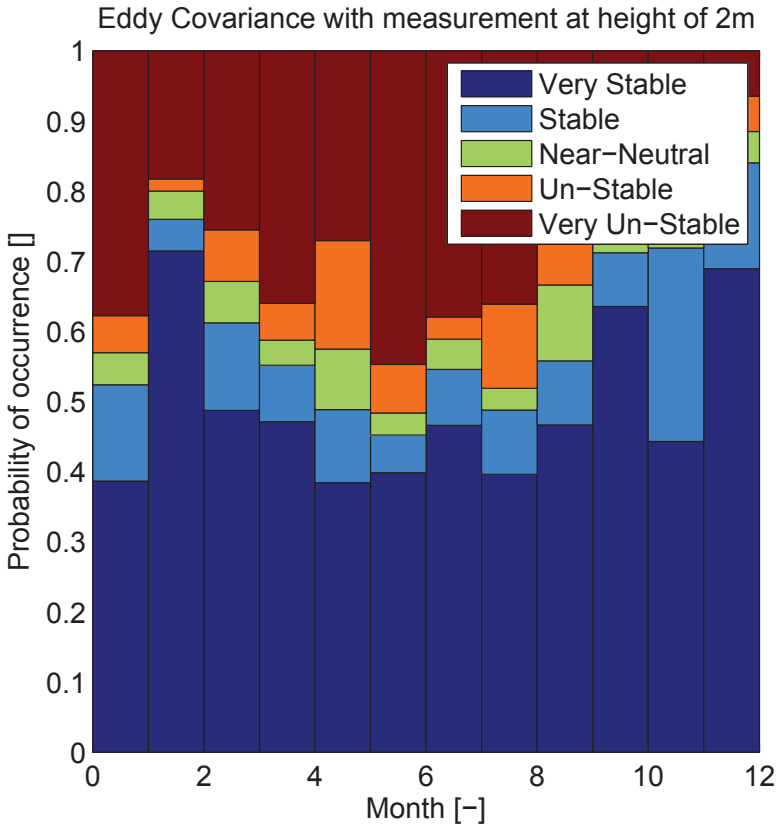

Figure C.4: Lindenberg - Monthly distribution of Eddy Covariance Method at a height of 2m

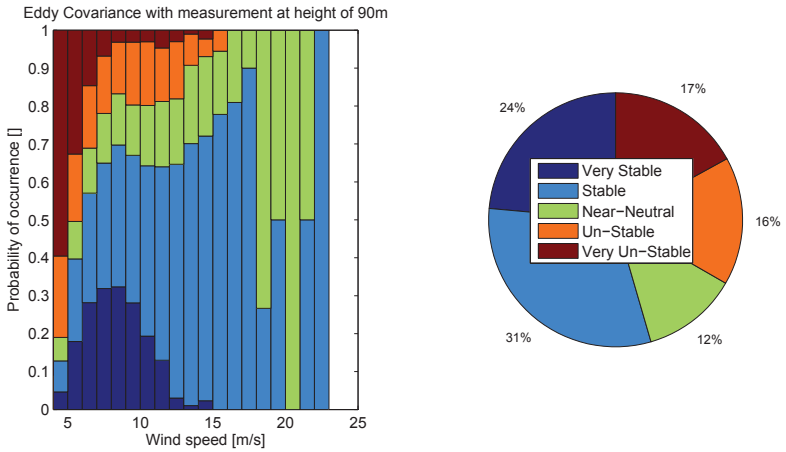

Figure C.5: Lindenberg - Eddy Covariance Method at a height of 90m

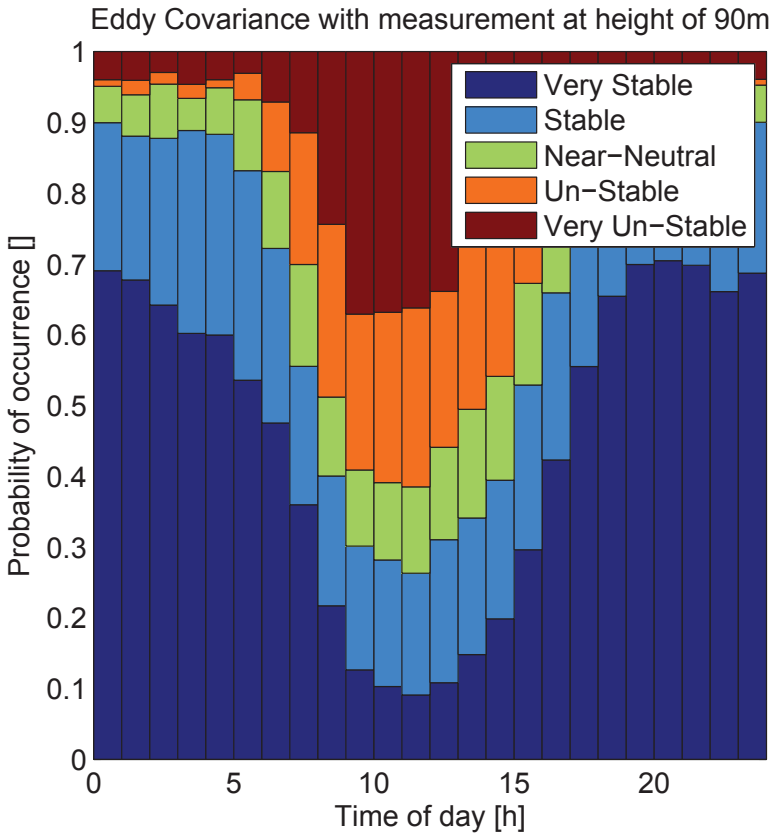

Figure C.6: Lindenberg - Hourly distribution of Eddy Covariance Method at a height of 90m

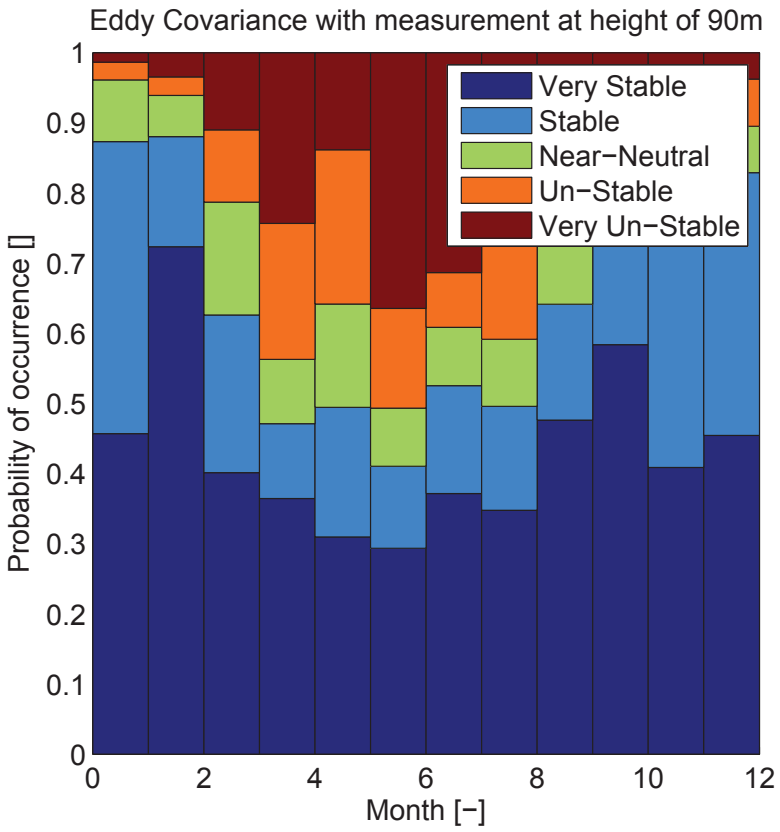

Figure C.7: Lindenberg - Monthly distribution of Eddy Covariance Method at a height of 90m

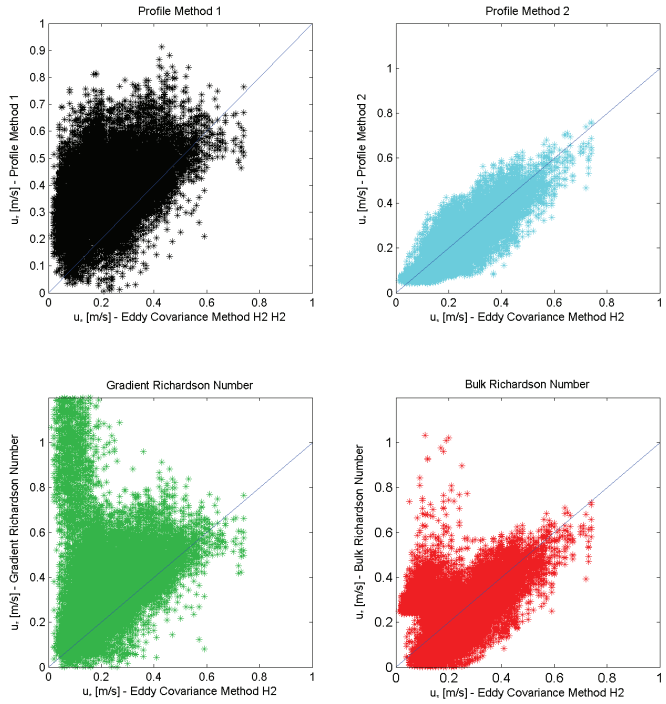

Figure C.8: Lindenberg - Comparison of Friction Velocity (u_*) at a height of 2m without the filter for the Surface Boundary Layer height

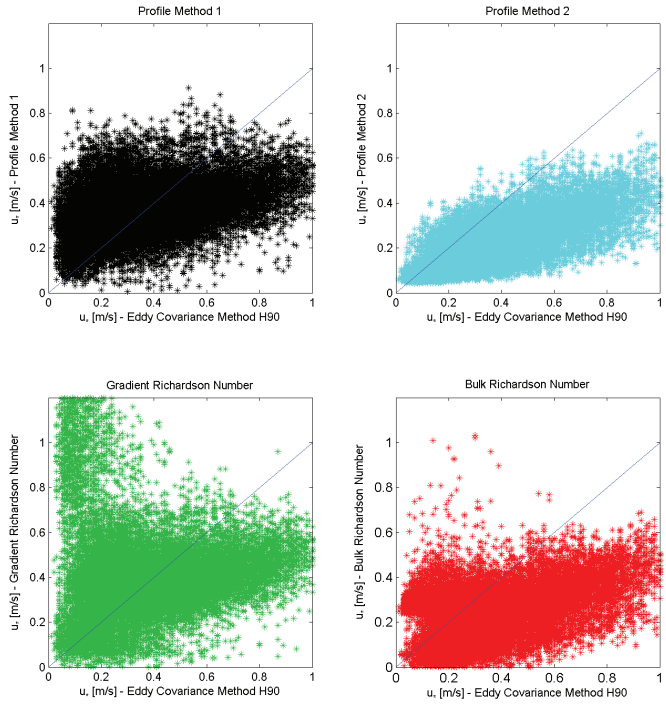

Figure C.9: Lindenberg - Comparison of Friction Velocity (u_*) at a height of 90m without the filter for the Surface Boundary Layer height

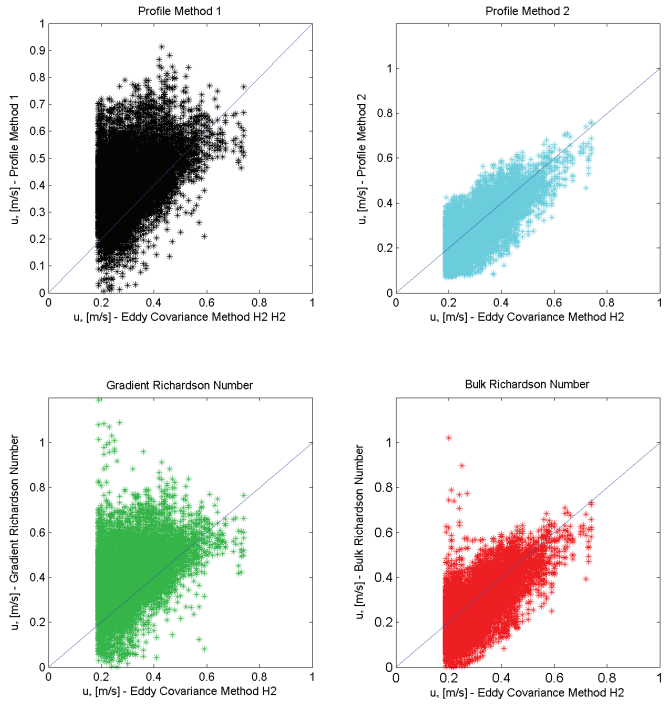

Figure C.10: Lindenberg - Comparison of Friction Velocity (u_*) at a height of 2m with the filter for the Surface Boundary Layer height

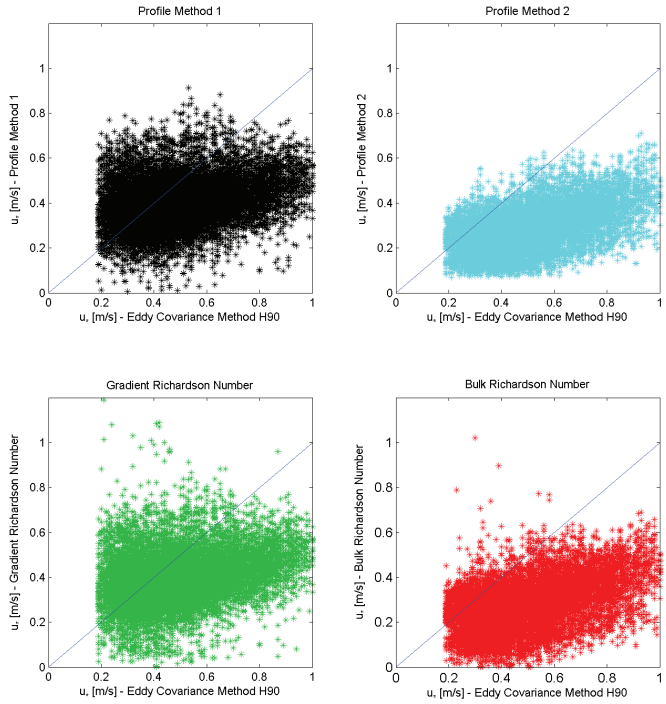

Figure C.11: Lindenberg - Comparison of Friction Velocity (u_*) at a height of 90m with the filter for the Surface Boundary Layer height

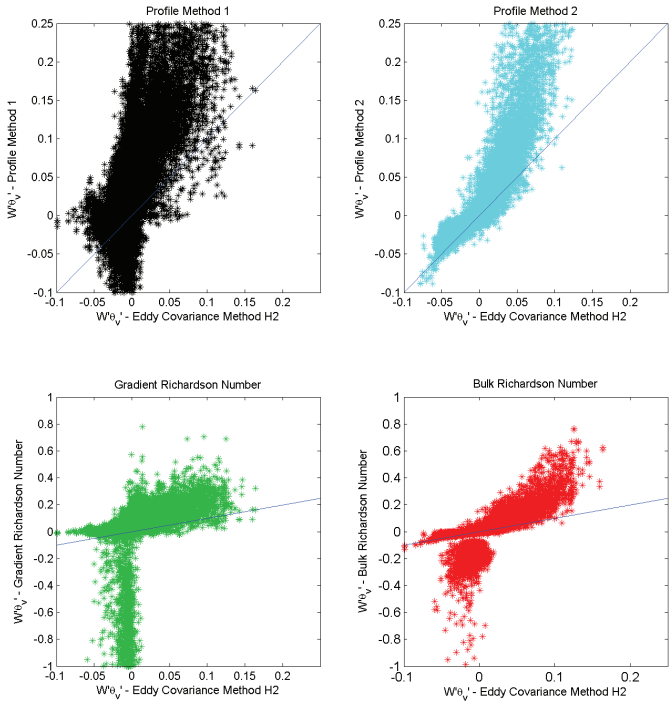

Figure C.12: Lindenberg - Comparison of Heat flux ($\overline{w'\theta'}$) at a height of 2m without the filter for the Surface Boundary Layer height

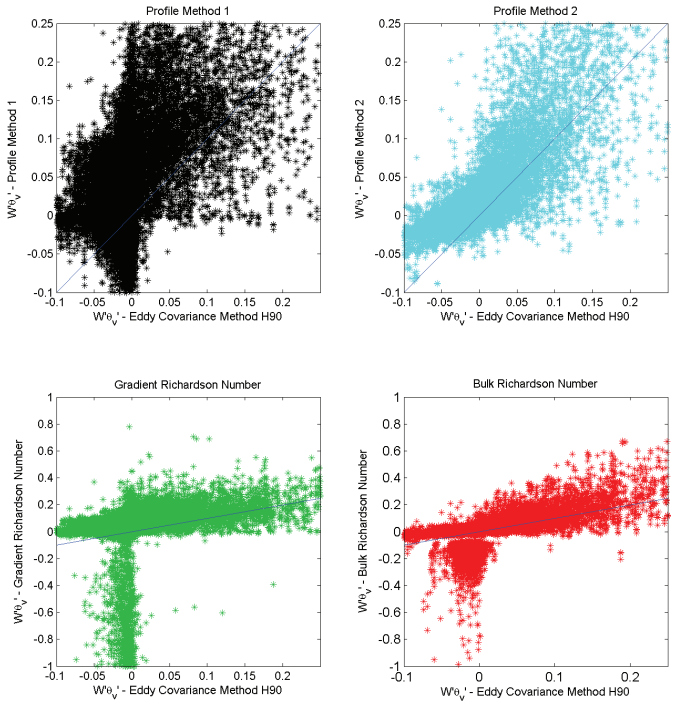

Figure C.13: Lindenberg - Comparison of Heat flux ($\overline{w'\theta'}$) at a height of 90m without the filter for the Surface Boundary Layer height

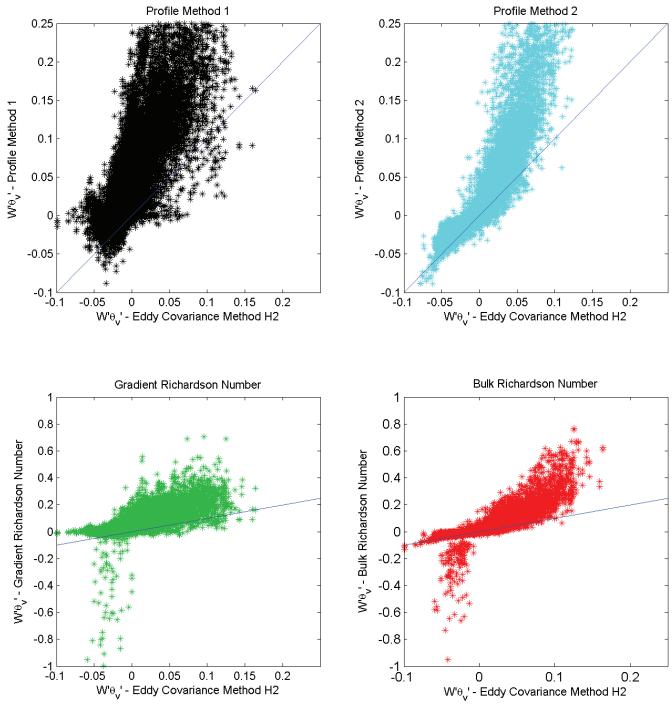

Figure C.14: Lindenberg - Comparison of Heat flux ($\overline{w'\theta'}$) at a height of 2m with the filter for the Surface Boundary Layer height

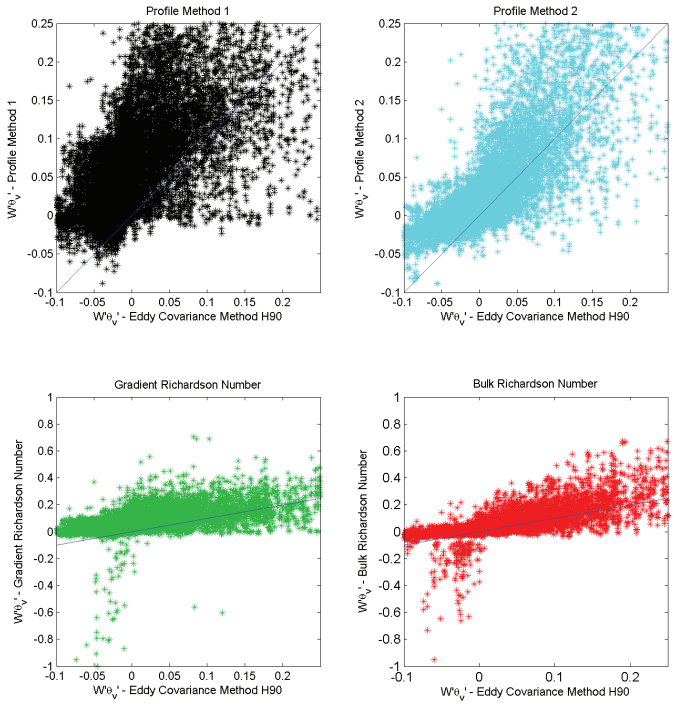

Figure C.15: Lindenberg - Comparison of Heat flux ($\overline{w'\theta'}$) at a height of 90m with the filter for the Surface Boundary Layer height

Appendix D

National Test Centre Høvsøre

D.1 Introduction

At the end of the 1990s, it was decided by Danish politicians to establish a large National Test Centre at Høvsøre, located on the West coast of Jutland in Denmark. The main goal for the test centre was to develop and test wind turbine concepts, methods and data gathering of wind turbine tests.

In addition to the wind turbines, the National Test Centre also includes two met masts. One met mast, which will be used in this research, is 114 meters high and is instrumented with following instrumentation:

- Cup and sonic wind speed measurements at 6 heights
- Wind direction and absolute temperature measurements at 3 heights
- Pressure and Relative humidity measurements at 2 heights
- Precipitation and radiation

The test site at Høvsøre has the advantage that the wind conditions allow an almost undisturbed wind flow from the North Sea for wind turbines. Due to the uninterrupted flow over sea and flat terrain to the West of the test site, the wind conditions are very well defined at the turbines. The 114 meter high met mast is located South of the test turbines. As stated before the met mast is equipped with sensors to measure wind speed, direction, temperature, pressure and humidity. For the atmospheric stability analysis five measurement heights will be used 10, 40, 60, 80 and 100 meter. They will be compared to the sonic measurements at heights of 10, 40 and 100 meter [37].

The met mast data were obtained from Danish Technical University for January 1 to December 31, 2010.

D.2 Data processing

Before the atmospheric stability can be determined from the given data, a couple of factors have to be taken into account which are extensively discussed in chapter 4 and 5.

The coastal line to the West and wind turbines to the North of the met mast disturb the free airflow. To exclude these influences a selection of the wind direction is made. The wind directions from 50 ° to 150 ° are used in the atmospheric stability analysis at Høvsøre. This resulted in a total data reduction of around 76%.

D.3 Results - National Test Centre Høvsøre

In this chapter, the Høvsøre data is used to analyse the behaviour of multiple methods to estimate the atmospheric stability and execute a comparison with the Eddy Covariance Method based on sonic measurements at three heights.

D.3.1 Overall statistics of atmospheric stability

For the overall statistics of Høvsøre, the distribution per year of multiple methods is compared to the Eddy Covariance Method, assuming that the Eddy Covariance Method gives the best representation of the real atmospheric stability.

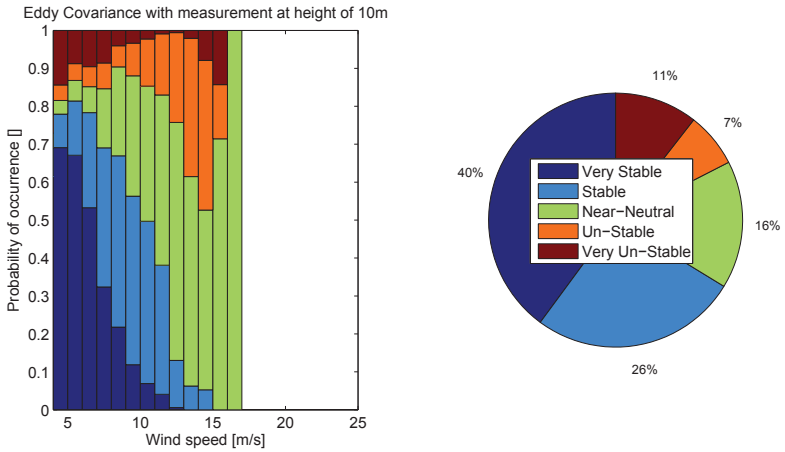

Figure D.1: Høvsøre - Eddy Covariance Method with sonic measurements at a height of 10 meter

Figures D.1, D.2 and D.3, show the stability distribution according to the Eddy Covariance Method divided into five classes, at a height of 10, 40 and 100 meters respectively. On the left side of the figures the stability per wind speed bin and on the right side the yearly distribution. The specification of the five classes can be found in table 4.4 in section 4.4.1.

What can be observed from these figures is the large differences between the yearly distributions at different heights. When the results are compared to the results of Lindenberg, some differences can observed. At Lindenberg a decrease of extreme conditions with height can be observed. However at Høvsøre a decrease of stable conditions at 40 meters, compared to the results at 10

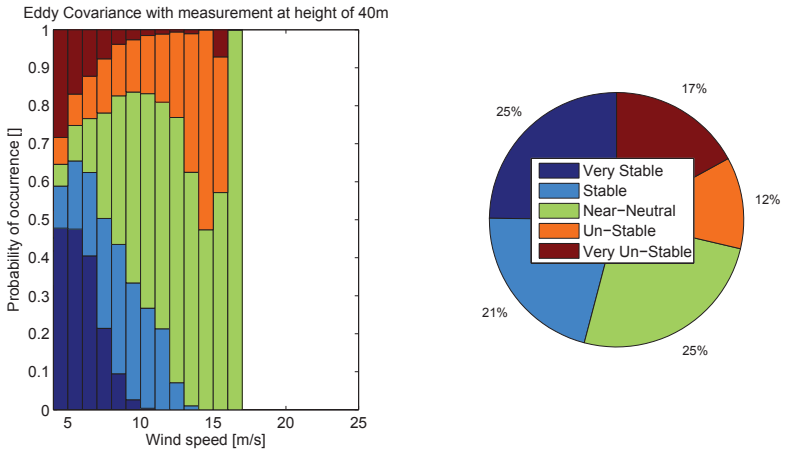

Figure D.2: Høvsøre - Eddy Covariance Method with sonic measurements at a height of 40 meter

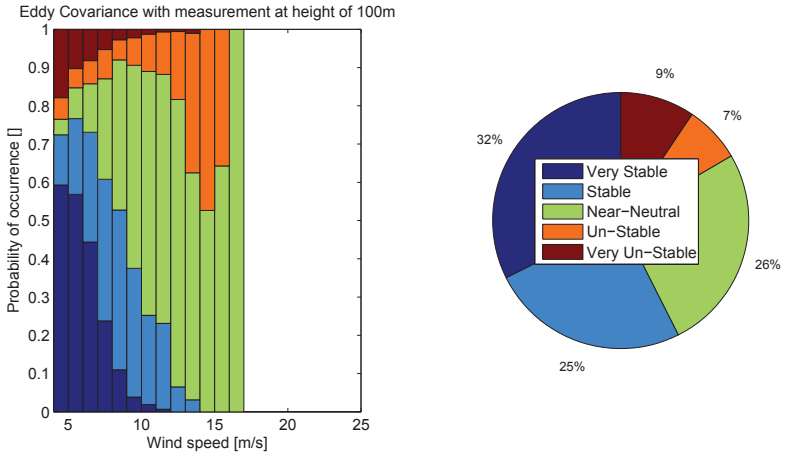

Figure D.3: Høvsøre - Eddy Covariance Method with sonic measurements at a height of 100 meter

meters. The results of the Eddy Covariance Method at 100 meters are compared to the results of 40 meters, a slight increase can be observed of the stable conditions. For the unstable conditions at Høvsøre the opposite can be observed. First an increase of unstable conditions after which an decrease of unstable conditions could be observed from the lower measurements to the higher measurements.

From the PDF in figure D.4, it can be observed that two methodologies, the Bulk Richardson Number and Profile Method 2, give very similar results to the Eddy Covariance Method. The atmospheric stability estimation of the Bulk Richardson Number at 40 meters is very close atmospheric stability estimation of the Eddy Covariance Method at 40 and 100 meters. A small over-prediction of unstable conditions and an under-prediction of the stable conditions can be observed. The results of the Profile Method 2 at 40 meters are also very similar to the Eddy Covariance Method at 40 and 100 meters, with an over-prediction of neutral.

The results of the Profile Method 1 and Gradient Richardson Number are significantly different. According to the results with both methodologies the conditions are mainly extreme, with a

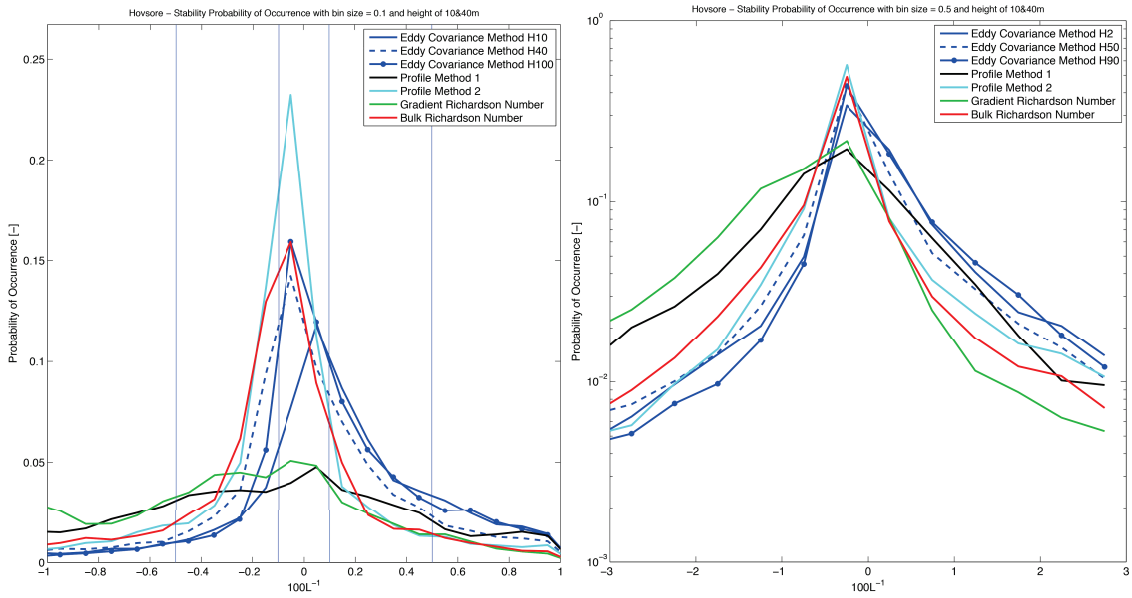

Figure D.4: Høvsøre - Comparison of Atmospheric Stability Distribution with the PDF of the stability parameter $\frac{z}{L}$. The left figure is plotted on normal scale and the right figure on semi-logarithmic scale

tendency to very stable.

The atmospheric stability analyses of Cabauw and Lindenberg showed the same results, the Bulk Richardson Number and Profile Method 2 give significantly better results than the other two methodologies. The further research in this chapter will therefore focus on the Bulk Richardson Number and Profile Method 2.

D.4 Statistical analysis of the friction velocity (u_*) and heat flux ($\overline{w'\theta'_v}$) for multiple measurement heights

A maximum measurement height of 40 meters is used in this chapter until now, to determine the stability with MOST at Høvsøre. In this chapter a statistical analysis will be executed by a direct comparison of the friction velocity and heat flux of each moment in time with one methodology and the Eddy Covariance Method. The differences between multiple methodologies and measurement heights will be visualized in terms of slope and correlation, which can be found in figures D.5, D.6, D.7, D.8.

Friction velocity (u_*)

The slope of the Bulk Richardson Number is around 1 when compared to the Eddy Covariance Method at 10 meters. Comparing the results of the Bulk Richardson Number with the Eddy Covariance Method at higher altitudes a small under-prediction can be observed. The slope of the Profile Method 2 however, shows a significant over-prediction of the friction velocity for all cases.

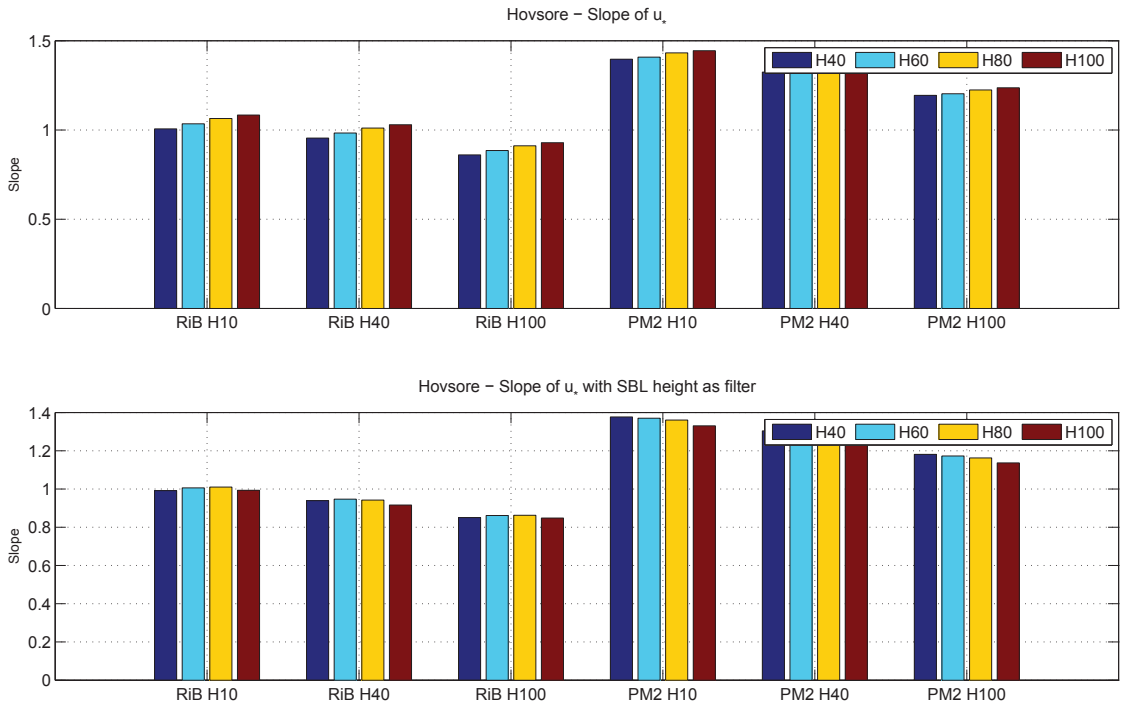

Figure D.5: Høvsøre - Slope of Friction Velocity (u_*) with and without the Surface Boundary Layer height as a filter for four methods
RiB - Bulk Richardson Number, PM2 - Profile Method 2

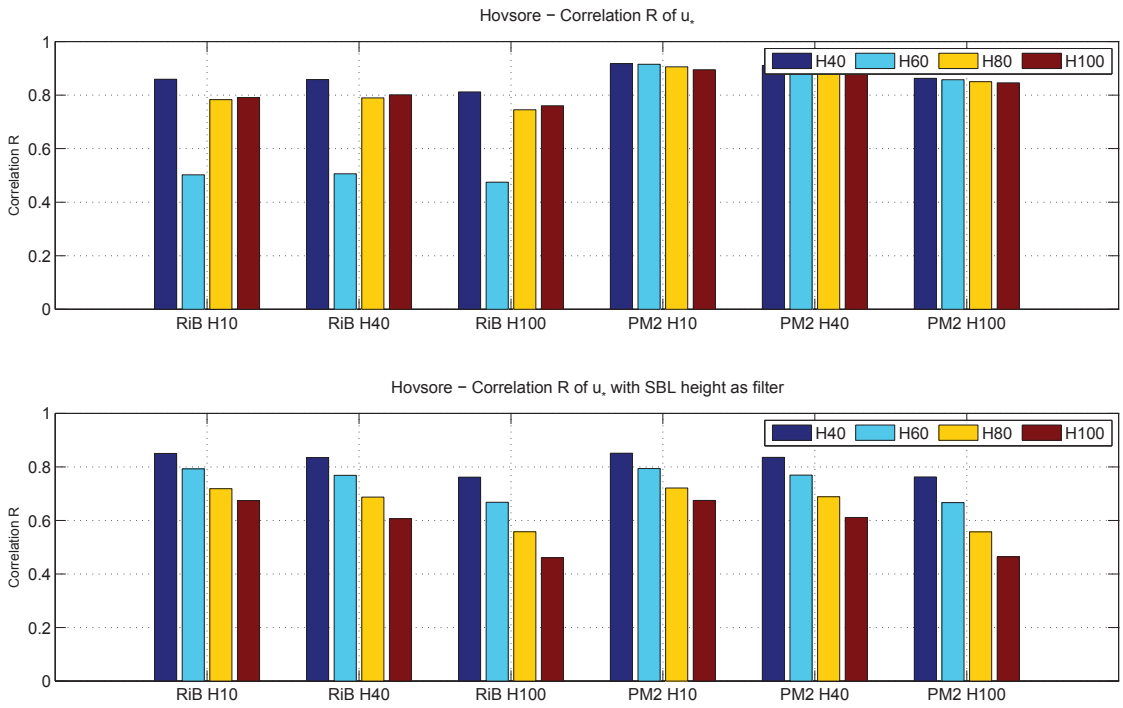

Figure D.6: Høvsøre - Correlation of Friction Velocity (u_*) with and without the Surface Boundary Layer height as a filter for four methods
RiB - Bulk Richardson Number, PM2 - Profile Method 2

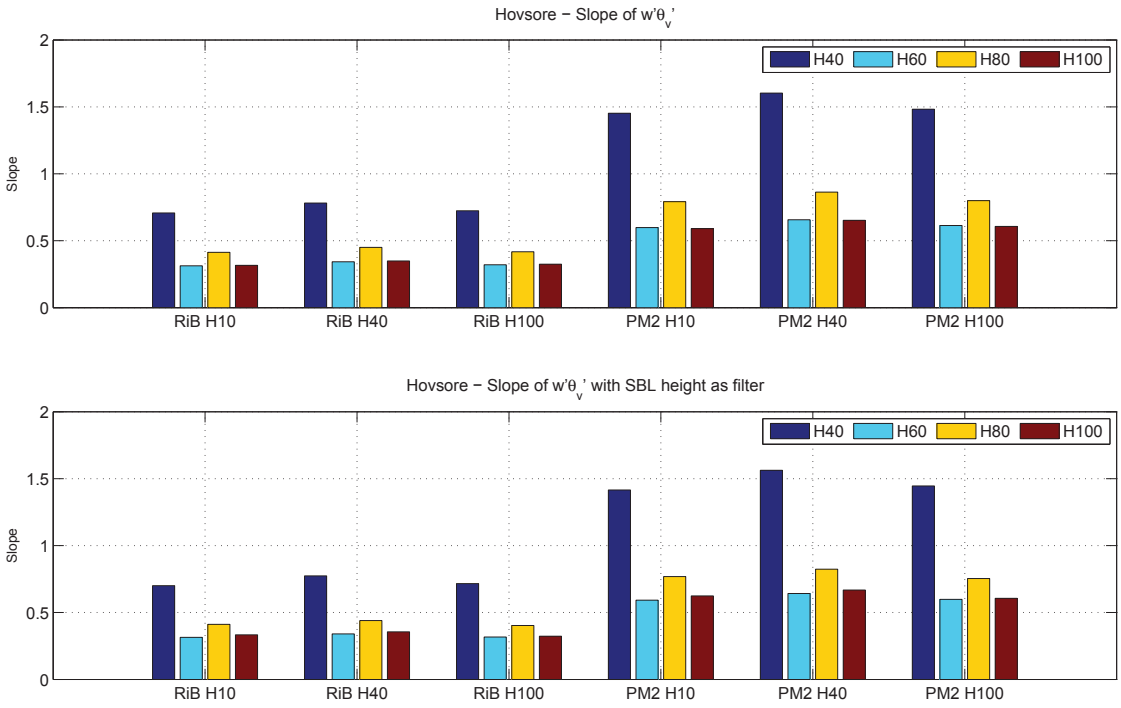

Figure D.7: Høvsøre - Slope of Heat flux $(\overline{w'\theta'_v})$ with and without the Surface Boundary Layer height as a filter for four methods
RiB - Bulk Richardson Number, PM2 - Profile Method 2

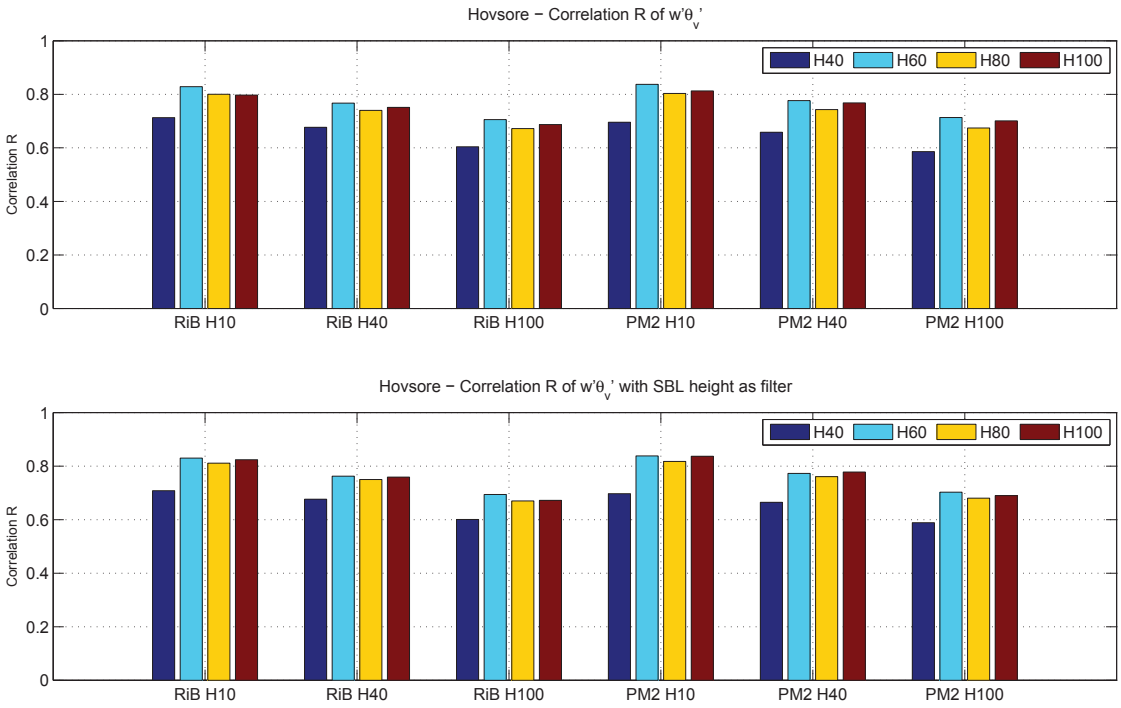

Figure D.8: Høvsøre - Correlation of Heat flux $(\overline{w'\theta'_v})$ with and without the Surface Boundary Layer height as a filter for four methods
RiB - Bulk Richardson Number, PM2 - Profile Method 2

Profile Method 2 has the highest correlation and is the most consistent. Especially the Richardson Number methods are effected with measurements outside the Surface Boundary Layer, similar to the results of Cabauw and Lindenberg.

In contrast to the results of Cabauw and Lindenberg where an overall an increase of slope could be observed when higher altitudes are selected. The slope of both methods at Høvsøre is almost constant with multiple measurement heights. However due to the small decrease of correlation with height, preferable a maximum measurement height of around 40-60 meters would be used.

Heat flux ($\overline{w'\theta'_v}$)

The heat flux for all methodologies gives an under-prediction, except when a measurement height of 40 meters is used. A significant increase in slope can be observed when a measurement height of 40 meters is used. The Profile Method 2 with a measurement height of 80 meter is the closest to the Eddy Covariance Method at all heights.

The correlation of the Profile Method 2 & Bulk Richardson Number are very similar again.

D.5 Equivalent load calculations of a wind turbine blade root

The results are shown in table D.1. The table shows the equivalent load for the Eddy Covariance Method, Profile Methods and Richardson Number Methods and the deviation of each method with the Eddy Covariance Method in percentage. This is conducted for two cases, with and without the Surface Boundary Layer height as filter.

Next to equivalent load using the atmospheric stability distributions, in each table the equivalent load determined using the IEC guideline can be found. This guideline assumes only neutral conditions where the turbulence intensity is a function of the wind speed and not of the atmospheric conditions.

From table D.1 a couple of observations can be made based on the equivalent load estimations using multiple methodologies.

An overall over-prediction of all methods can be observed when compared to the Eddy Covariance Method, with the Profile Method as an exception. The best agreement is similar to the results of Cabauw and Lindenberg. Both the Profile Method 2 and Bulk Richardson Number give an equivalent load estimation between -1% and 3% compared to the Eddy Covariance Method.

Again an increase of the equivalent load was found when the Surface Boundary Layer height filter is used. This resulted in an increase of the equivalent load of around 5%.

The equivalent load of the IEC guideline shows an over prediction of around 30%, depended on the situation. This shows the conservative results of the IEC guideline.

D.6 Summary & Conclusions based on the Høvsøre data

In this appendix, the atmospheric stability analysis is executed with five methods using the 2010 Høvsøre data. Before the analysis could be executed, two filter types are used to handle the data

Method	$F_{eq10min}$ $[kNm]$	$\Delta_{EddyCH10}$	$\Delta_{EddyCH40}$	$\Delta_{EddyCH100}$
Eddy Covariance Method H10	809	-	1%	2%
Eddy Covariance Method H40	803	-1%	-	-1%
Eddy Covariance Method H100	793	-2%	-1%	-
IEC Guideline	1047	29%	28%	29%
Profile Method 1	993	23%	24%	25%
Profile Method 2	800	-1%	-0.3%	1%
Gradient Richardson Number	972	20%	21%	23%
Bulk Richardson Number	819	1%	2%	3%
Using the Surface Boundary Layer height as a filter ($c_i = 0.15$ and $z_s = 10\%$ of z_i)				
	$F_{eq10min}$ $[kNm]$	$\Delta_{EddyCH10}$	$\Delta_{EddyCH40}$	$\Delta_{EddyCH100}$
Eddy Covariance Method H10	865	-	1%	2%
Eddy Covariance Method H40	856	-1%	-	1%
Eddy Covariance Method H100	848	-2%	-1%	-
IEC Guideline	1109	30%	30%	31%
Profile Method 1	1037	21%	21%	22%
Profile Method 2	853	-1%	-0.4%	1%
Gradient Richardson Number	1038	21%	21%	22%
Bulk Richardson Number	875	1%	2%	3%

Table D.1: Høvsøre - Equivalent load of a wind turbine blade root using the height filter at the bottom table.

correctly. First, all extreme values and sensor errors are removed from the dataset and second the steady state check is executed. MOST requires stationary flow and the steady state filter removes data point where the deviation from previous values exceeds certain conditions, mentioned in section 4.3.1. To exclude the influences of the coast and wind turbines all wind directions outside 50 ° to 150 ° are excluded from the atmospheric stability analysis. This resulted in a total data reduction of around 76%.

Overall the results and conclusions are very similar to the findings at Cabauw and Lindenberg.

Appendix E

Verifications of Assumptions

E.1 Stationary conditions filter impact

In this section the impact of the stationary conditions filter is analysed, by comparing the overall distributions and correlations of the friction velocity and heat flux.

Starting with the comparison of the overall distribution of the Eddy Covariance Method, Profile Method and Bulk Richardson Number. The figures E.1, E.2 and E.3 show the overall distribution without the stationary conditions filter. Comparing these figures with figures 4.6, figure 4.9, figure 4.10 with the stationary conditions filter, a small increase of unstable conditions for all three the methodologies.Further investigation of the impact of this small increase showed a small increase of the equivalent load of around 2% for the Eddy Covariance Method.

The correlation of the friction velocity and heat flux can be found in table E.1 and E.2. Showing for the Richardson Number a small decrease of both correlation of the friction velocity and heat flux when the Stationary conditions filter is not used. The Profile Method 2 shows however a small increase of correlation when the Stationary conditions filter is not used.

These results are similar to the results found by Sathe [45], where was seen that hardly any influence of the stationary conditions filter.

Method	R	R without stationary conditions filter	R with z_s filter	R with z_s filter without stationary conditions filter
Bulk Richardson Number	0.67	0.61	0.91	0.91
Profile Method 2	0.89	0.95	0.90	0.91

Table E.1: Correlation R - Friction velocity (u_*)

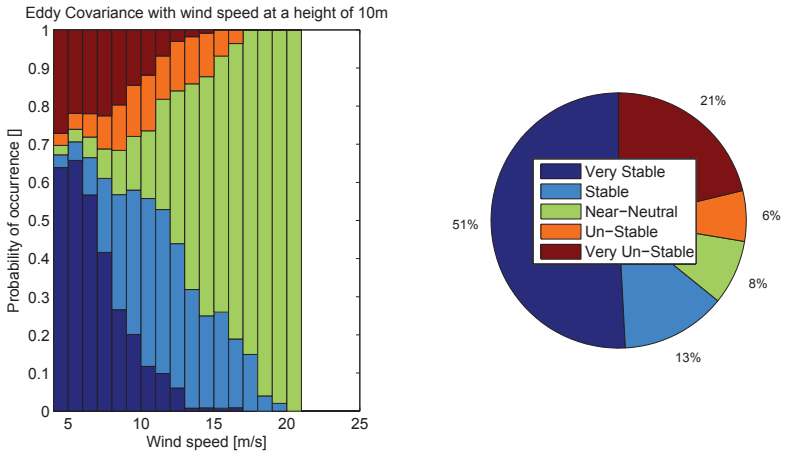

Figure E.1: Cabauw - Atmospheric Stability distribution for the Eddy Covariance Method without Stationary filter

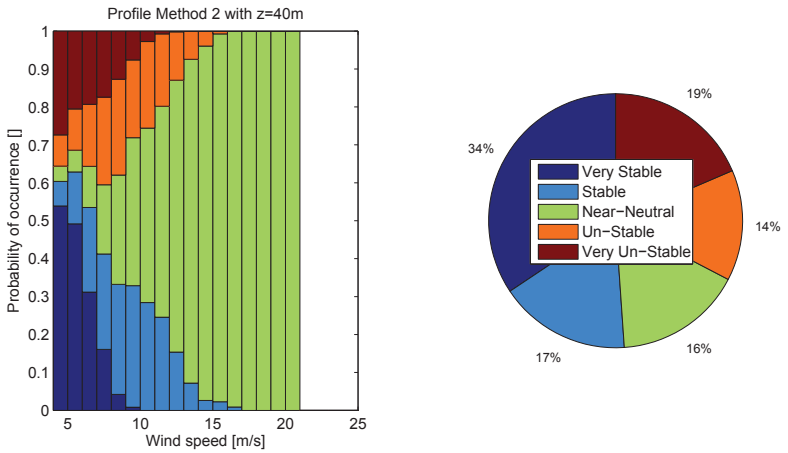

Figure E.2: Cabauw - Atmospheric Stability distribution for the Profile Method 2 without Stationary filter

Method	R	R without stationary conditions filter	R with z_s filter	R with z_s filter without stationary conditions filter
Bulk Richardson Number	0.02	0.01	0.88	0.88
Profile Method 2	0.86	0.88	0.87	0.88

Table E.2: Correlation R - Heat flux ($\overline{w'\theta'_v}$)

E.2 Surface Temperature

At Cabauw, instead of the real surface temperature at 0 meters, the temperature measured at 20 centimeters above the ground is used to determine the atmospheric stability. Due to the heat transfer of the surface to the air a small difference will be observed between the actual surface temperature and the temperature at 20 centimeters above the ground.

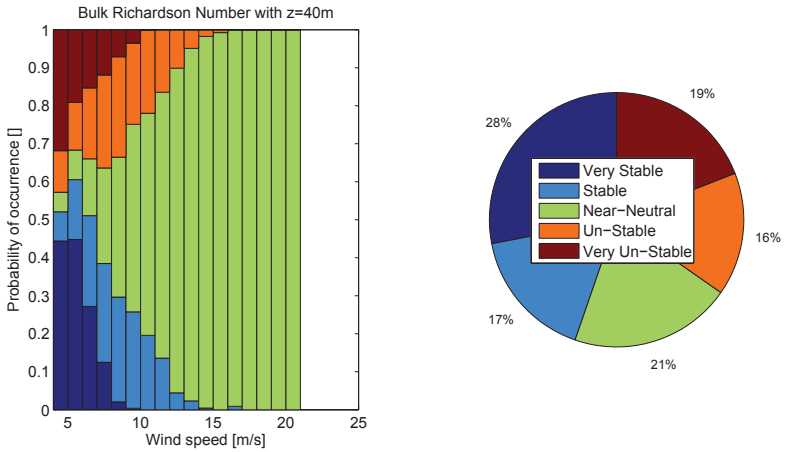

Figure E.3: Cabauw - Atmospheric Stability distribution for the Bulk Richardson Number without Stationary filter

To look at the impact of this temperature difference, a first order estimation of the temperature difference is executed, by looking at the difference in virtual potential temperature between 10 meters and 200 meters. The average temperature difference is approximately 0.7 K. Therefore it is assumed, the temperature difference between the actual surface temperature and temperature to 20 centimeters is approximately 0.1 K.

A small sensitivity study has been performed, shown in Figures E.4 and E.5. This is the measured temperature difference between 20 centimeters and 40 meters. In addition, an offset is introduced in the the measured temperature difference of plus/minus 0.1K. Both figures shows that this has only a small effect on the distribution, therefore it can be assumed that the temperature measurement at 20 centimeters is sufficient.

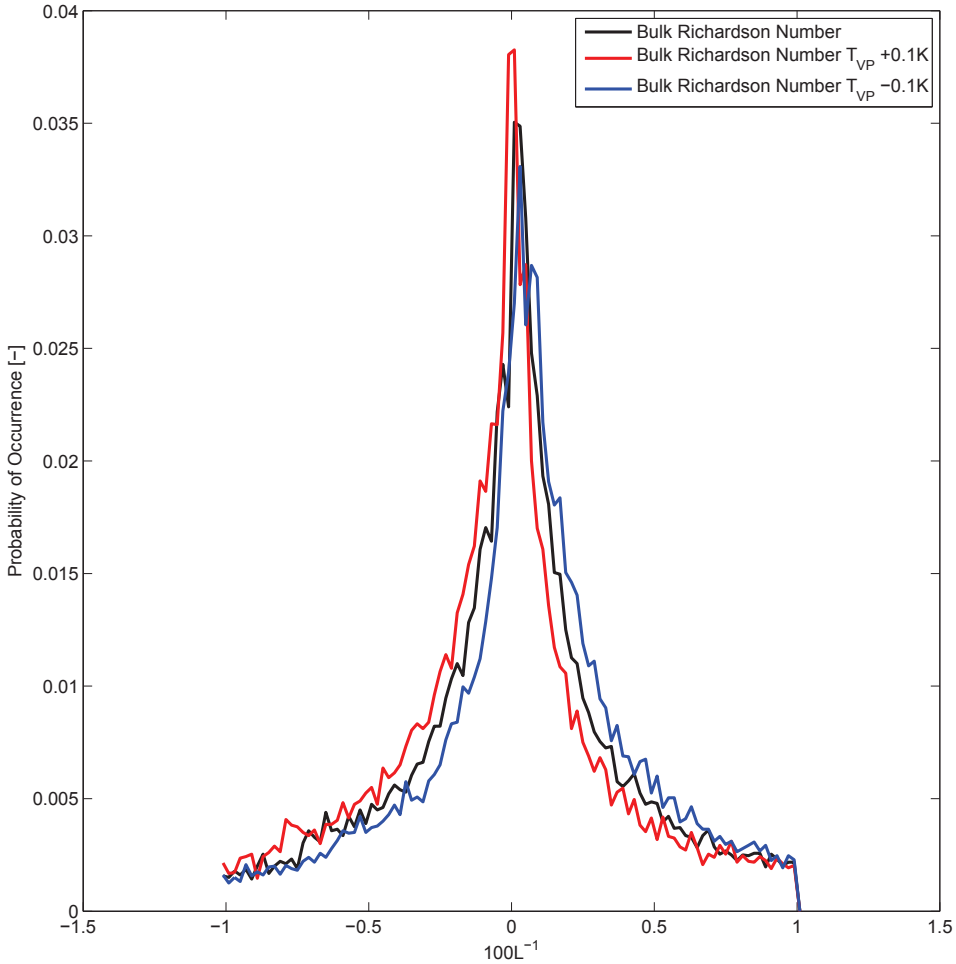

Figure E.4: Cabauw - Sensitivity analysis of surface temperature for Bulk Richardson Number

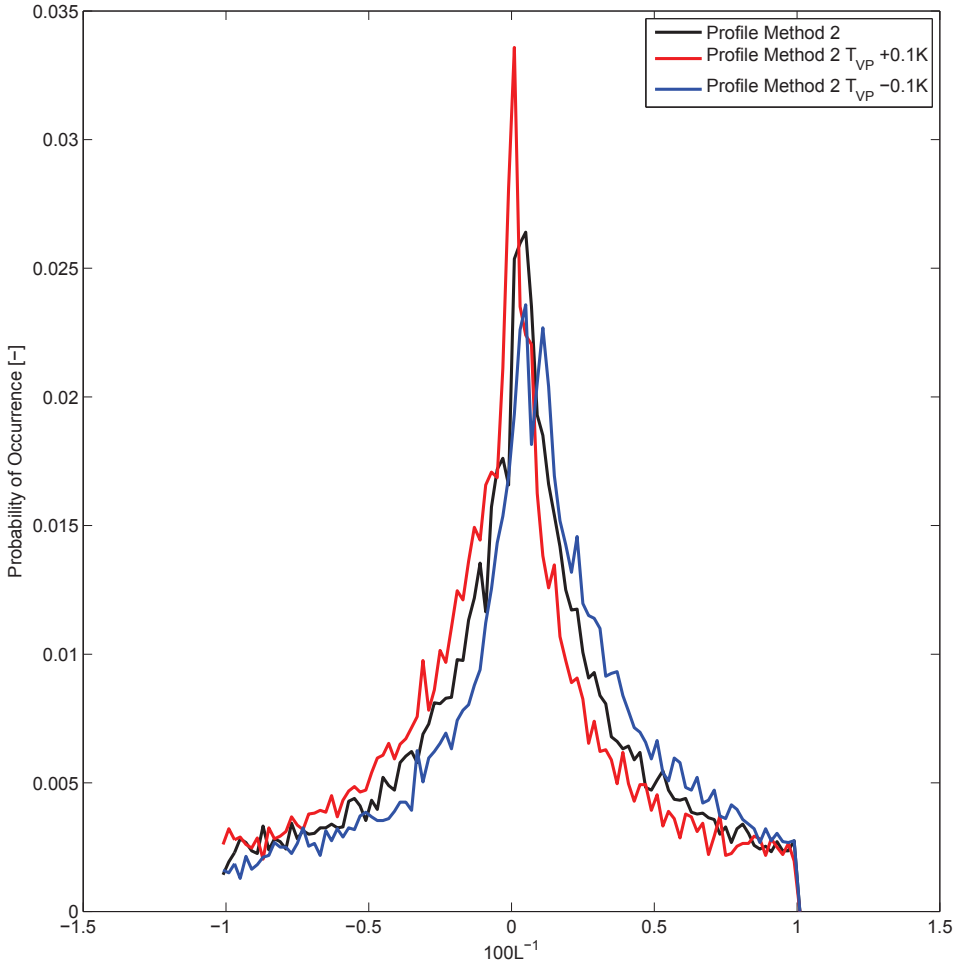

Figure E.5: Cabauw - Sensitivity analysis of surface temperature for Profile Method 2

E.3 Friction velocity routine check

In chapter 4 and 5 statistical analysis are executed on the slope and correlation of the friction velocity and heat flux. To check the routine an ideal dataset of the friction velocity is created with the following parameters: $N = 10000$, mean=0.5 m/s and standard deviation of 0.1.

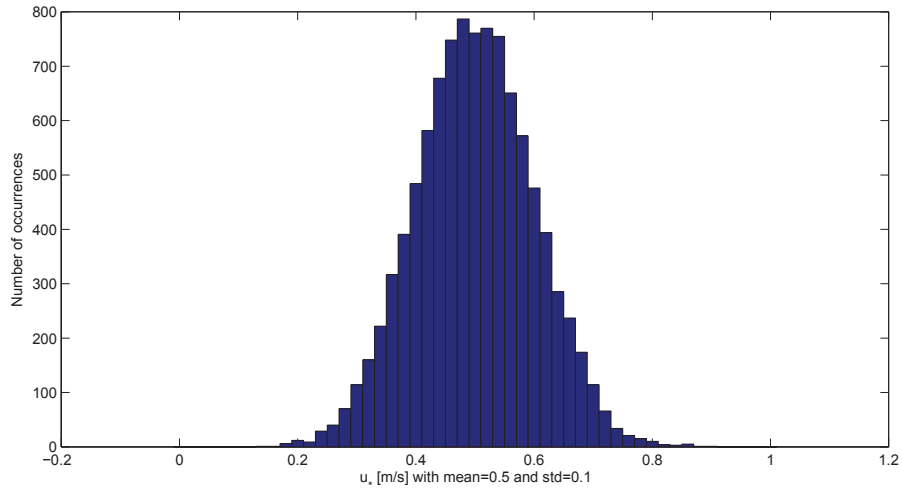

Figure E.6: Histogram routine check vector with ideal u* with mean of 0.5 and standard deviation 0.1

Using this ideal dataset, with varying u_*, constant $\overline{w'\theta'_v} = -5 * 10^-3 \frac{W}{m^2}$, $T = 280K$,$\Delta z = 40m$ and $z_0 = 0.1m$ the wind speed and temperature difference at each datapoint can be calculated using equations of the Profile Method 2.

The found wind speeds and temperature can be used to determine the friction velocity with the Profile Method 2. In figure E.7 the friction velocity of the ideal dataset is plotted against the new recalculated friction velocity. Ideally the new found friction velocity (u_*) should be the same as the starting point and exactly on the blue line. The figure shows that for almost all cases this requirement is achieved, however for small values a small deviation can be found. This is due to the iterative process which is used by the Profile Method 2 to determine the stability.

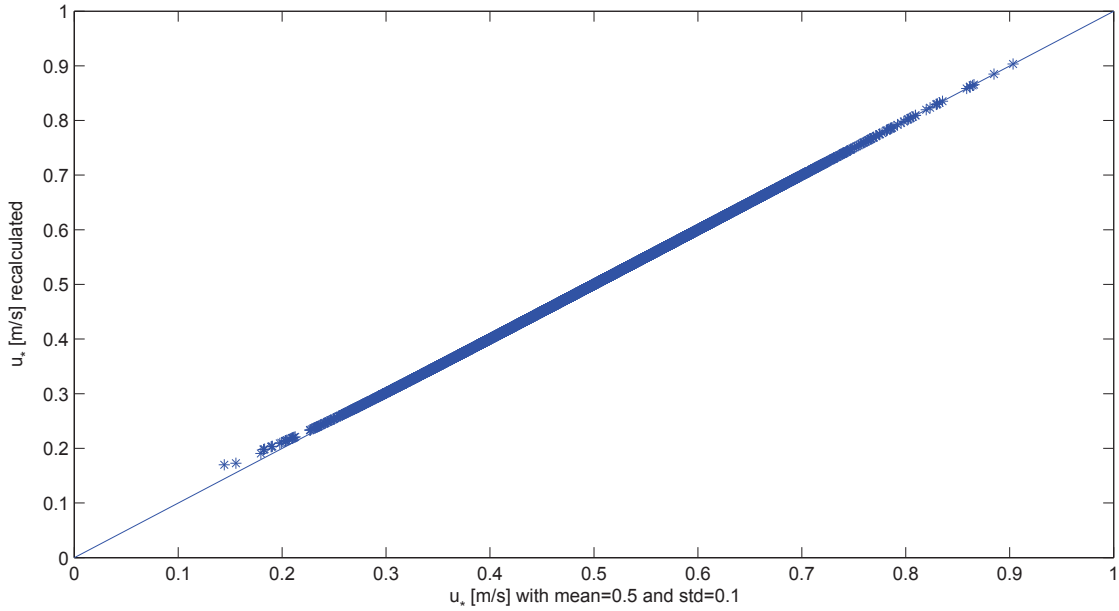

Figure E.7: Routine check, with on the x-axis the ideal dataset of u_* and the y-axis the recalculated u_*

Appendix F

Richardon Number

F.1 Derivation Ri_g from Ri_f

The flux Richardson Number is the ratio of the buoyant production of turbulence to the mechanical shear production of turbulence.

$$Ri_f = \frac{\frac{g}{\overline{\theta_v}}\overline{w'\theta'}}{\overline{w'u'}\frac{\partial \overline{U}}{\partial z}} \tag{F.1}$$

Assuming correlation to be proportional to their vertical gradients:

$$\overline{w'\theta'_v} = K_\theta \frac{\partial \overline{\theta_v}}{\partial z} \tag{F.2}$$

$$\overline{w'u'} = K_U \frac{\partial \overline{U}}{\partial z} \tag{F.3}$$

The K_θ and K_U are the eddy coefficients respectively for heat and momentum, the gradient Richardson Number can be obtained:

$$Ri_g = \frac{\frac{g}{\overline{\theta_v}} K_\theta \frac{\partial \overline{\theta_v}}{\partial z}}{K_U (\frac{\partial \overline{U}}{\partial z})^2} \tag{F.4}$$

By approximating $\frac{K_\theta}{K_U} \approx 1$ and assuming $\frac{\partial}{\partial z} = \frac{\Delta}{\Delta z}$

$$Ri_g = \frac{g\overline{\Delta\theta_v}\Delta z}{\overline{\theta_v}(\Delta \overline{U})^2} \tag{F.5}$$

F.2 Theoretical substantiation - Richardson Number Parameterization

Logarithmic profile used all over the world

$$U = \frac{u_*}{\kappa} ln(\frac{z}{z_0}) \tag{F.6}$$

For the Gradient Richardson number:

$$Ri_G = \frac{g}{\theta_v} \frac{\frac{\partial \theta_v}{\partial z}}{(\frac{\partial U}{\partial z})^2} \tag{F.7}$$

And for the stability parameter $\zeta = \frac{z}{L}$

$$\zeta = -\frac{\kappa g z}{\theta_v} \frac{\overline{w'\theta'_v}}{u_*^3} \tag{F.8}$$

From definition the dimensionless wind gradient and temperature gradient can be defined as.

$$\phi_m(\frac{z}{L}) = \frac{\kappa z}{u_*}(\frac{\partial U}{\partial z}) \tag{F.9}$$

$$\phi_h(\frac{z}{L}) = \frac{\kappa z}{\theta_*}(\frac{\partial \theta_v}{\partial z}) \tag{F.10}$$

Combining the turbulent fluxes and gradients, results in the following:

$$\overline{w'\theta'_v} = -K_\theta \frac{\partial \theta_v}{\partial z} \tag{F.11}$$

$$\overline{w'u'} = -K_U \frac{\partial U}{\partial z} \tag{F.12}$$

From this the Eddy-transfer coefficients can be defined:

$$\alpha = \frac{K_\theta}{K_U} = \frac{\overline{w'\theta'_v}\frac{\partial U}{\partial z}}{\overline{w'u'}\frac{\partial \theta_v}{\partial z}} \tag{F.13}$$

By definition from Stull [53]:

$$-\overline{w'u'} = u_*^2 \tag{F.14}$$

$$-\overline{w'\theta'_v} = u_*\theta_* \tag{F.15}$$

From the definitions above it can be concluded that

$$\alpha = \frac{\overline{w'u'}}{u_*\theta_*}\frac{\phi_m}{\phi_h} = \frac{\phi_m}{\phi_h} \tag{F.16}$$

$$\zeta = \alpha \phi_m Ri_G \tag{F.17}$$

Thus,

$$\frac{\zeta}{\phi_m} = \alpha Ri_G \tag{F.18}$$

According to the Businger-Dyer functions in Table 2.2 for stable conditions the ϕ function for stable conditions is $\phi_m = 1 + \beta\zeta$ where $\beta = -5$ and assumed that $\alpha = 1$.

Resulting in:

$$\frac{\zeta}{1+\beta\zeta} = Ri_G \tag{F.19}$$

$$\frac{1+\beta\zeta}{\zeta} = \frac{1}{Ri_G} \tag{F.20}$$

$$\frac{1}{\zeta} = \frac{1}{Ri_G} - \beta \tag{F.21}$$

$$\zeta = \frac{1}{\frac{1}{Ri_G} - \beta} = \frac{Ri_G}{Ri_G} \frac{1}{\frac{1}{Ri_G} - \beta} = \frac{Ri_G}{1 - \beta Ri_G} \tag{F.22}$$

This is exactly what is used in the Gradient Richardson Method for unstable conditions. However for the Bulk Richardson Number the function is:

$$\zeta = \frac{ARi_G}{1 - \beta Ri_G} \tag{F.23}$$

with A=10. The difference can be explained by the application, the derivation of the function of the Gradient Richardson Number is done locally with ∂z almost zero, however the Bulk Richardson Number uses a gradient temperature and wind speed of more than 10 meters which results in different parameters due to the averaging over a layer or multiple layers.

For unstable conditions the following can be found, excluding extreme unstable conditions;

$$\phi_m = [1 - C\zeta]^{\frac{1}{4}} \tag{F.24}$$

$$\phi_h = [1 - C\zeta]^{\frac{1}{2}} \tag{F.25}$$

$$\alpha = \frac{1}{\phi_m} \tag{F.26}$$

Resulting in $\zeta = Ri_G$
It has to taken into account, that according to the dimensionless analysis the to the power of $\frac{1}{4}$ and $\frac{1}{2}$ in respectively in equation F.24 and F.25 are not entirely correct. The constants are determined in the famous Businger-Dyer Kansas experiment.

F.2.1 Parametrization Richardson Number

With the derivation of above the parameters used in the relation between the Richardson Number and the Monin-Obukhov length for unstable conditions can be derived from data and compared with the literature.

$$\zeta = \frac{z}{L} = ARi_B \frac{1}{L} = \frac{A}{z} Ri_B \tag{F.27}$$

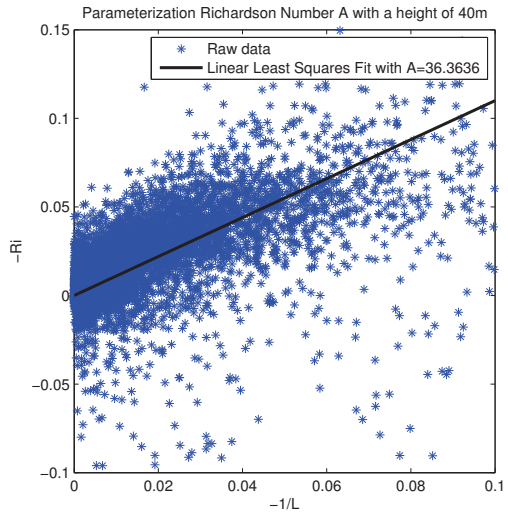

Figure F.1: Cabauw - Parametrization Richardson Number without the Surface Boundary Layer filter at a height of 40m.

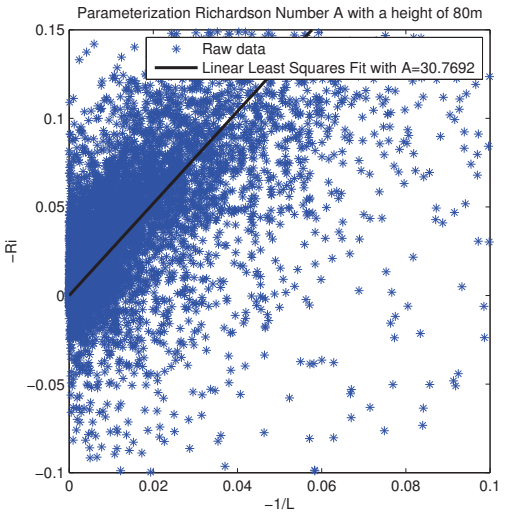

Figure F.2: Cabauw - Parametrization Richardson Number without the Surface Boundary Layer filter at a height of 80m.

A sensitivity study is executed to see the influence of different parameters

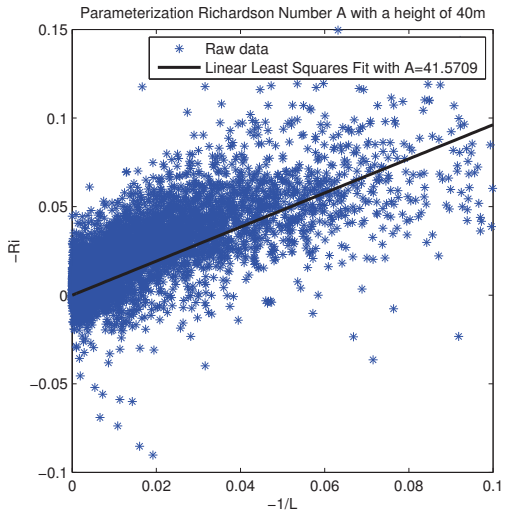

Figure F.3: Cabauw - Parametrization Richardson Number with the Surface Boundary Layer filter at a height of 40m.

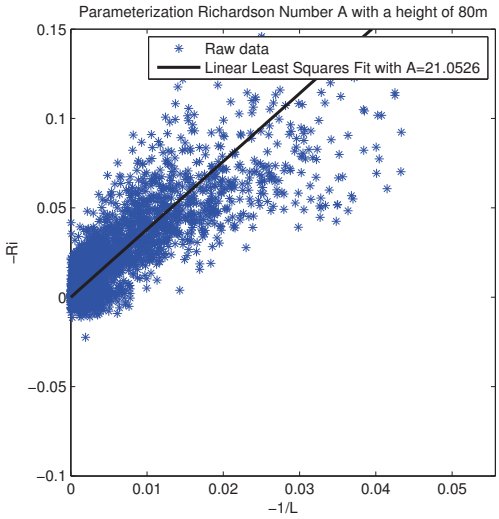

Figure F.4: Cabauw - Parametrization Richardson Number with the Surface Boundary Layer filter at a height of 80m.

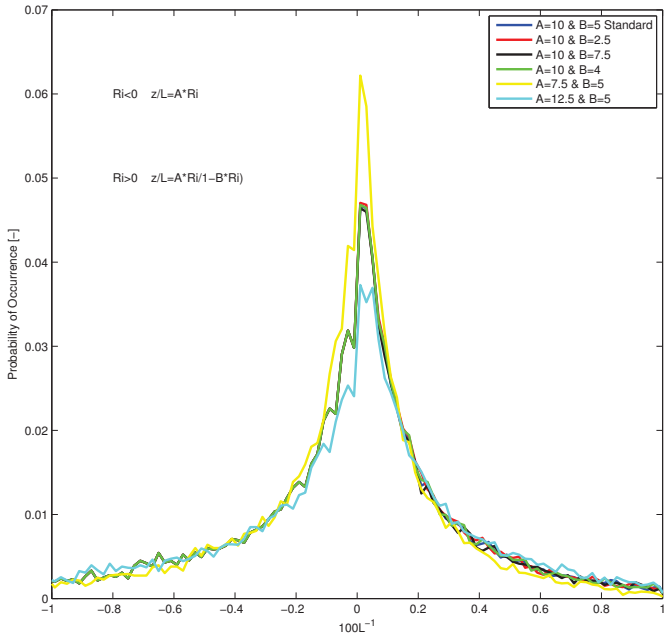

Figure F.5: Cabauw - Sensitivity study parametrization Richardson Number

F.3 Verification of equivalent load calculations with literature

In paper [28], Holstlag used the simulation software bladed to determine the equivalent load for each condition, wind speed and stability and determined the equivalent load for the NREL wind turbine at the FLOW met mast IJmuiden, 85 kilometers offshore, for January 1 to December 31 2012.

To verify the steps taken to determine the equivalent load in this thesis: An equivalent load calculation was conducted with the FLOW met mast IJmuiden for the year 2012 and the results were within 2% of the result found by Holstlag [28].

This small difference can be explained, because Holtslag assumed the stability distribution per wind speed pin was Normal distributed. At the FLOW met mast IJmuiden this was certainly the case, however at Cabauw and Lindenberg not and therefore stability distribution was divided into multiple bins and each bin was individual selected, which explains the small difference between the equivalent load found by Holtslag and me.

Appendix G

Methods - Literature

Method	Literature
Eddy Covariance Method	[20, 42, 38, 48, 11, 43, 13]
Profile Method 1	[39, 45, 26, 48, 24, 25]
Profile Method 2	[39, 45, 26, 48, 24, 25]
Gradient Richardson Number	[39, 44, 45]
Bulk Richardson Number	[20, 43, 44, 11, 36, 27, 39, 45, 58, 48, 11]
Pasquill-Gifford Method	[61, 1, 54, 39]
WRF	[43]
Flux relations	[10][3][36][3][21]

Table G.1: Methods from Literature